CHANGES IN INSULIN RESISTANCE ASSOCIATED WITH CHRONIC AIRWAY ALLERGEN EXPOSURES IN A SPONTANEOUSLY OBESE, NONHUMAN PRIMATE MODEL OF ALLERGIC ASTHMA

by

Hannah G. Woolard

July, 2021

Director of Thesis: Stefan Clemens, PhD

Co-director: Robert L. Wardle, PhD

Major Department: Physiology

Obesity and asthma are two major well-recognized and interconnected major health problems, but the mechanisms that underlie the association of these two chronic inflammatory disease states are still unknown. Novel insights including the central role of inflammation and metabolic dysfunction, have been reported but even more complexity has arisen by the many co-morbidities common to both obesity and asthma. Of particular interest is the role of insulin resistance, which has been heavily implicated as the possible missing link required for understanding the etiology and underlying pathophysiological mechanisms resulting in a more severe, difficult to treat asthma. Hence, the proposed research project presented in this thesis was conducted to specifically investigate the relationship/interaction/association between the development of insulin resistance (induced by obesity) and allergen-induced allergic asthma. From an established non-human primate model of allergic asthma, we studied a cohort of obese, male 10-year-old rhesus macaques with varying historical degrees of airway hyperreactivity and changes in insulin resistance. We hypothesized chronic aero-HDM exposures would induce increased airway hyperreactivity and pulmonary inflammation which would be associated with

the worsening development of insulin resistance. To test this hypothesis, we paired animals according to historical AHR, then exposed one animal from each pair to aero-HDM and the other to aero-saline/SHAM, monthly for 6 months. We assessed body composition, insulin resistance via intravenous glucose tolerance test, the early asthmatic response AHR to aero-HDM/saline, as well as the late asthmatic response AHR to aero-Mch and pulmonary inflammation via bronchoalveolar lavage.

We found increased AHR to aero-HDM coincident with eosinophil-dominate pulmonary inflammation for all five HDM-exposed study animals, mirroring the early-onset, eosinophilic obese asthma endotype. SHAM-exposed animals did not manifest increases in AHR to aero-saline nor aero-Mch, yet two animals manifested increased eosinophilic pulmonary inflammation (similar to HDM-exposed animals) and interesting one animal manifested neutrophilic inflammation mirroring the non-eosinophilic, neutrophil-dominant inflammatory endotype reported in the literature for the late-onset, non-atopic obese asthma phenotype. Due to high variability and limited time points, no significant changes were observed for the IR indices however an interesting negative trend between changes in AHR and HOMA-IR, an index of insulin resistance, was observed for 3/5 HDM-exposed animals suggesting increased AHR was associated with decreased HOMA-IR/improved IR, not supporting our original hypothesis. Further studies identifying and understanding the unique inflammatory biomarkers and mechanisms linking allergic asthma, obesity, insulin resistance, and related sequalae are necessary for targeted therapeutic development and the proper treatment of the heterogeneous nature of obesity associated asthma and the inevitable metabolic consequences.

CHANGES IN INSULIN RESISTANCE ASSOCIATED WITH CHRONIC AIRWAY ALLERGEN EXPOSURES IN A SPONTANEOUSLY OBESE, NONHUMAN PRIMATE MODEL OF ALLERGIC ASTHMA

A Thesis

Presented to the Faculty of the Department of Physiology

Brody School of Medicine at East Carolina University

In Partial Fulfillment of the Requirements for the Degree

Masters of Science in Biomedical Sciences

by

Hannah G. Woolard

July, 2021

CHANGES IN INSULIN RESISTANCE ASSOCIATED WITH CHRONIC AIRWAY ALLERGEN EXPOSURES IN A SPONTANEOUSLY OBESE, NONHUMAN PRIMATE MODEL OF ALLERGIC ASTHMA

by

Hannah G. Woolard

APPROVED BY:

DIRECTOR OF THESIS:

(Stefan Clemens, PhD)

CO-DIRECTOR OF THESIS:

(Robert L. Wardle, PhD)

COMMITTEE MEMBER:

(David N. Collier, MD, PhD)

COMMITTEE MEMBER:

(Jamie C. DeWitt, PhD)

DIRECTOR OF THE MASTER'S
OF BIOMEDICAL SCIENCES
PROGRAM:

(Richard A. Franklin, PhD)

DEAN OF THE GRADUATE
SCHOOL:

(Paul J. Gemperline, PhD)

DEDICATION

I dedicate this thesis to the twenty animals that made this project possible – their memory and scientific contribution will never be forgotten.

ACKNOWLEDGEMENTS

I would like to first acknowledge my committee including Dr. Stefan Clemens, Dr. Robert Wardle, Dr. David Collier and Dr. Jamie DeWitt for their guidance, patience, and scientific insight. I would also like to thank the Departments of Physiology, Pharmacology/Toxicology, Comparative Medicine, and the Brody Brothers Endowment Fund for providing the resources, support and guidance to perform my graduate research project using their equipment and facilities.

I would like to express my sincerest gratitude to Dr. Stefan Clemens, who not only stepped into a role last minute outside of his research field but moved mountains for me to complete my thesis and degree. This thesis would not have been possible without your lead and I will be forever grateful.

Additionally, I would like to thank Dr. Jamie DeWitt for her encouragement, support, advocacy, and comfort throughout this entire process. You exhibit true excellence as a person and scientist. Thank you from the bottom of my heart.

I would like to acknowledge the multiple collaborators who contributed to this project including Dr. Robert Lust, Dr. Michael VanScott, Dr. Michelle Ratliff, Ms. Lyndsay Richards, Dr. Sky Reece, Dr. Kymberly Gowdy, Dr. Kelsey Fisher-Wellman, as well as the Oregon National Primate Research Center (ONPRC).

I would like to express my heartfelt gratitude to the DCM veterinarians and staff including Dr. Dorcas O'Rourke, Dr. Karen Oppelt, Dr. Cecile Baccanale, Dr. Kali Campbell, Peggy Pittman, Jason St. Antoine, Matt Verzwyvelt, Tammy Barnes, Ryan Blum, and Courtney Williford as well as Aaron Hinkle, Jerry Register, Edward Walker, Jennifer Johnson, Hampton Farmer, Zach Aardweg, and Anan Hiralal.

My incredible support system including Michelle McCarthy, Megan Kelly, M.K. Donovan, Sarah Crump, and Kim Fisher, have provided unwavering love and encouragement. And lastly, I would like to acknowledge my mom, Gray, dad, John, big brother, Logan, and sister/best friend, Jennifer. You four have never stopped supporting, encouraging, motivating, and most importantly loving me unconditionally during the most difficult and trying time of my life. This thesis is a product of YOUR love, strength, and support.

TABLE OF CONTENTS

LIST OF TABLES

LIST OF FIGURES

LIST OF SYMBOLS AND ABBREVIATIONS

AAALAC	American Association for Accreditation of Laboratory Animal Care
Aero-HDM	Aerosolized house dust mite
Aero-Mch	Aerosolized methacholine
Aero-saline	Aerosolized saline
AHR	Airway hyperreactivity
AU/mL	Antigen units per milliliter
AUCGlucose	Area under the curve for glucose
AUCG	Area under the curve for glucose
AUCInsulin	Area under the curve for insulin
AUCI	Area under the curve for insulin
BAL	Bronchoalveolar lavage
BMICRL	Body mass index using crown-to-rump length
BW	Body weight
Cdyn	Dynamic lung compliance
CRL	Crown-to-rump length
DBP	Diastolic blood pressure
EAR	Early asthmatic response
ECU	East Carolina University
EH&S	Environmental Health and Safety
ELISA	Enzyme-linked immunoassay
FBG	Fasting blood glucose
FPI	Fasting plasma insulin
HDM	House dust mite antigen
HOMA-IR	Homeostatic model assessment for insulin resistance
HR	Heart rate
IACUC	Institutional Animal Care and Use Committee
IBC	Institutional Biosafety Committee
IR	Insulin resistance
IVGTT	Intravenous glucose tolerance test
KG	Glucose disapperance rate
LAR	Late asthmatic response
Mch	Methacholine
NHP	Nonhuman primate
NIH	National Institute of Health
PC100	Provocative concentration of methacholine that induces a 100% increase in R_L
PC40	Provocative concentration of methacholine that induces a 100% increase in C_{dyn}

PFT	Pulmonary function test
PNT	Pneumotachometer
QUICKI	Quantitative insulin sensitivity check
RL	Lung resistance
RM ANOVA	Repeated measures analysis of variance
RR	Respiratory rate
SBP	Systolic blood pressure
SpO2	Peripheral oxygen saturation
T2DM	Type 2 diabetes mellitus
TP	Time point
WBC	White blood cell
WC	Waist circumference

INTRODUCTION

Problem and Significance

Obesity and asthma continue to be significant global public health concerns, accounting for much of the mortality and morbidity worldwide (Abate et al., 2018; Mattiuzzi & Lippi, 2020). In the last two decades, novel insights regarding the relationship between these two disease states have been reported (Pite et al., 2020; Wu, T. D., 2021). Not only does evidence support the finding that obesity increases the prevalence of asthma, but it also significantly increases the severity of asthma (Miethe, Karsonova, Karaulov, & Renz, 2020; Tashiro & Shore, 2019). This relationship is so compelling that a new asthma phenotype was created to describe the unique phenomenon observed in obese asthmatics characterized by worse asthma exacerbations, increased hospitalization, and non-responsiveness to traditional asthma therapeutics (in particular inhaled corticosteroids) compared to lean asthma counterparts (Dixon & Poynter, 2016; Tashiro & Shore, 2019). Additionally, significant associations as well as molecular links have been reported between obesity-induced insulin resistance and allergic asthma (Bantulà, Roca-Ferrer, Arismendi, & Picado, 2021; Pite et al., 2020).

While considerable research of this multifactorial disease state has provided important insights, including the central, predominate role of inflammation linking obesity, insulin resistance (IR), and allergic asthma, the underlying, interacting molecular mechanisms involved are still relatively unknown (Wu, 2021). Understanding the complex etiology and interaction effect between these multifactorial pathologies is a necessity for proper management and treatment of the obese asthmatic subgroup and is even more critical with the increasing prevalence of obesity, Type 2 diabetes mellitus (T2DM), and asthma (Dixon & Holguin, 2019; Miethe et al., 2020; Wu, 2021).

To investigate the associations between obesity, IR and allergic asthma, we used a non-human primate (NHP) model to assess airway hyperreactivity (AHR) and associated changes in IR during a six-month study. The background, hypotheses, and the specific aims of the proposed research project will be presented first, followed by individual chapters presenting the methods, results, discussion, and overall conclusions of the study.

Background

Obesity, metabolic dysfunction and T2DM

Obesity is a common risk factor associated with multiple disease pathologies in various organ systems/tissues within the body(Defronzo, 2009; Hansen, B. C., 2014). In 2016, 650 million cases of obesity were reported globally(Mattiuzzi & Lippi, 2020). In the US, the prevalence rate is ~43%, while 30% of North Carolina residents are considered obese(Centers for disease control and prevention.national center for chronic disease prevention and health promotion, division of nutrition, physical activity, and obesity.data, trend and maps.; Hales, Carroll, Fryar, & Ogden,). One of the first identified chronic disease associated with obesity is Type 2 Diabetes Mellitus (T2DM), first manifested as insulin resistance (IR) (Defronzo, 2009; Wu, H. & Ballantyne, 2020). In 2017, ~463 million cases of T2DM were reported worldwide, with a ~11% prevalence rate in the US (National diabetes statistics report, 2020 | CDC.2020; Abate et al., 2018). T2DM is a chronic disease characterized by elevated blood glucose (hyperglycemia) coincident with insulin deficiency/insulin resistance (Defronzo, 2009; Wu, 2021). T2DM is the predominate consequence of insulin resistance in the tissue. Furthermore, a 33% prevalence rate has been reported for hyperinsulinemia, resulting from decreased insulin sensitivity, in the United States (Ioannou, Bryson, & Boyko, 2007; Kumar & O'Rahilly, 2005; Pound, Kievit, &

Grove, 2014). The underlying mechanisms associated with obesity, IR, and overt T2DM implicate a central commonality that links these three metabolic abnormalities – "metaflammation" (Periyalil, Gibson, & Wood, 2013a; Wu & Ballantyne, 2020).

Metaflammation - linking obesity-induced IR and T2DM

Obesity was first hypothesized as an inflammatory condition at the beginning of the 21st century (Das, 2001). Evidence over the past two decades supported this hypothesis leading to the currently accepted characterization of obesity as a systemic low-grade inflammatory state resulting from excessive macronutrients in adipose tissue (Fantuzzi, 2005; Hotamisligil, 2017; Periyalil, Gibson, & Wood, 2013b). In an obese state, inflamed adipocytes, produce pro-inflammatory cytokines resulting in systemic inflammation and oxidative stress (Ellulu, Patimah, Khaza'ai, Rahmat, & Abed, 2017; Fantuzzi, 2005; Husemoen et al., 2008; Periyalil et al., 2013; Wu & Ballantyne, 2020).

Insulin resistance (IR), a known sequalae of obesity, is the major contributing factor in the development of T2DM (Freeman & Pennings, 2021; Kumar & O'Rahilly, 2005). IR is first evident by the hypersecretion of insulin resulting in elevated insulin levels despite no changes or improvements in glucose clearance (Defronzo, 2009; Freeman & Pennings, 2021) . The development and manifestation of IR has been associated with obesity and type 1 inflammation of adipose tissues (Bantulà et al., 2021; Wu & Ballantyne, 2020). The obesity induced systemic state of low, yet chronic inflammation has been shown to cause defects in glucose tolerance and the development of IR (Wu & Ballantyne, 2020). Pro-inflammatory cytokines (TNF-α, IL-6, IL-1β) and adipokines (elevated leptin, reduced adiponectin) produced by excess adipose tissue in an obese state, have been implicated in the pathogenesis of IR (Bantulà et al., 2021; Kumar &

O'Rahilly, 2005; Pite et al., 2020; Wu & Ballantyne, 2020). Further investigation of the inflammatory mediated pathways linking obesity and IR is needed.

Obese asthma phenotype

As compared to lean asthmatics, obese asthmatics are generally characterized as having more severe symptoms, more frequent exacerbations, more frequent hospitalizations, poorer quality of life; and obese asthmatics are generally non- or less responsive to traditional controller medications (in particular, inhaled corticosteroids) than are lean asthmatics (Israel & Reddel, 2017; Peters, Dixon, & Forno, 2018; Shore, 2008; Tashiro & Shore, 2019). Within the obese asthma phenotype, there are two main subgroups: one is characterized by early-onset atopy/allergic asthma and high Th-2 inflammation; the other is characterized by late-onset non-allergic asthma with less airway hyperreactivity and obstruction, and less atopy (Bantulà et al., 2021; Gomez-Llorente, Romero, Chueca, Martinez-Cañavate, & Gomez-Llorente, 2017). These two phenotype subgroups describe already present allergic asthma complicated by obesity and asthma development due to obesity, respectively (Bantulà et al., 2021; Miethe et al., 2020; Tashiro & Shore, 2019).

An association between obesity and asthma was first observed/reported in a study of US nurses in 1999 (Camargo, Weiss, Zhang, Willett, & Speizer, 1999). Since then, possible links between obesity and asthma have been studied extensively (including studies of epidemiological data, the physiological mechanics of excess body mass on the lung, as well as studies of numerous molecular inflammatory biomarkers/mediators) (Dixon & Holguin, 2019; Haldar et al., 2008; Wu & Ballantyne, 2020). Not only does epidemiological and clinical evidence support the obese

asthma phenotype, metabolomics also supports obesity-associated asthma phenotype at the molecular level (Pite et al., 2020; Wu, 2021). However, a complete understanding of the cellular and inflammatory mechanisms associated with obese asthma is still unclear (Gomez-Llorente et al., 2017; Periyalil et al., 2013). Multiple studies suggest the etiology and pathophysiology of obesity-related asthma cannot be explained by obesity alone (Dixon & Rincón, 2016; Gomez-Llorente et al., 2017; Peters, Suratt, Bates, & Dixon, 2018; Sadeghimakki & McCarthy, 2019). Recently, insulin resistance, dyslipidemia, and hypertension, three major metabolic dysfunctions associated with obesity and T2DM, have been shown to be independently associated with asthma (Gomez-Llorente et al., 2017; Sadeghimakki & McCarthy, 2019; Serafino-Agrusa, Spatafora, & Scichilone, 2015). Being that T2DM is first manifested as insulin resistance, the relationship between obesity-induced IR and asthma is critical for understanding and treating the obese asthma phenotype (Dixon & Rincón, 2016; Wu, 2021).

Insulin resistance and asthma

An association between insulin resistance and asthma is supported in the literature (Kim et al., 2014; Singh, Prakash, Linneberg, & Agrawal, 2013). Insulin resistance/hyperinsulinemia was described as a predictor of incident asthma-like symptoms in adults, manifested as lower lung function, bronchial hyperresponsivity and lung remodeling (Bantulà et al., 2021; Forno, Erick, MD, MPH, Han, Muzumdar, & Celedón, Juan C., MD, DrPH, 2015; Kim et al., 2014; Singh et al., 2013). Collectively, a negative correlation between insulin resistance and lung function has been reported and, interestingly this correlation is independent of obesity and BMI (Cardet, Ash, Kusa, Camargo, & Israel, 2016; Husemoen et al., 2008; Sadeghimakki & McCarthy, 2019; Thuesen, Husemoen, Hersoug, Pisinger, & Linneberg, 2009) (Bantulà et al., 2021; Wu &

Ballantyne, 2020). TNF-alpha and IL-6 are two pro-inflammatory mediators implicated in the association of insulin resistance and asthma resulting in an IR-induced "switch" towards a Th1 immune response/inflammation. This suggests a possible mechanism in which insulin resistance contributes to the pathogenesis of severe asthma associated with obesity requiring further investigation (Miethe et al., 2020; Pite et al., 2020; Wu, 2021).

Taken together, the literature clearly demonstrates the association between obesity and asthma resulting in a more severe and difficult to treat phenotype (Israel & Reddel, 2017; Tashiro & Shore, 2019). While significant progress has been made uncovering the role of systemic inflammation in obesity-associated asthma, researchers have only scratched the surface investigating this increasingly complex and entangled interrelationship (Pite et al., 2020; Singh et al., 2013; Wu, 2021).

Preliminary data

In 2013, twenty young, naïve Rhesus macaques were sensitized by i.p. injection of house dust mite antigen (HDM) adsorbed to alum; airway sensitization and maintenance were accomplished by exposure to aerosolized HDM (aero-HDM) at 2-week intervals. Periodically, we assessed the late phase asthmatic response 24 hours after aero-HDM exposure: airway hyperreactivity was assessed by aerosolized methacholine challenge; pulmonary inflammation was assessed by bronchoalveolar lavage. Occasionally animals were also exposed to an experimental asthma therapeutic.

In 2018, ten animals had developed obesity and were suspected to harbor other clinical manifestations of obesity-induced metabolic dysfunction. Using archived frozen serum samples, we reconstructed the biochemical history of adiposity development and glucose metabolism – a

story that was evolving coincident with chronic exposures to Diet A, standard monkey chow, and aero-HDM. By age 10 years, four of the largest animals showed signs of insulin resistance and/or dyslipidemia development; one animal had hyperglycemia/diabetes by age 8 years – 4 to 6 years earlier than would be expected based on non-human primate literature.

In July 2019, six months after switching to lower carbohydrate/higher protein Diet B, and > 12 months since the last aero-HDM exposure: all animals lost weight coincident with larger animals resolving insulin resistance, dyslipidemia, and diabetes. Larger animals had higher pulmonary inflammation and higher airway hyperreactivity to aerosolized methacholine compared to smaller animals. These airway reactivity and inflammatory profiles resemble those of many humans who have obesity-related asthma, a phenotype that is less well understood and often difficult to treat due to underlying mechanisms that differ from those of other asthmatic phenotypes.

Chronic allergic asthma model in spontaneously obese nonhuman primates

Animal models of spontaneous obesity, IR, T2DM

Spontaneous obesity and T2DM has been reported in multiple species including nonhuman primates, dogs, and cats (Loeb & Quimby, 1989). Additionally, rodent models have been used to study obesity, insulin resistance, and T2DM using genetically modified knockout mice as well as experimentally induced obesity (Kumar & O'Rahilly, 2005; Loeb & Quimby, 1989; Younas et al., 2019). However, NHPs are regarded as the superior animal model for metabolic studies (Havel, Kievit, Comuzzie, & Bremer, 2017). More specifically, the amino acid structure of the insulin molecule is identical (all 22 amino acids) in rhesus macaques and humans(Peterson, Nehrlich, Oyer, & Steiner,). “NHPs differ significantly from laboratory rodents and are

metabolically more similar to humans in a number of characteristics, including the major site of de novo lipogenesis (liver vs. adipose tissue) and major classes of circulating lipoproteins and in the physiology of thermogenesis and insulin-meditated glucose utilization." (Havel et al., 2017). Insulin-mediated glucose utilization is the focus of the proposed investigation.

Animal models of asthma

A variety of animal models are used to study asthma including mice, rabbits, cats, dogs, sheep, horses and nonhuman primates. The nonhuman primate (NHP) model of chronic allergic asthma manifests characteristics remarkably similar to chronic allergic asthma of humans: genetic, anatomical and physiological similarities; lung structure, mechanics and inflammatory responses to allergens (Abee, Mansfield, Tardif, & Morris, 2012; AYANOGLU et al., 2011; Miller, Royer, Pinkerton, & Schelegle, 2017; Plopper & Hyde, 2008; Schelegle et al., 2001a; Van Scott et al., 2004).

Our unique NHP model mirrors the heterogeneity in human asthma and metabolic dysfunction (Havel et al., 2017; Miller et al., 2017; Plopper & Hyde, 2008). Like humans, our colony of NHPs are socialized, group-housed animals (*Laboratory animal medicine* 2015; Abee et al., 2012; Hansen, 2014; Hansen, Barbara C., 2012). The similarities between human and NHP anatomy, physiology, metabolism, and immunology are unmatched (Barbara C. Hansen & Xenia T. Tigno, 2007; Coffman & Hessel, 2005; Hansen, 2014; Havel et al., 2017; Liddie, Okamoto, Gromada, & Lawrence, 2019; Miller et al., 2017; Plopper & Hyde, 2008; Pound et al., 2014). Such a highly translatable disease model is ideally suited to study development, progression, physiological and immunological interactions, mechanistic insights for development of

combined treatment as well as identifying distinct biomarkers for diagnosis and early detection (Havel et al., 2017; Miller et al., 2017).

Exhaustive review of the literature returned only one publication addressing NHP adiposity and pulmonary function (Young, Skeans, Austin, & Chapman, 2003). Therefore, to our knowledge, our current chronic allergic and obese NHP model is unique and warrants further investigation, including the putative role of inflammation in the development of the obese asthma phenotype and associated insulin resistance and Type 2 diabetes.

Research purpose and specific aims

Inflammation, and especially inflammation associated with obesity, is thought to contribute to the progressive development of IR, and ultimately T2DM. Consistent with this hypothesis, we have shown that macaques sensitized to HDM show a broad range of sensitization (aka inflammation); and individual animals that displayed enhanced sensitization to aerosolized HDM were more likely to develop spontaneous obesity as well as insulin resistance (Woolard et al., 2020). After termination of aero-HDM exposure, all animals were placed on a "healthier diet", resulting in loss of some excessive weight and resolution of insulin resistance (and other manifestations of metabolic dysfunction) in affected animals.

Here we hypothesize that resuming chronic exposure to aero-HDM will induce chronic pulmonary inflammation that will synergize with obesity related inflammation to exacerbate the development of obesity-related insulin resistance – with the severity of IR correlated to the degree of aero-HDM sensitivity. To test this hypothesis, we paired macaques (N=5 pairs) according to historical airway hyperresponsiveness, then exposed one animal from each pair to aero-HDM, while the other animal was exposed to aerosolized saline/SHAM treatment, monthly

for 6 months. The primary outcomes were measures of abdominal obesity, glucose and insulin responses to IVGTT, and the related indices of insulin resistance and glucose tolerance. Secondary outcomes were measures of pulmonary function/AHR, and pulmonary inflammation as assessed by bronchoalveolar lavage.

Specific Aim 1

Assess the relationship between early asthmatic response (EAR) and development of IR in obese nonhuman primates.

We hypothesize that more robust EAR pulmonary function response will be associated with more severe insulin resistance.

Specific Aim 2

Assess the relationship between late asthmatic response (LAR) and development of IR in obese nonhuman primates.

We hypothesize that more robust LAR pulmonary function and inflammation response will be associated with more severe insulin resistance.

MATERIALS AND METHODS

All animal studies were conducted according to the National Institute of Health's (NIH) *Guide for the Care and Use of Laboratory Animals*. All research protocols were approved by East Carolina University's (ECU) Institutional Animal Care and Use Committee (IACUC), Institutional Biosafety Committee (IBC) and Environmental Health and Safety (EH&S).

Animals

In 2013, ten naïve, male, 3 to 5-year-old, US-bred (Mannheimer Foundation Inc., Homestead, FL) rhesus macaques (Macaca mulatta) arrived at East Carolina University. Animals were group-housed in ECU animal facilities according to AAALAC and IACUC guidelines. Upon arrival, eight animals were housed in stainless steel cages in groups of 3 to 5; over the years, three stable groups of 2 to 3 animals each were established. Exceptions were made on arrival and over the years for two individual animals to be single-housed as a result of extreme aggression towards or from other animals. Although physically separated, single-housed animals were housed in the same room with grouped animals- maintaining animal safety while still allowing indirect visual and social interaction with other animals. Animals had ad libitum access to water and were fed twice daily with standard monkey chow LabDiet® 5038 (18% Protein, 13% Fat, 69% Carbohydrate; LabDiet®, St. Louis, MO), supplemented once daily with enrichment usually consisting of fruits/vegetables.

Experimental design

Defining relative airway hyperresponsivity, AHR rank. A relative index of aero-HDM-sensitivity was determined using historical pulmonary function test (PFT) data for each of the ten prospective study animals. This index was given the name "AHR rank" and was defined using the following six parameters: maximum provocative dose of aero-HDM (AU/mL), aero-HDM delivery time (minutes), maximum ΔR_L (change expressed relative to aero-saline response, % saline), maximum ΔC_{dyn} (% saline), maximum ΔRR (% saline), and minimum SpO_2. The criteria for ranking each of these parameters are listed in Table 1.

Table 1. Parameters and criteria for defining "AHR rank"

AHR rank	Max Provocative [HDM] (AU/mL)	Delivery time (min)	Max ΔR_L (% saline)	Min ΔC_{dyn} (% saline)	Max ΔRR (% saline)	Min SpO_2 (%)
1	1	1	>90%	<-40%	>150%	<75
2	10	2	65-89%	-30 to -39%	100-149%	75-79
3	100	3	40-64%	-20 to -29%	50-99%	80-84
4	500	4	15-39%	-10 to -19%	25-49%	85-89
5	2500	6	<15%	>-10%	<25%	>90

The six pulmonary function parameters were determined for each PFT day and then assigned a rank from 1 to 5 using the criteria outlined in Table 1. An overall average AHR rank was then determined for each animal. Table 2 shows individual animals average rank for the six parameters and the overall average AHR rank. Animals were then matched/paired according to overall AHR rank, with pairs being made on similar/closeness of the AHR rank- pairs included

S235 and T199, T215 and 09-04, S88 and T103, T91 and T10, and S35 and T159. Pairs were then randomly assigned to aero-HDM or SHAM exposure groups.

Table 2. Average AHR rank and overall average AHR rank for ten study animals

	Average AHR rank						
Animal ID	**Max [HDM] (AU/mL)**	**Delivery (min)**	**Max ΔR_L (% saline)**	**Min ΔC_{dyn} (% saline)**	**Max ΔRR (% saline)**	**Min SpO_2 (%)**	**Overall AHR rank**
S235	3.0	2.0	1.5	1.1	1.2	1.0	**1.6**
T199	3.0	3.1	1.5	1.0	1.0	1.2	**1.8**
T215	3.9	2.8	1.5	1.0	1.0	1.0	**1.9**
09-04	5.0	4.1	2.2	1.0	1.4	1.3	**2.48**
S88	4.9	3.8	3.2	1.0	1.0	1.1	**2.50**
T103	5.0	4.0	4.2	1.5	1.0	2.5	**3.0**
T91	4.9	4.0	4.8	1.3	1.1	3.0	**3.2**
T10	5.0	4.0	4.5	2.5	1.4	2.9	**3.4**
S35	4.8	4.0	4.3	2.7	2.1	4.5	**3.7**
T159	4.8	4.1	4.8	4.7	4.4	4.8	**4.6**

Prior to initiating exposures, one animal that was assigned to the SHAM group was withdrawn from the study for health reasons. The HDM-exposed group (N=5) received monthly exposures to aerosolized-HDM; the SHAM-exposed group (now N=4) received aerosolized-saline/SHAM (Figure 1).

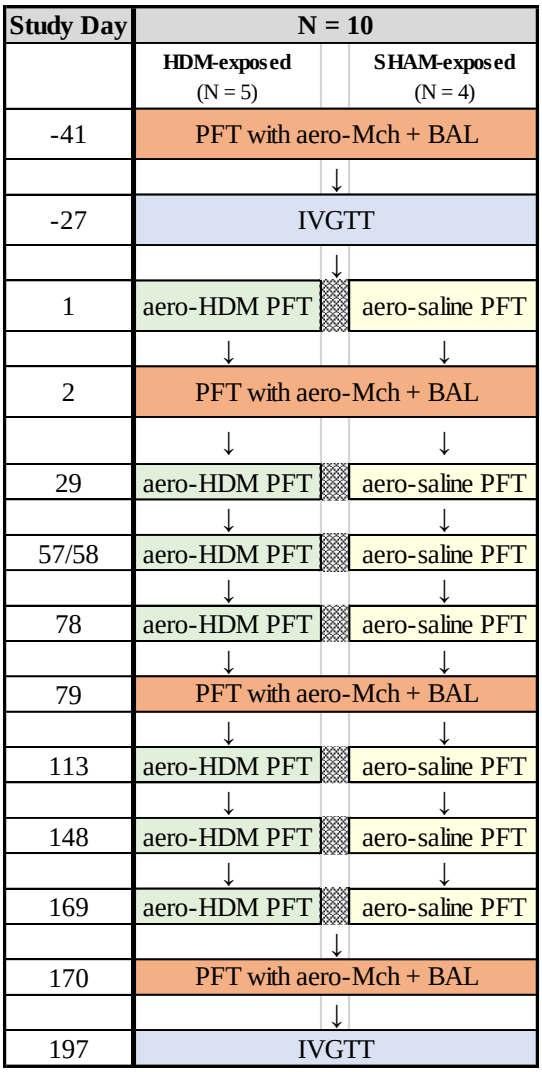

Figure 1. Experimental study protocol timeline of events

Prior to Day -41/Pre-HDM baseline, ten male rhesus macaques were paired according to historical aero-HDM sensitivity using overall AHR rank. Then, one animal of each pair was randomly assigned to receive monthly aero-HDM exposures, and the other animal of each pair was assigned to receive monthly aero-saline/SHAM exposure. On Day -41/Pre-HDM baseline, Six weeks before initiating monthly aero-HDM/SHAM exposures, pulmonary function was assessed to determine non-specific AHR to aero-Mch and pulmonary inflammation was assessed via BAL. Note, one animal that was assigned to the SHAM group was withdrawn from the study for health reasons before Day 1, the first monthly exposure. On Day -27, four weeks before beginning aero-HDM/SHAM exposures, glucose tolerance and insulin resistance were assessed via intravenous glucose tolerance test. Beginning Day 1, HDM-exposed animals (N=5) received monthly exposures to aerosolized-HDM; SHAM-exposed animals (now N=4) received aerosolized-saline/SHAM (Figure 1). After the first, fourth, and seventh exposure, aero-Mch PFT and BAL were conducted 24-hours after aero-HDM/SHAM exposures on Days 2, 79, and 170.

Methodology

Measurements of body composition

Body weight (BW, in kg) and waist circumference (WC, in cm) were measured for all study time points. WC was measured using a non-elastic sewing tape, perpendicular to the spine and at the level of the umbilicus, with the animal positioned in left lateral[61]mbency (Kemnitz & Francken, 1986; Raman et al., 2005). Body mass index for the rhesus macaques (BMI_{CRL}, in kg/m^2) was determined by replacing height in the human BMI calculation with the animal's crown-to-rump length (CRL). CRL was measured for each animal (with the exception of S35) at Days -27 and 1 using a shore-board, "a calibrated ruler with a fixed headrest" with the animal in supine position (Hansen, 2014; Raman et al., 2005). The measured CRL, recorded in cm, was converted to m for the following calculation:

$$BMI_{CRL} = \text{Body weight (in kilograms)}/\text{CRL (in m)}^2$$

Obesity was defined by the following criteria:

1. Body weight >15 kg. (Hansen, 2014)
2. Waist circumference ≥ 40 cm. (XIUQIN ZHANG et al., 2011)
3. BMI ≥ 40 kg/m^2. (Kemnitz & Francken, 1986)

Intravenous glucose tolerance test (IVGTT)

This IVGTT protocol was adapted from protocols previously described (Bremer et al., 2011; Hansen, Barbara C., 2004; Staup, Aoyagi, Bayless, Wang, & Chng, 2016a). Animals were fasted for 16-18 hours overnight. On the day of the procedure, anesthesia was induced with Telazol® (4-6 mg/kg, i.m.) and maintained with additional Telazol® (up to 2 mg/kg, i.m.) if needed. Depth of sedation and vitals (HR, SpO_2, SBP, DBP; CARDELL Veterinary Vital Signs Monitor Model

9403) were recorded throughout the procedure. Following Telazol® induction, animals were instrumented with two saline/heparin-lock equipped intravenous catheters in separate limbs: one catheter was used for drawing blood, the other catheter was used for dextrose administration only. Catheter patency was maintained by periodic flushes with heparinized saline (0.06 mg/kg); blood sample integrity was maintained by discarding the first 0.5 ml of blood withdrawn with each collection. Blood was taken 5 minutes before (TP=-5) and immediately before (TP=0) a 50% dextrose bolus (250 mg/kg) was delivered over 30 seconds. Blood was collected at 3, 5, 7, 10, 15, 20, & 30 minutes after the completion of the dextrose administration. Blood glucose measurements were taken in duplicate using the same model of blood glucometer (Presto AgaMatrix Pro) immediately after each draw. The remaining collected blood (~1.5 mL) was transferred to a 3 mL Lithium Heparin blood collection tube and then placed on ice until processing for insulin. Blood tubes were centrifuged and two aliquots of 0.5 mL plasma per timepoint were collected, frozen and stored at -80 °C for later insulin assay. Duplicate blood glucose values were averaged for all time points. Plasma samples were analyzed for insulin values using ELISA assay technique (Mercodia Insulin ELISA assay, cat no. 10-1113-10; Mercodia Inc. Winston[57,67]m, NC) (Liddie et al., 2019; Wang, Xueqian et al., 2015). Outcome measurements included blood glucose (mg/dL) and plasma insulin (mU/L) for each of the nine timepoints over the course of the 30-minute glucose tolerance test. Fasting blood glucose (FBG; mg/dL) and fasting plasma insulin (FPI; mU/L) were determined as the concentrations of blood glucose and plasma taken at 0 minutes (immediately before administering the bolus of dextrose).

Calculated indexes of insulin sensitivity included 1/FPI, the homeostatic model assessment for insulin resistance (HOMA-IR) and quantitative insulin sensitivity check (QUICKI). HOMA-IR

was calculated using fasting blood glucose (mg/dL) and fasting plasma insulin (mU/L) and the following formula (Bremer et al., 2011; Lee et al., 2011):

$$\text{HOMA-IR} = [\text{FBG} * \text{FPI}]/405$$

QUICKI, a surrogate index of insulin sensitivity, was calculated using FBG (mg/dL) and FPI (mU/L) and the following formula (Lee et al., 2011):

$$\text{QUICKI} = 1 / [\log (\text{FPI}) + \log (\text{FBG})]$$

Calculated indexes of glucose tolerance included the glucose clearance rate (K_G), and area under the curves for glucose ($AUC_{Glucose}$) and insulin ($AUC_{Insulin}$). K_G is calculated by the slope of a linear trend of best fit of the natural logarithm of the blood glucose concentrations at time points 3, 5, 7, 10, 15, 20, 30 (Jen & Hansen, 1988; Lundbaek, 1962). K_G was calculated using the least square method with the Microsoft Excel formula: =LINEST (LN(blood glucose in mg/dL at each TP from 3-30 minutes), 3, 5, 7, 10, 15, 20, 30 min) (Wang et al., 2015). Area under the curve for glucose and insulin was calculated using the trapezoid method (GraphPad Prism) (Bremer et al., 2011; Wang et al., 2015).

Assessment of pulmonary function and inflammation

This pulmonary function testing (PFT) protocol was adapted from protocols previously described (Schelegle et al., 2001b; Van Scott, Reece, Olmstead, Wardle, & Rosenbaum, 2013; Van Scott et al., 2004; Van Scott, Aycock, Cozzi, Salleng, & Stallings, 2005; Wang, Xiaojia, Reece, Olmstead, Wardle, & Van Scott, 2010). Animals were anesthetized with Telazol® (4-6 mg/kg, i.m.), weighed, instrumented with a 22 G catheter for blood withdrawal and intravenous drug

administration, then moved to a heated table with tubing set up for PFT and intratracheal aerosol administration. Depth of sedation and vitals (HR, SpO_2, SBP, DBP) were recorded throughout the procedure. A bolus of propofol (Propoflo®; 2 to 3 mg/kg, i.v., delivered at 2 mL/min) was given immediately before intubating the animal with an uncuffed endotracheal tube; an esophageal balloon was advanced into the abdomen via a long catheter, the other end of which extended outside the oral cavity. Thereafter, a light plain of anesthesia (less than surgical) was maintained with a constant intravenous infusion of Propofol (based on animal's body weight, ~0.125 to 0.200 mg/kg/min, as well as on anesthesia history). Propofol administration was generally the same on each study day for individual animals, only minor adjustments as needed to maintain a consistent relative state of sedation. Following intubation, the endotracheal tube was connected to the PFT tubing system/circuit containing an in-line nebulizer (AeroNeb Lab Nebulizer Unit #AG-AL100, Aerogen Ltd., Galway, Ireland) upstream for aerosol administration and containing an in-line pneumotachometer (Hans Rudolph Inc., Shawnee, KS) downstream for measurement of pulmonary airflow; the esophageal balloon catheter was connected to a pressure transducer for measurement of (transpulmonary) pressure. The pneumotachometer (PNT) and pressure transducer were electrically integrated with a computerized system designed by EMKA Technologies (Paris, France) that uses iox 2 software and conventional pressure-flow analyses to determine breath-by-breath indexes of pulmonary function. After connecting the animal to PFT tubing system, the esophageal balloon was repositioned from the abdomen into the mid-thorax so as to optimize changes in transpulmonary pressure and yield near historical baseline measurements of pulmonary function indexes. After the esophageal balloon position was secured, the aerosol exposure and PFT protocol was initiated.

After the esophageal balloon was secured, vitals were manually recorded into a computerized animal database while iox recorded "Baseline" measurements of pulmonary airflow and esophageal/transpulmonary pressure for 1 minute. The EMKA iox software is integrated with Excel to provide breath by breath readouts of pulmonary function indexes for the entire minute recording, which are then averaged, and the average stored in the animal database next to associated vitals. Following the "Baseline" recording, saline was aerosolized for 4 or 2 minutes, respectively, followed by recording vitals and pulmonary function indexes; followed by specific incremental doses of aerosolized HDM or Mch, each followed by recording associated vitals and pulmonary function indexes.

Pulmonary function indexes derived from iox 2 software and conventional pressure-flow analyses included lung resistance (R_L in cm H_2O/L/sec), dynamic lung compliance (C_{dyn} in mL/cm H_2O), respiratory rate (RR; breaths/minute), tidal volume (mL), minute volume (mL); associated vitals included peripheral oxygen saturation (SpO_2; %), heart rate (HR; bpm), systolic blood pressure (SBP; mmHg), and diastolic blood pressure (DBP; mmHg). Calculated measurements include maximum HDM- or Mch- induced changes in pulmonary function indexes (maximum ΔR_L, maximum ΔC_{dyn}, maximum ΔRR) expressed as a percentage of the daily baseline response to aerosolized saline (% saline); these values were recorded with the associated minimum SpO_2 induced by the aerosol challenge.

Early Asthmatic Response (EAR): Aerosolized-HDM/saline airway challenge and PFT

Greer Allergenic Extract Mite Mix (Standardized D. pteronyssinus/D. farina; 5000 AU/mL each) was diluted with sterile saline (1:10,000, 1:1,000, 1:100, 1:20, 1:4) resulting in daily working

HDM concentrations of 1, 10, 100, 500, 2500 AU/mL. Following the "Baseline" PFT indexes recording, aerosolized saline was delivered for 4 minutes; after quickly aspirating any droplets adhering to the inner surface of the endotracheal tube, PFT indexes and vitals were recorded for 1 minute. Following aero-saline, a series of three consecutive increasing concentrations of HDM were delivered to the aero-HDM exposure group. Each aero-HDM delivery was administered for 4 minutes (except some animals with great HDM sensitivity only received 2 minutes of the highest concentration of HDM) and followed by 1 minute recording of PFT and vitals. Increasing concentrations of HDM were delivered until reaching either 2500 AU/mL (less sensitive animals) or a concentration that induced the following criteria: 100% increase in lung resistance (% relative to the daily aero-saline induced baseline value), 40% decrease in dynamic lung compliance, and/or a $SpO_2 \leq 70\%$ (the latter prompts switching from a biased flow of inhaled medical air to inhaled 100% O_2). After administering the highest concentration of HDM, PFT indexes and vitals were recorded beginning one minute after ending HDM delivery, and at 10- and 15-minutes from the beginning of HDM delivery (provided that the animals were not too compromised from the challenge, i.e., SpO_2 was increasing appropriately after switching to inhaled 100% oxygen). After completing the HDM exposure arm of the protocol, all animals were administered aerosolized albuterol sulfate (0.083%) for 4 minutes to relieve bronchoconstriction, followed by a one minute PFT index and vitals recording.

For SHAM-exposed animals receiving aerosolized saline, a similar aerosolization protocol was designed to mirror the HDM exposures. Following baseline recording, animals were administered 4 minutes of aerosolized saline as per HDM-exposed group. Pulmonary function was measured for 1 minute following aerosolization. Next, a series of 3 separate saline deliveries

were administered for 4 minutes each followed by 1 minute recording. To mirror the HDM-exposed group's protocol, PFT indexes and vitals were also recorded at 10- and 15-minutes from the beginning of the final saline delivery. Finally, all animals were administered aerosolized albuterol sulfate (0.083%) for 4 minutes, followed by a one-minute PFT index and vitals recording.

In addition to the measured outcomes and calculated measurements described for the general assessment of pulmonary function, additional calculated measurements were determined specifically for the EAR aero-HDM/saline PFT protocol. In particular, the maximum provocative concentration of HDM was calculated as the concentration of HDM antigen in AU/mL that induced a 100% increase in R_L, 40% decrease in C_{dyn}, or a decline in arterial oxygen saturation (SpO_2) assessed by pulse oximetry to < 70% (AYANOGLU et al., 2011). The maximum provocative concentration of HDM provides the degree of HDM sensitivity for each animal in the HDM-exposed group (i.e. a highly sensitive animal such as S235 had a maximum provocative concentration of 100 AU/mL HDM; a less sensitive animal such as S35 had a maximum provocative concentration of 2500 AU/mL).

Late Asthmatic Response (LAR): Aerosolized-methacholine airway challenge and PFT

This protocol was based on protocols previously established. (AYANOGLU et al., 2011; Van Scott et al., 2004; Van Scott et al., 2005; Wang et al., 2010) Non-specific airway hyperreactivity was assessed by measuring pulmonary function following aerosolized administration of an airway smooth muscle muscarinic receptor agonist, methacholine (A2251, Sigma-Aldrich, St. Louis, MO). Serial dilutions of a 10.24 mg/ml stock solution yielded daily working

concentrations of 0.001, 0.01, 0.02, 0.04, 0.08, 0.16, 0.32, 0.64, 1.28, 2.56, 5.12, 10.24 mg/mL methacholine (Mch). Aerosolized methacholine (aero-Mch) challenges were conducted: once several weeks before initiating aero-HDM exposures (pre-treatment baseline); and 24 hours after the first, fourth and seventh monthly aero-HDM/saline exposures to assess the late asthmatic response. After recording daily baseline and aero-saline PFT indexes and vitals, incremental doubling doses of aero-Mch were administrated until a set of respiratory parameters were met: 100% increase in lung resistance (R_L; % relative to the daily aero-saline induced baseline value), 40% decrease in dynamic lung compliance (C_{dyn}), or inability to maintain SpO_2 above 70% while breathing 100% oxygen. Once these parameters were met, all animals were administered aerosolized albuterol sulfate (0.083%) for 4 minutes to relieve bronchoconstriction, followed by a one minute PFT index and vitals recording.

In addition to the measured outcomes and calculated measurements described for the general assessment of pulmonary function, additional calculated measurements were determined specifically for the LAR aero-Mch PFT protocol: PC_{100} was defined as the provocative concentration of Mch that induced a 100% increase in R_L; and PC_{40} was defined as the provocative concentration of Mch that induced a 40% decrease in C_{dyn} (AYANOGLU et al., 2011).

Late Asthmatic Response (LAR): Bronchoalveolar lavage (BAL)

Using previously described methods (AYANOGLU et al., 2011; Schelegle et al., 2001; Van Scott et al., 2004; Van Scott et al., 2005; Wang et al., 2010), pulmonary inflammation was assessed by a bronchoalveolar lavage (BAL) conducted: once several weeks before initiating

aero-HDM exposures (immediately after the pre-treatment baseline Mch challenge); and immediately after Mch challenges 24 hours after the first, fourth and seventh monthly aero-HDM/saline exposures. Immediately before the "blind" BAL procedure (not guided by use of a bronchoscope), animals received a bolus of propofol (2-3 mg/kg, i.v.) and inhaled air flooded 100% O_2. A lubricated, flexible Tygon tubing (O.D. 2.5 mm) was advanced through the endotracheal tube into the lungs where it was wedged into a peripheral lung compartment. After wedging, 10 mL of sterile saline was instilled followed by 2 mL of air to flush the tubing completely; gentle aspiration was then applied to collect the lavage fluid from the lungs into a 15 mL conical tube. The amount of BAL fluid recovered was recorded in the animal database. Total WBC cell counts were determined using a Coulter Counter (Beckman Coulter Instruments, Miami, FL). Four microscope slides were prepared for each animal via Cytospin 2 (Catalogue #: 59900102; Shandon Southern Products Ltd., Astmoor, England) and stained with Hema 3 (Item #: 22122911; Fisher Scientific, Suwanee, GA). Differential cell counts (lymphocytes, eosinophils, neutrophils, macrophages, and epithelial cells) were conducted using a Leica DM4000B Microscope (Type: DFC420C, 12 V/600 mA; Leica Microsystems Inc., Buffalo Grove, IL), counting 100 cells per slide. Cell counts from the four slides for each animal were then averaged to calculate % cells and actual/total number of cells.

Outcome measurements of pulmonary inflammation included % lymphocytes, eosinophils, neutrophils, macrophages, and epithelial cells, averaged from four duplicate slides with 100 cells counted per slide. Calculated estimates of total number of lymphocytes, eosinophils, neutrophils, macrophages, and epithelial cells was achieved by multiplying the average % cells for each cell type by the total WBC count ($x10^6$ cells) determined on the day of BAL via Coulter Counter, and

assuming recovery of all 10 mL of the instilled saline. Recovered WBC ($x10^6$ cells) was also calculated by multiplying the total WBC ($x10^6$ cells) by the actual volume of BAL fluid (mL) recovered.

Statistical analysis

Data are presented as mean ± standard deviation unless otherwise indicated. Figures with average percent baseline (normalized data) were normalized to baseline measurements. The effects of monthly aero-HDM challenges on body composition, IR, pulmonary function and pulmonary inflammation were tested by comparing the SHAM-exposed (N = 4) and HDM-exposed (N = 5) groups with each other and over the course of the study using two-factor analysis of variance (ANOVA) with repeated measures (RM). For each two-factor RM ANOVA conducted, the main effects and interaction effect was evaluated. When appropriate, post-hoc tests were conducted to establish differences between groups as well as at specific study day/time points. All statistical analyses were performed using SPSS software (IBM SPSS Statistics, Armonk, NY). A $p<0.05$ was considered statistically significant.

RESULTS

Introduction

In order to assess responses to glucose challenges and pulmonary function and inflammation in SHAM and aerosolized house dust mite exposed non-human primates. These experiments were performed over a period of 6 months during which 7 monthly aero-HDM/sham challenges were conducted. This chapter will first present body composition data of these animals measured prior to each experimental exposure, we will then present data obtained from an intravenous glucose tolerance test before and after the 6-month period, followed by pulmonary function and inflammation data collected over the period of experimental treatment exposures.

Body composition

Body composition was used to characterize and determine obesity in the nine study animals. In addition, changes in body composition were assessed and evaluated for associated changes in insulin resistance, AHR, and pulmonary inflammation during seven monthly aero-HDM/SHAM exposures. The body composition data collected during the study include body weight, waist circumference and BMI_{CRL}.

Body weight

Body weight was measured prior to each experimental procedure (Figure 2, Panel A). At Day -41, the average body weight for HDM-exposed animals (18.2±1.9 kg) was ~ 3 kg greater than in SHAM-exposed animals (15.6±0.7 kg). The average body weight for SHAM-exposed group did not significantly change over time (Figure 2**,** Panel B). HDM-exposed animals showed a trend for a decrease in average body weight over the study (Figure 2**,** Panel C). The average body

weight for the HDM-exposed group on Day 169 was 17.6±1.7 kg, a 3% decrease from Day -41 (Figure 2**,** Panel B): in particular, two HDM-exposed animals identified as Animal ID S35 and S235, had a 7% and 5% decrease in body weight, respectively, on Day 169 relative to Day -41 (Figure 2**,** Panel A). Two-factor ANOVA with repeated measures did not show statistically significant main effects for time or group and no interaction effect.

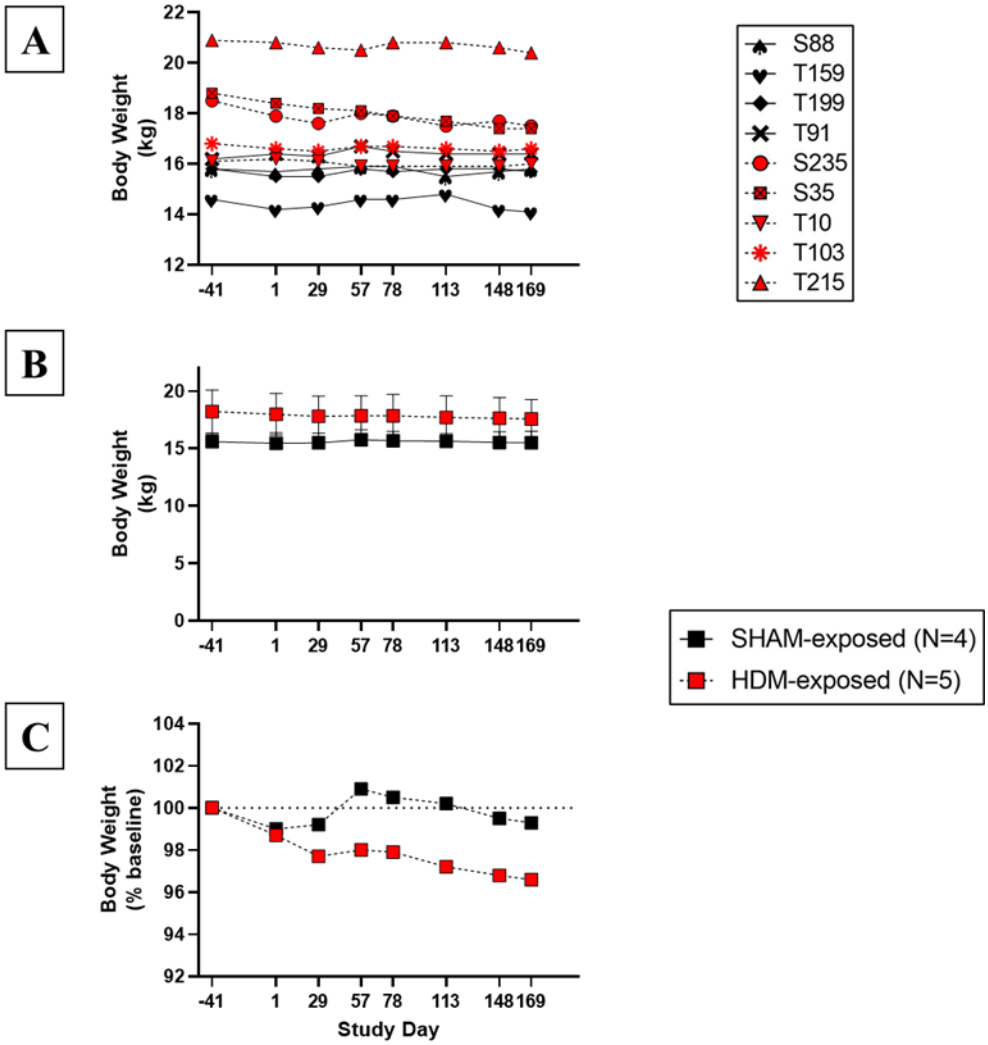

Figure 2. Raw and normalized changes in body weight (BW)

Body weight (kg) was measured at Day -41/Pre-HDM Baseline and before each monthly experimental exposure to aero-HDM/SHAM. (**A**) Raw measured body weight at each study day for all nine study animals: SHAM-exposed animals (n=4) shown in black with a solid line and HDM-exposed animals (n=5) in red with a dashed line. (**B**) The average body weight for SHAM and HDM-exposed animals (group mean ± SD). (**C**) Normalized body weight (to Day -41/Pre-HDM baseline) for both exposure groups. Normalized data is expressed as group mean ± SD for SHAM (red square; solid line) and HDM-exposed (black square; dashed line) groups. Two-factor ANOVA with repeated measures did not show statistically significant main effects for time or group and no interaction effect.

Waist circumference

In addition to body weight, waist circumference was measured at each study day for both exposure groups (Figure 3**,** Panel A). At Day -41, HDM-exposed animals average waist circumference (68.7±5.9 cm) was 9.0 cm larger than SHAM-exposed controls (59.7±5.4 cm). From Day -41 to 169, no change in average WC was observed for HDM-exposed animals and, although not statistically significant, a relative 4% increase was observed for SHAM animals (Figure 3**,** Panel C). Average waist circumference for HDM-exposed animals was significantly higher compared to the SHAM group on Day -41 ($p=0.049$), Day 1 ($p=0.014$), Day 57 ($p=0.043$), Day 78 ($p=0.042$) and Day 169 ($p=0.049$), represented as * in Figure 3**,** Panel B.

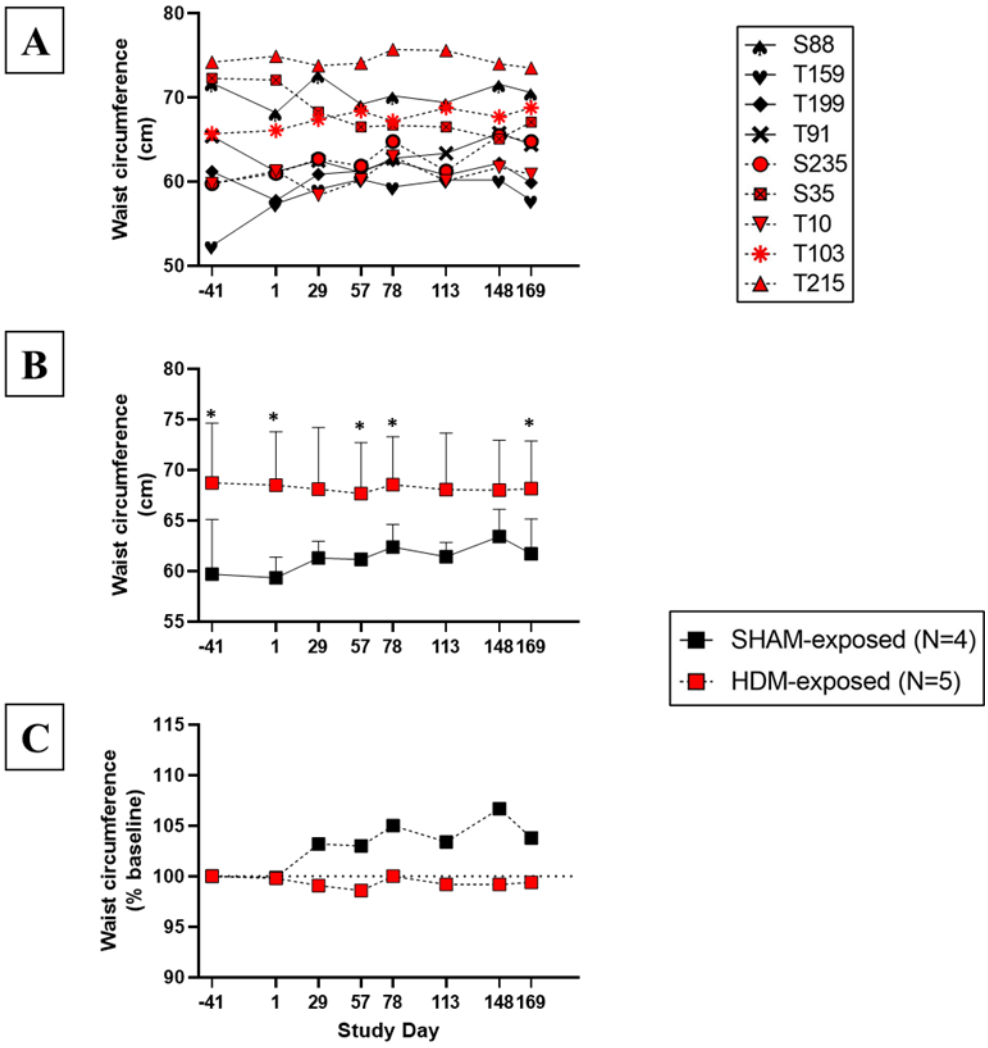

Figure 3. Raw and normalized changes in waist circumference (WC)

Waist circumference (cm) was measured at Day -41/Pre-HDM Baseline and before each monthly experimental exposure to aero-HDM/SHAM. (**A**) Raw measured waist circumference at each study day for all nine study animals: SHAM-exposed animals (n=4) shown in black with a solid line and HDM-exposed animals (n=5) in red with a dashed line. (**B**) The average WC for SHAM and HDM-exposed animals (group mean ± SD). (**C**) Normalized WC (to Day -41/Pre-HDM baseline) for both exposure groups. Normalized data is expressed as group mean ± SD for SHAM (red square; solid line) and HDM-exposed (black square; dashed line) groups. Two-factor ANOVA with repeated measures showed statistically significant main effects for HDM-exposed group ($p<0.05$), no main effects for time and no interaction effect. Two-sample t-test determined statistically significant group differences at Days -41, 1, 57, 78, and 169 ($p<0.05$=*).

BMI_{CRL}

Crown-to-rump length (CRL) was measured on Day -41 and Day 1, before beginning monthly experimental exposures for SHAM and HDM-exposed animals (except for Animal S35 on Day -41). Using CRL (measured in cm; converted to meters), body mass index for rhesus macaques (BMI_{CRL} in kg/m^2) was calculated for each study animal (Figure 4**,** Panel A).

The BMI_{CRL} range on Day -41 and Day 1 for all nine study animals was 42.8-58.7 kg/m^2 and 43.5-60.3 kg/m^2, respectively; for both days, HDM-exposed animal, T215, had the largest BMI_{CRL} and SHAM-exposed animal, T159, had the lowest (Figure 4**,** Panel A). For both Days -41 and 1, the average BMI_{CRL} for HDM-exposed animals was greater than controls; average BMI_{CRL} was ~12.7 kg/m^2 greater in HDM-exposed animals compared to than SHAM (Figure 4**,** Panel B).

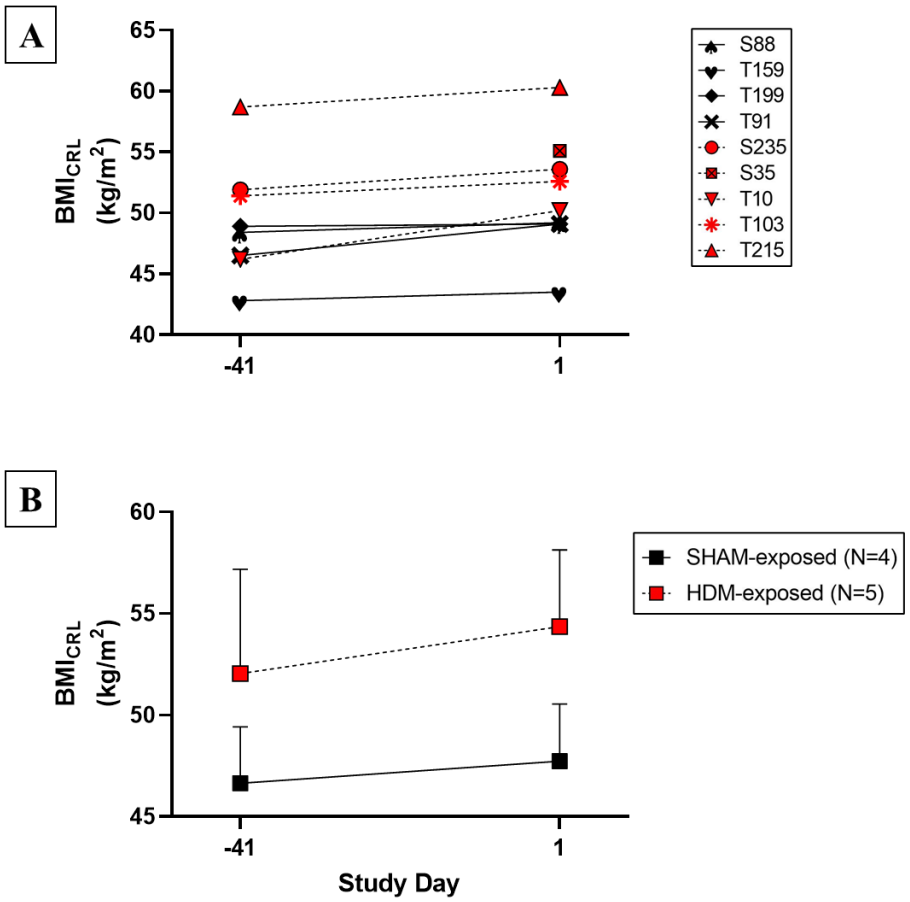

Figure 4. Raw BMI_{CRL} measured at Day -41 and Day 1

Crown-to-rump length CRL was measured for each animal at Day -41/Pre-HDM Baseline and Day 1, with the exception of Animal S35 on Day -41. Using CRL (measured in cm; converted to meters), body mass index for rhesus macaques (BMI_{CRL} in kg/m^2) was calculated. (**A**) Calculated BMI_{CRL} for all nine study animals: SHAM-exposed animals (n=4) shown in black with a solid line and HDM-exposed animals (n=5) in red with a dashed line. (**B**) The average BMI_{CRL} for SHAM and HDM-exposed animals (n=4 for Day -41) (group mean ± SD) for SHAM (red square; solid line) and HDM-exposed (black square; dashed line) groups. Two-factor ANOVA with repeated measures did not show statistically significant main effects for time or group and no interaction effect.

Fasting glucose and insulin concentrations, insulin resistance and glucose tolerance

The objective of Aim 1 was to assess changes in insulin resistance and glucose tolerance before and after monthly aero-HDM/SHAM exposures over six months. This was done by conducting two 30-minute intravenous glucose tolerance tests (on Days -27 and Day 197), measuring changes in glucose and insulin levels before, and in response to, a bolus of 50% dextrose (250 mg/kg). Glucose response data are presented first, followed by coincident insulin responses.

Glucose response during IVGTT

A 30-minute intravenous glucose tolerance test was conducted at Day -27 (before initiation of the first aero-HDM/saline airway challenge, i.e., pre-treatment) and at Day 197 (about one month after completing the last/seventh airway challenge, i.e., post-treatment). Average glucose responses at nine timepoints were determined (Table 3 and Figure 5). Average glucose responses were very similar between groups (Table 3) and were roughly the same before and after treatment, with the exception of a slightly lower average glucose value at the -5 timepoint for HDM-exposed animals at Day 197 (Figure 5). Two-factor ANOVA with repeated measures showed statistically significant main effects for time ($p<0.05$), no main effects for treatment and no interaction effect.

Table 3. Glucose responses during IVGTT at Day -27 and Day 197

Plasma Glucose (mg/mL)					
SHAM-exposed (N = 4)			HDM-exposed (N = 5)		
Time (min)	**Day -27**	**Day 197**	**Time (min)**	**Day -27**	**Day 197**
-5	73	73	-5	73	67
0	68	69	0	68	65
3	202	210	3	206	202
5	183	194	5	190	189
7	179	181	7	182	174
10	167	171	10	169	168
15	152	155	15	154	146
20	132	139	20	131	133
30	104	111	30	107	103

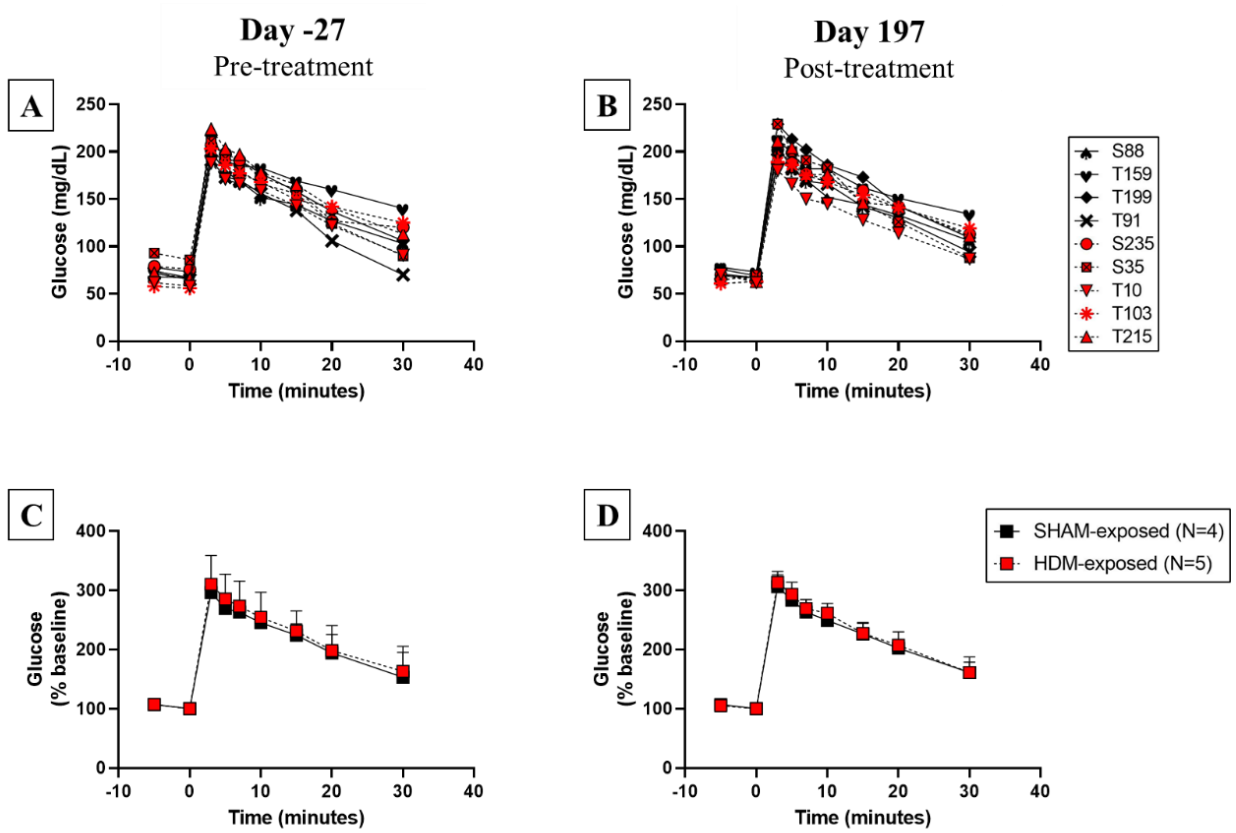

Figure 5. Raw and normalized blood glucose during IVGTT at Day -27 and Day 197

Panels (A) and (B), respectively, illustrate the raw glucose responses pre-treatment and post-treatment for individual animals. Panels (C) and (D) illustrate the normalized glucose responses (% relative to baseline=glucose value at TP=0 minutes), expressed as group averages (mean ± SD). SHAM-exposed animals (N=4) are shown in black symbols with a solid line; HDM-exposed animals (N=5) are shown in red symbols with a dashed line. Two-factor ANOVA with repeated measures showed statistically significant main effects for time ($p<0.05$), no main effects for treatment and no interaction effect.

Insulin response during IVGTT

Insulin responses were highly variable among individual animals within each exposure group (Figure 6**,** Figure 7). Average insulin responses at nine timepoints were determined (Table 4). Unlike glucose, insulin responses showed different trends between groups, and before and after treatment. At Day -27 baseline, insulin values measured at the first (TP=-5 min) and last timepoints (TP=30 min) were higher in HDM-exposed animals (52 and 116 mU/L, respectively) compared to SHAM (29 and 94 mU/L). Additionally, maximum insulin values were the same for both exposure groups but peaked much sooner for the HDM-exposed animals (272 mU/L at 3 min from the end of dextrose infusion) than for SHAM (271 mU/L at 10 min). At Day 197, fasting plasma insulin immediately before dextrose infusion for SHAM-exposed animals (19 mU/L at 0 min) was 32% lower than before treatment; the maximum insulin response for SHAM-exposed animals (211 mU/L at 10 min) was 22% lower than before treatment. Differences in average insulin responses from Day -27 to 197 were also observed for the HDM-exposed animals. At Day 197, fasting plasma insulin 5 min before and immediately before dextrose infusion (29 and 28 mU/L, respectively) were 44% and 22% lower than before treatment; the maximum insulin response (250 mU/L at 10 min) was only 9% lower than before treatment (Figure 6**,** Figure 7). Two-factor ANOVA with repeated measures showed statistically significant main effects for time ($p<0.05$), no main effects for treatment and no interaction effect.

Table 4. Insulin responses during 30-minute IVGTT at Day -27 and Day 197

Plasma Insulin (mU/L)					
SHAM-exposed (N = 4)			HDM-exposed (N = 5)		
Time (min)	**Day -27**	**Day 197**	**Time (min)**	**Day -27**	**Day 197**
-5	29	26	-5	52	29
0	28	19	0	36	28
3	190	191	3	272	219
5	180	168	5	236	210
7	204	196	7	253	227
10	271	211	10	242	250
15	241	209	15	212	214
20	176	181	20	167	168
30	94	117	30	116	110

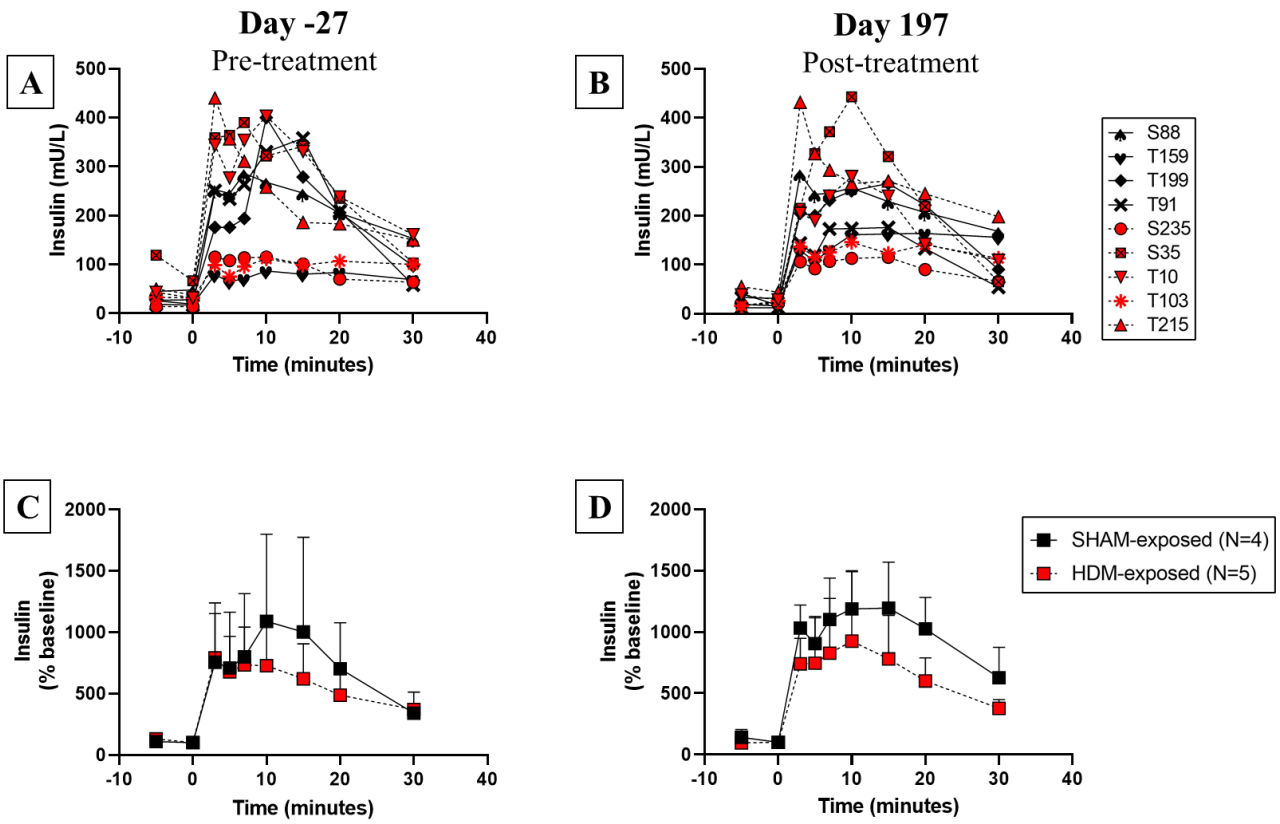

Figure 6. Raw and normalized blood plasma insulin during IVGTT at Day -27 and Day 197

Panels (A) and (B), respectively, illustrate the raw insulin responses pre-treatment and post-treatment for individual animals. Panels (C) and (D) illustrate the normalized insulin responses (% relative to baseline=insulin value at TP=0 minutes), expressed as group averages (mean ± SD). SHAM-exposed animals (N=4) are shown in black symbols with a solid line; HDM-exposed animals (N=5) are shown in red symbols with a dashed line. Two-factor ANOVA with repeated measures showed statistically significant main effects for time ($p<0.05$), no main effects for treatment and no interaction effect.

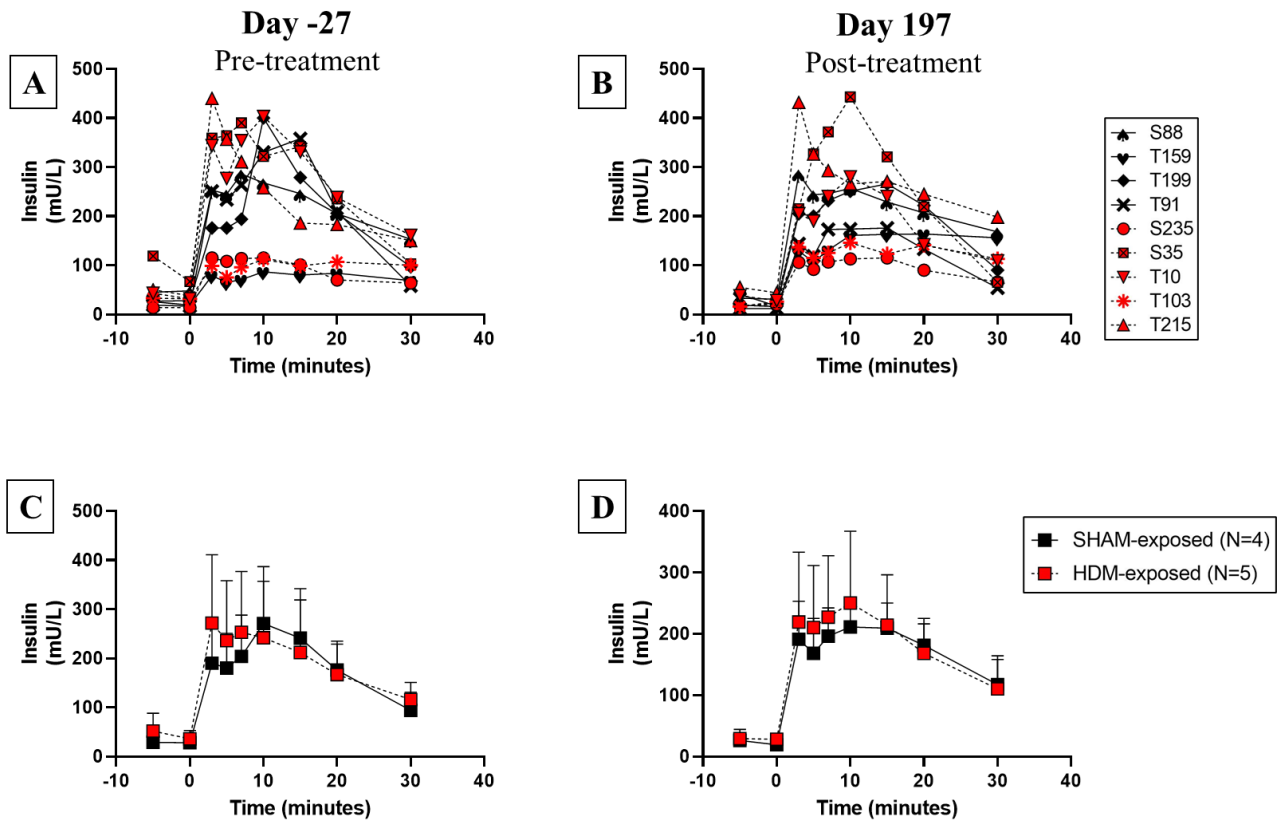

Figure 7. Raw blood plasma insulin during IVGTT at Day -27 and Day 197

Panels (A) and (B), respectively, illustrate the raw insulin responses pre-treatment and post-treatment for individual animals. Panels (C) and (D) illustrate the raw insulin responses expressed as group averages (mean ± SD). SHAM-exposed animals (N=4) are shown in black symbols with a solid line; HDM-exposed animals (N=5) are shown in red symbols with a dashed line. Two-factor ANOVA with repeated measures showed statistically significant main effects for time ($p<0.05$), no main effects for treatment and no interaction effect.

Indices of insulin resistance and glucose tolerance

Using glucose and insulin values measured during a 30-minute IVGTT on Day -27 (pre-treatment) and Day 197 (post-treatment), seven indices of insulin resistance and glucose tolerance were determined. Four indices of insulin resistance (FPI, HOMA-IR, QUICKI, AUC_I) will be presented first, followed by three indices of glucose tolerance (FBG, K_G and AUC_G).

Fasting Plasma Insulin (FPI)

At Day -27 and Day 197, the average FPI for HDM-exposed animals was greater than SHAM (Figure 8**,** Panel B). Average decrease in FPI for both exposure groups was observed at Day 197, 30% decrease for SHAM-exposed and 31% decrease for HDM-exposed (Figure 8**,** Panel B). HDM-exposed animals changes in FBG pre- and post-treatment were highly variable; 3/5 animals had a 10% or greater decrease in FPI and 2/5 had a 10% or higher increase at Day 197 (Figure 8**,** Panel A). On the other hand, all four SHAM-exposed animals had a 10% or greater decrease in FPI (Figure 8**,** Panel A). Two-factor ANOVA with repeated measures did not show statistically significant main effects for time or group and no interaction effect. FPI ranged from 17-48 mU/L on Day -27 and 12-31 mU/L on Day 197 for SHAM and 14-67 mU/L on Day -27 and 20-44 mU/L on Day 197 for HDM-exposed (Figure 8**,** Panel A).

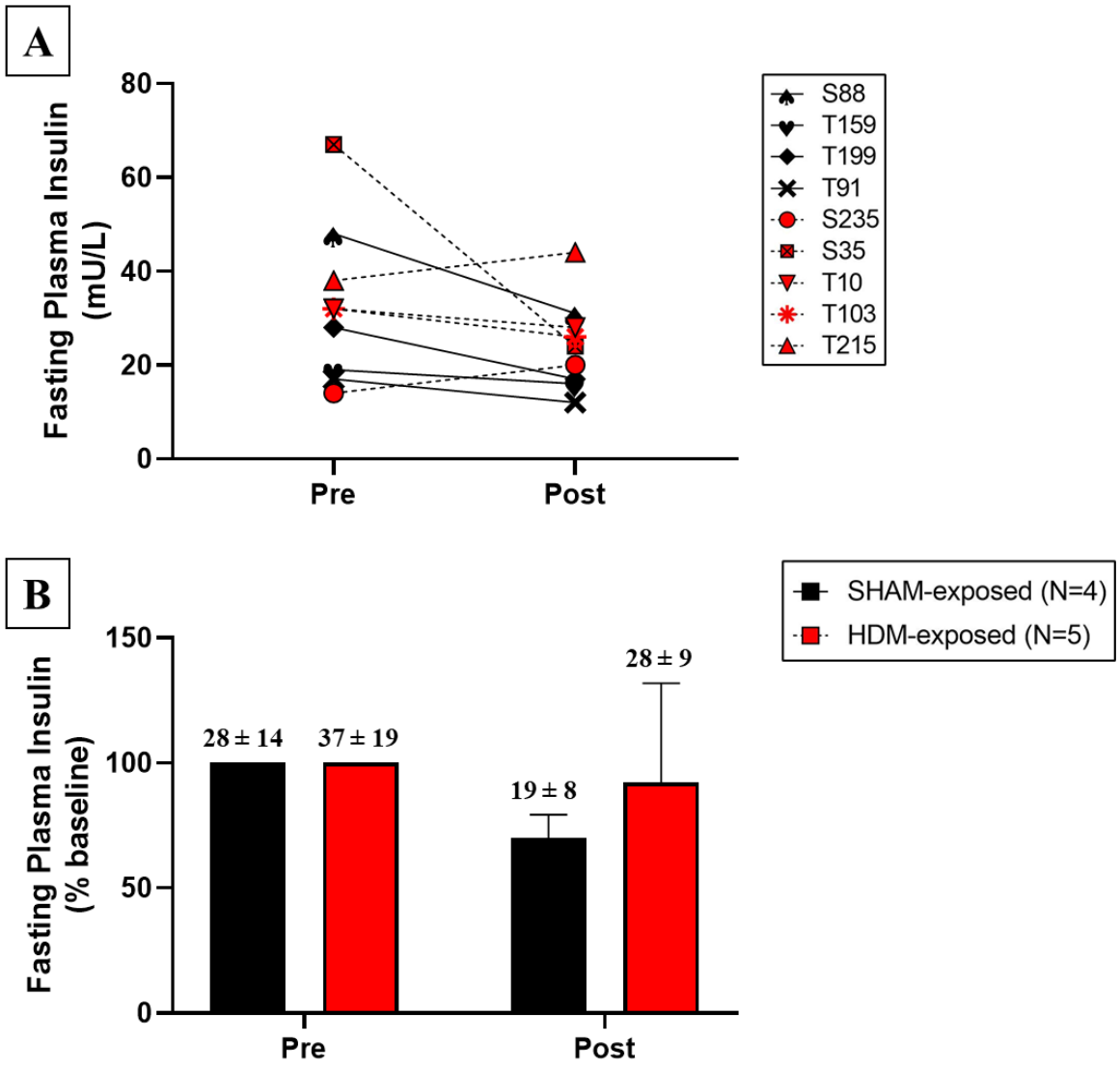

Figure 8. Raw and normalized FPI during IVGTT at Day -27 and Day 197

Fasting plasma insulin (mU/L) for all nine study animals at pre-treatment and post-treatment. Fasting plasma insulin was defined as the insulin value measured at 0 min (TP=0 in IVGTT), immediately prior to administering 50% dextrose bolus during an IVGTT. Individual animals are identified by a unique symbol; SHAM-exposed animals shown in black with a solid line and HDM-exposed animals in red with a dashed line (A). Normalized FPI to baseline (Day -27/pre-treatment) expressed as group averages for SHAM, black bar, and HDM-exposed, red bar (B). Raw group averages for Day -27, pre-treatment, and Day 197, post-treatment, are shown as mean ± SD above black and red bars in Panel B. Two-factor ANOVA with repeated measures did not show statistically significant main effects for time or group and no interaction effect.

HOMA-IR

The average HOMA-IR on Days -27 and 197 were greater for HDM-exposed animals (Figure 9**,** Panel B). An average decrease of 29% and 32% was observed on Day 197 for HDM-exposed and SHAM, respectively. Within the HDM-exposed group, 2/5 animals showed 10% or greater increase in HOMA-IR while the other three showed a trend for decreased HOMA-IR. One HDM-exposed animal, S35, had a 72% decrease in HOMA-IR on Day 197 (Figure 9**,** Panel A). All four SHAM-exposed animals showed a >10% decrease in HOMA-IR (Figure 9**,** Panel A). Two-factor ANOVA with repeated measures did not show statistically significant main effects for time or group and no interaction effect. Descriptive stats: HOMA-IR ranged from 2.7-7.9 on Day -27 and 2.0-5.1 on Day 197 for SHAM and 2.6-14.1 on Day -27 and 3.2-6.9 on Day 197 for HDM-exposed (Figure 9**,** Panel B).

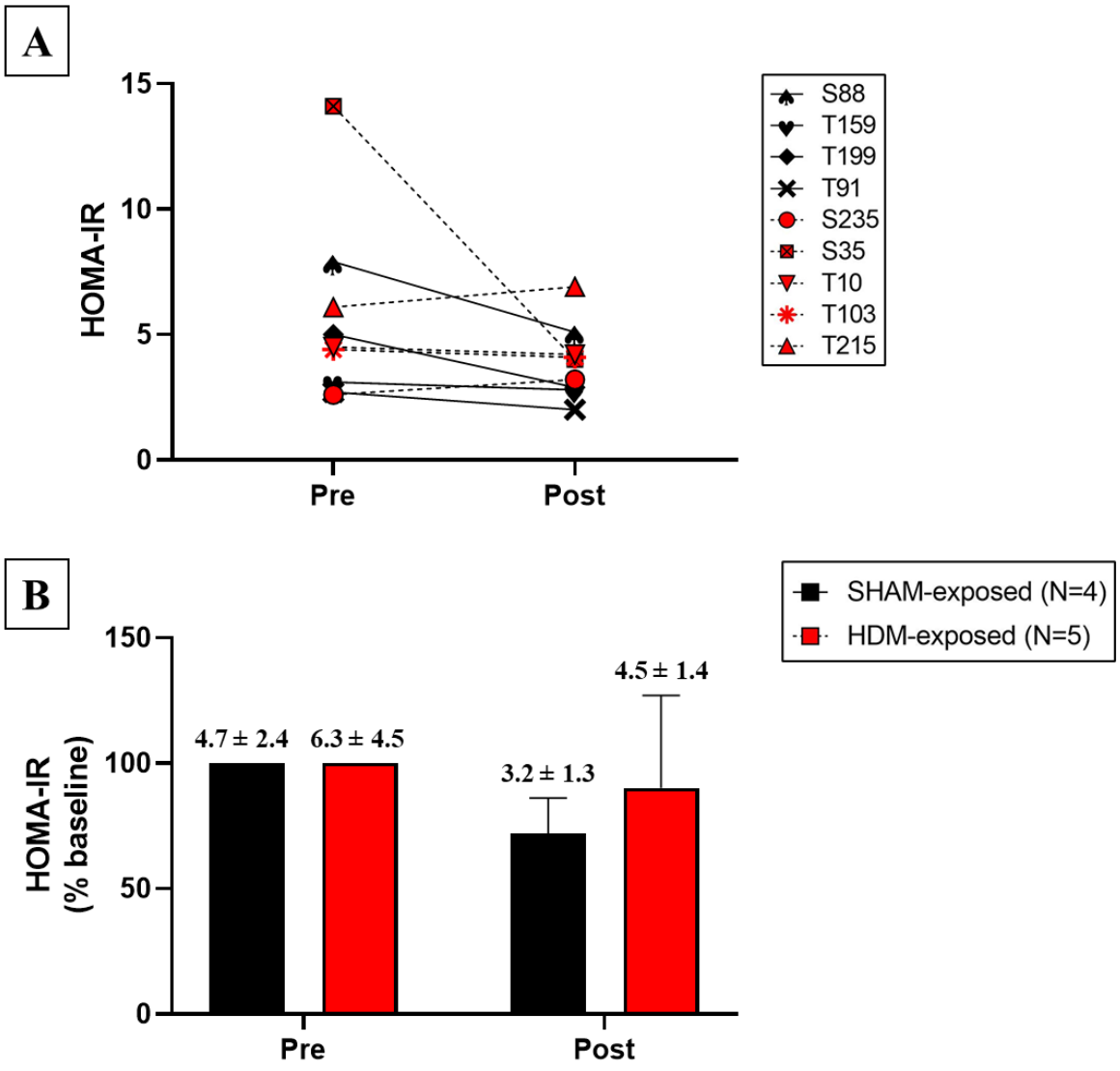

Figure 9. Raw and normalized HOMA-IR during IVGTT at Day -27 and Day 197

Calculated HOMA-IR values for all nine study animals' pre-treatment and post-treatment. Individual animals are identified by a unique symbol; SHAM-exposed animals shown in black with a solid line and HDM-exposed animals in red with a dashed line (A). Normalized HOMA-IR to baseline (Day -27/pre-treatment) expressed as group averages for SHAM, black bar, and HDM-exposed, red bar (B). Raw group averages for Day -27, pre-treatment, and Day 197, post-treatment, are shown as mean ± SD above black and red bars in Panel B. Two-factor ANOVA with repeated measures did not show statistically significant main effects for time or group and no interaction effect.

QUICKI

On Days -27 and 197, average QUICKI was greatest in SHAM-exposed animals (Figure 10**,** Panel B). An average percent increase of 2% and 5% were observed on Day 197 for HDM-exposed and SHAM-exposed animals, respectively. An increase of >10% in QUICKI on Day 197 was observed in two of the nine study animals one from each exposure group: HDM-exposed animal S35 had a 15% increase in QUICKI post-treatment and SHAM-exposed animal T199 had increase of 10% (Figure 10**,** Panel A). Two-factor ANOVA with repeated measures did not show statistically significant main effects for time or group and no interaction effect. Descriptive stats: QUICKI ranged from 0.29-0.33 on Day -27 and 0.30-0.34 on Day 197 for SHAM and 0.27-0.33 on Day -27 and 0.29-0.32 on Day 197 for HDM-exposed (Figure 10**,** Panel B).

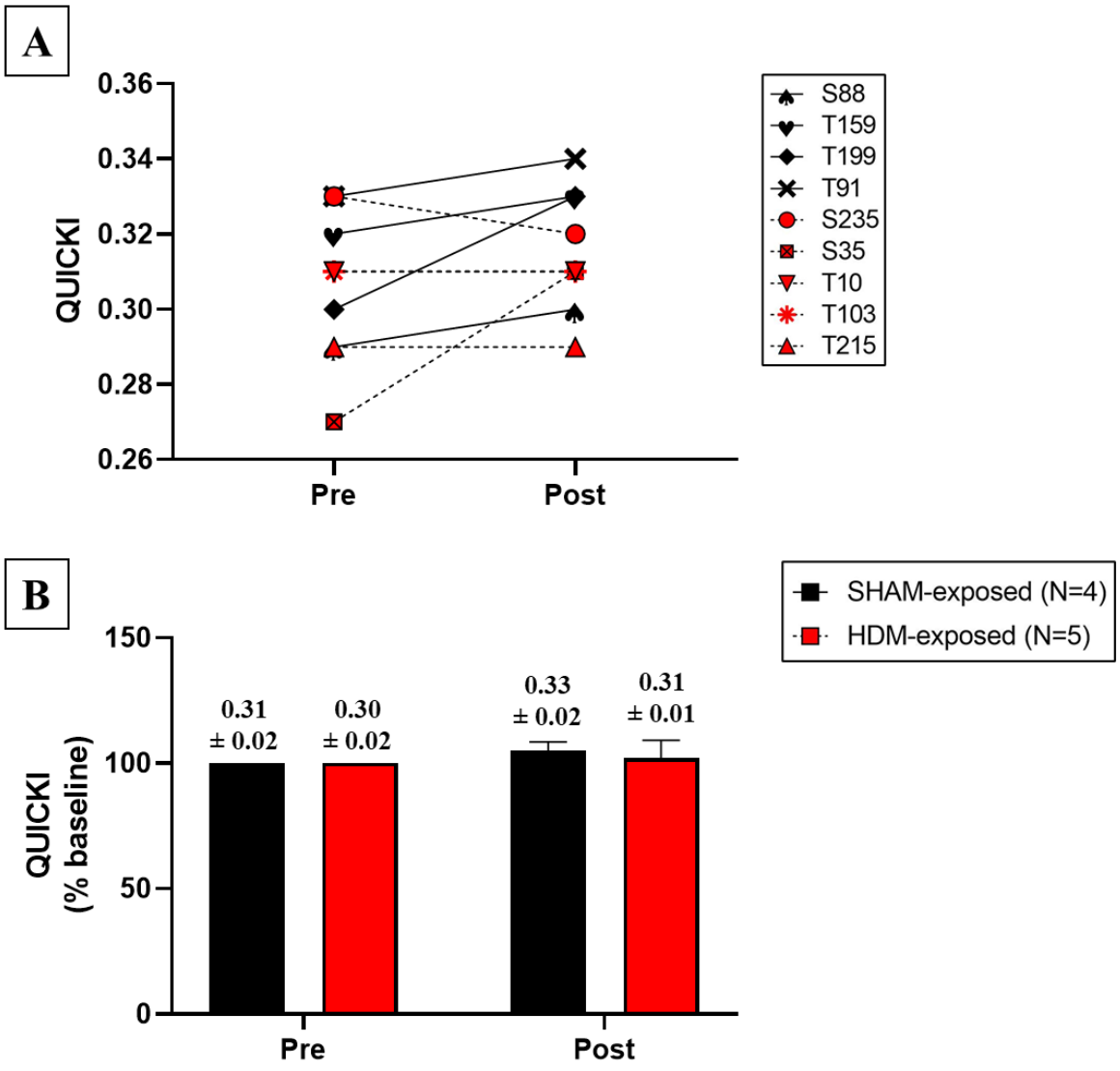

Figure 10. Raw and normalized QUICKI during IVGTT at Day -27 and Day 197

Calculated QUICKI values for all nine study animals' pre-treatment and post-treatment. Individual animals are identified by a unique symbol; SHAM-exposed animals shown in black with a solid line and HDM-exposed animals in red with a dashed line (A). Normalized QUICKI to baseline (Day -27/pre-treatment) expressed as group averages for SHAM, black bar, and HDM-exposed, red bar (B). Raw group averages for Day -27, pre-treatment, and Day 197, post-treatment, are shown as mean ± SD above black and red bars in Panel B. Two-factor ANOVA with repeated measures did not show statistically significant main effects for time or group and no interaction effect.

Area Under the Curve for Insulin (AUC_I)

At Day -27, the average AUC_I for both exposure groups were roughly the same (Figure 11**,** Panel B). An average decrease in AUC_I relative to Day -27 was observed on Day 197 for both groups (Figure 11**,** Panel B). Changes in AUC_I for individual animals within exposure groups varied (Figure 11**,** Panel A). Noteworthy changes in AUC_I for individual animals within the HDM-exposure group include: 2/5 with an average >10% increase and one animal (T10) with a 33% decrease in AUC_I. Among SHAM-exposed, a 42% decrease in AUC_I was observed in one animal (T91) and a 98% increase was observed for Animal T159 (Figure 11**,** Panel A). Two-factor ANOVA with repeated measures did not show statistically significant main effects for time or group and no interaction effect. Descriptive stats: AUC_I ranged from 2095-6286 mU/L*min on Day -27 and 3667-5936 mU/L*min on Day 197 for SHAM and 2609-7640 mU/L*min on Day -27 and 2575-7211 mU/L*min on Day 197 for HDM-exposed (Figure 11**,** Panel B).

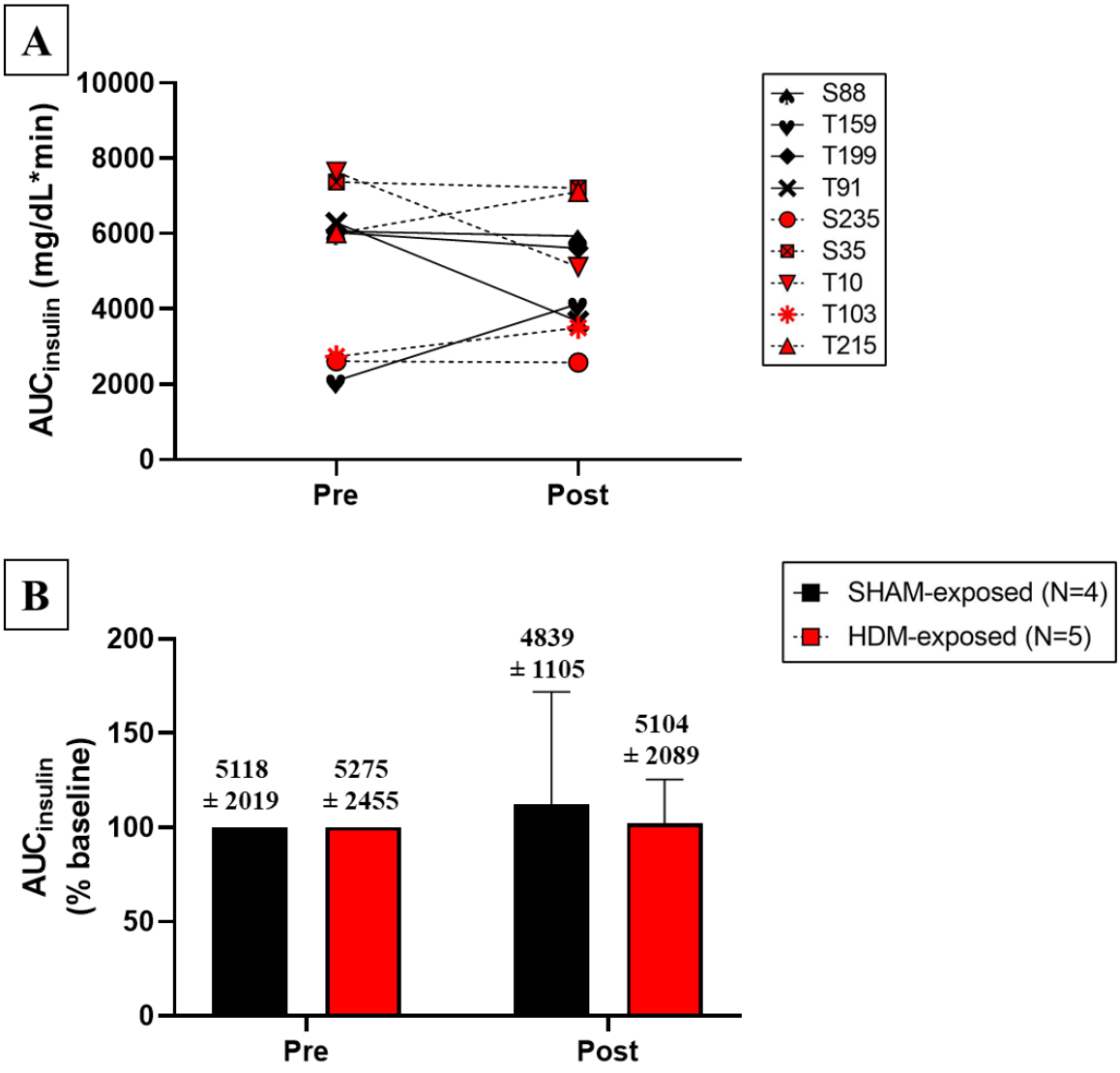

Figure 11. Raw and normalized $AUC_{Insulin}$ during IVGTT at Day -27 and Day 197

Calculated AUC_I values for all nine study animals' pre-treatment and post-treatment. Individual animals are identified by a unique symbol; SHAM-exposed animals shown in black with a solid line and HDM-exposed animals in red with a dashed line (A). Normalized AUC_I to baseline (Day -27/pre-treatment) expressed as group averages for SHAM, black bar, and HDM-exposed, red bar (B). Raw group averages for Day -27, pre-treatment, and Day 197, post-treatment, are shown as mean ± SD above black and red bars in Panel B. Two-factor ANOVA with repeated measures did not show statistically significant main effects for time or group and no interaction effect.

Fasting Blood Glucose (FBG)

Fasting blood glucose (mg/dL) was defined as the glucose value measured immediately prior to administering a bolus of 50% dextrose (250 mg/kg; TP=0 min). Pre-treatment FBG was highly variable, especially among individuals of the HDM-exposed group (Figure 12), while post-treatment FBG was less variable. At Day -27 (pre-treatment), both groups had an average FBG of 68 mg/mL (Figure 12**,** Panel B). Post-treatment FBG did not change relative to Day -27 in SHAM-exposed animals, however, a slight decrease was observed in the HDM-exposed group to 65±3 mg/dL. Individual animal changes in FBG pre- and post-treatment were highly variable; high variability was also observed within exposure groups (Figure 12**,** Panel A). Two-factor ANOVA with repeated measures did not show statistically significant main effects for time or group and no interaction effect. Pre-treatment FBG ranged from 65-73 mg/dL, post-treatment FBG ranged from 67-73 mg/dL for SHAM; pre-treatment FBG ranged from 56-86 mg/dL, post-treatment FBG ranged from 62-70 mg/dL for HDM-exposed (Figure 12**,** Panel A). 2/5 HDM-exposed animals showed a >10% decrease in FBG and 1/5 showed a >10% increase on Day 197 (Figure 12**,** Panel B).

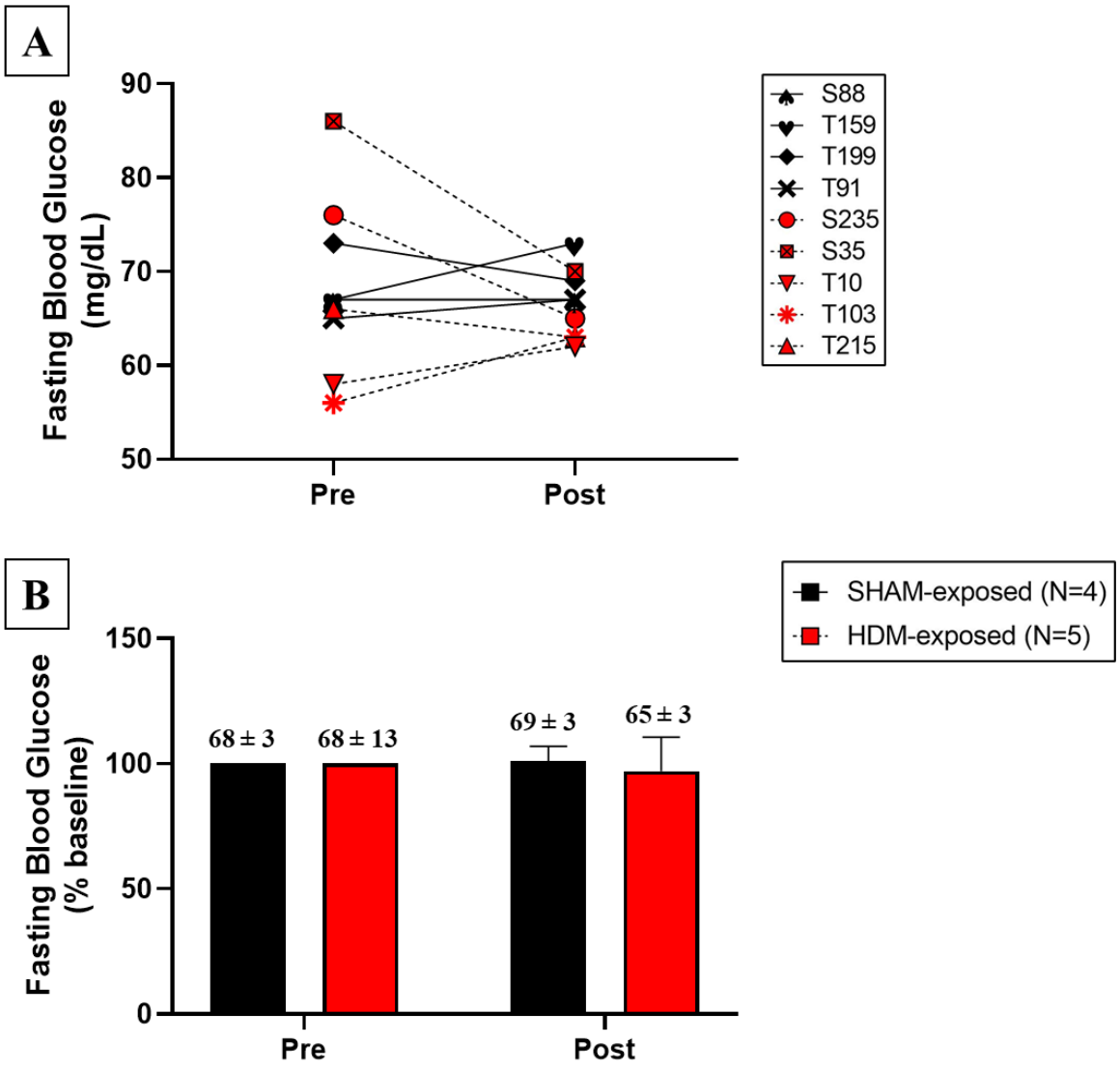

Figure 12. Raw and normalized FBG during IVGTT at Day -27 and Day 197

Fasting blood glucose (mg/dL) was defined as the glucose value measured immediately prior to administering a bolus of 50% dextrose (250 mg/kg; TP=0 min). Panel (A) illustrates raw values for all nine study animals, pre-treatment and post-treatment. Individual animals are identified by a unique symbol: SHAM-exposed animals shown in black with a solid line; HDM-exposed animals in red with a dashed line. Panel (B) illustrates the normalized FBG (% relative to pre-treatment baseline=glucose value at TP=0 minutes), expressed as group averages (mean ± SD). SHAM-exposed animals, black bars; HDM-exposed animals, red bars. Raw group averages are shown as mean ± SD above black and red bars in Panel B. Two-factor ANOVA with repeated measures did not show statistically significant main effects for time or group and no interaction effect.

Glucose disappearance rate (K_G)

At Day -27, the average K_G for SHAM- and HDM-exposed animals was 2.4 ± 0.5 and 2.5 ± 1.0 (Figure 13**,** Panel B). At Day 197, the average K_G for SHAM-exposed animals slightly decreased from Day -27, whereas HDM-exposed animals showed no change. Average AUC_G at Day 197, post-treatment, did not change relative to Day -27 in SHAM-exposed or HDM-exposed animals. Raw values and changes in K_G pre- and post-treatment were highly variable for individual animals and within exposure groups (Figure 13**,** Panel A). Two-factor ANOVA with repeated measures did not show statistically significant main effects for time or group and no interaction effect. Descriptive stats: K_G ranged from 1.3-3.7 on Day -27 and 1.7-2.7 on Day 197 for SHAM and 1.7-3.1 on Day -27 and 1.7-3.4 on Day 197 for HDM-exposed (Figure 13**,** Panel A). 1 SHAM-exposed (T159) and one HDM-exposed animal showed a ≥10% increase in K_G; one other SHAM animal (T91) had a 30% decrease in K_G at Day 197 (Figure 13**,** Panel A).

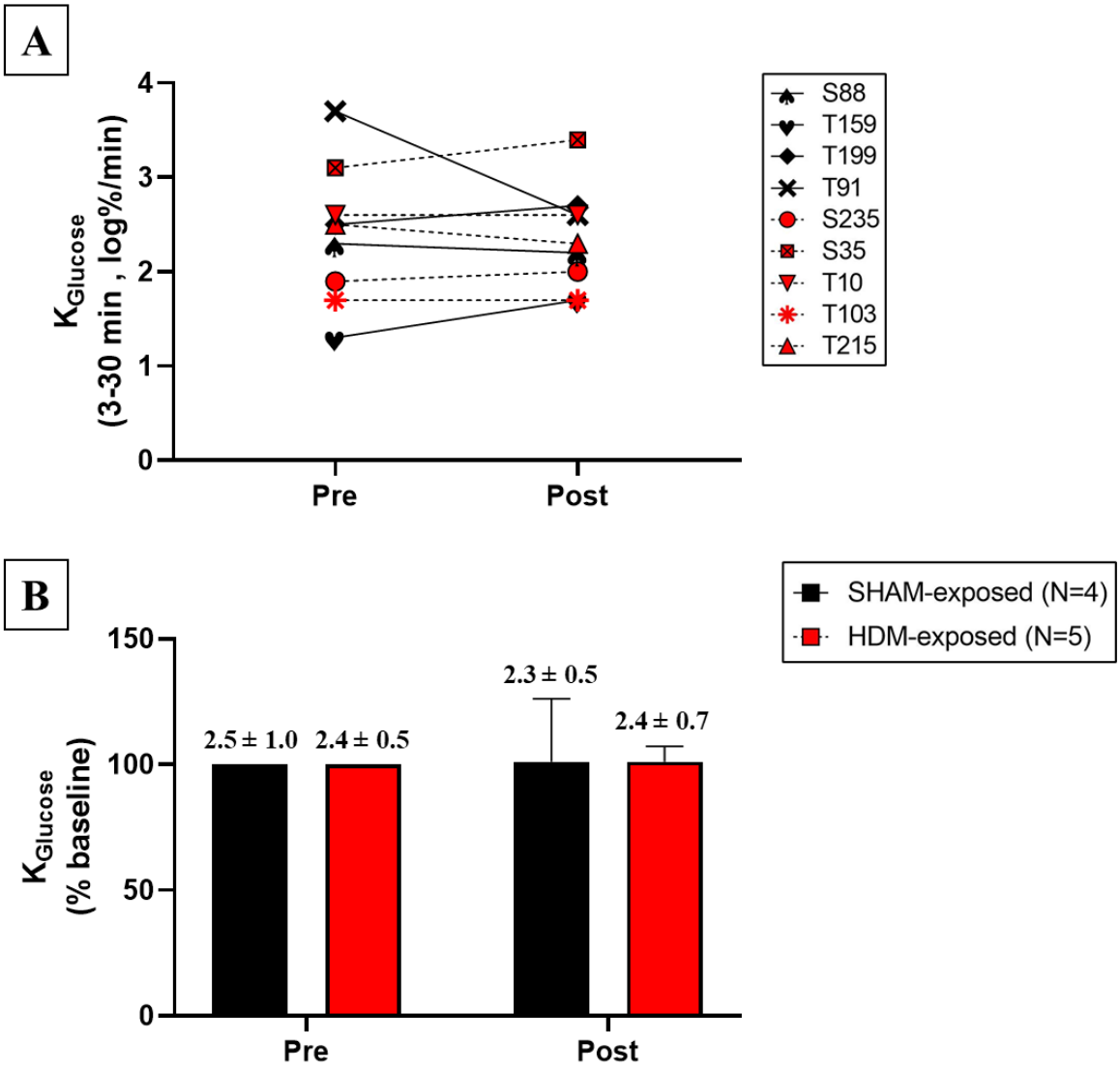

Figure 13. Raw and normalized K_G during IVGTT at Day -27 and Day 197

Calculated glucose disappearance rate between time points 3-30 minutes (K_G) for all nine study animals' pre-treatment and post-treatment. Individual animals are identified by a unique symbol; SHAM-exposed animals shown in black with a solid line and HDM-exposed animals in red with a dashed line (A). Normalized K_G to baseline (Day -27/pre-treatment) expressed as group averages for SHAM, black bar, and HDM-exposed, red bar (B). Raw group averages for Day -27, pre-treatment, and Day 197, post-treatment, are shown as mean ± SD above black and red bars in Panel B. Two-factor ANOVA with repeated measures did not show statistically significant main effects for time or group and no interaction effect.

Area Under the Curve for Glucose (AUC_G)

Both pre-treatment (Day -27) and post-treatment (Day 197) AUC_G were highly variable among individuals of each group (Figure 14**,** Panel B). Both groups had an average pre-treatment AUC_G of ~4000 mg/dL*min, which did not differ from average post-treatment AUC_G in SHAM-exposed or HDM-exposed animals (Figure 14**,** Panel B). Two-factor ANOVA with repeated measures did not show statistically significant main effects for time or group and no interaction effect. Pre-treatment AUC_G ranged from 3389-4473 mg/dL*min, post-treatment AUC_G ranged from 3811-4405 mg/dL*min for SHAM; pre-treatment AUC_G ranged from 3657-4272 mg/dL*min, post-treatment AUC_G ranged from 3397-4149 mg/dL*min for HDM-exposed (Figure 14**,** Panel B). One SHAM-exposed animal had a 12% increase in AUC_G on Day 197, while one HDM-exposed animal had an 11% decrease (Figure 14**,** Panel A).

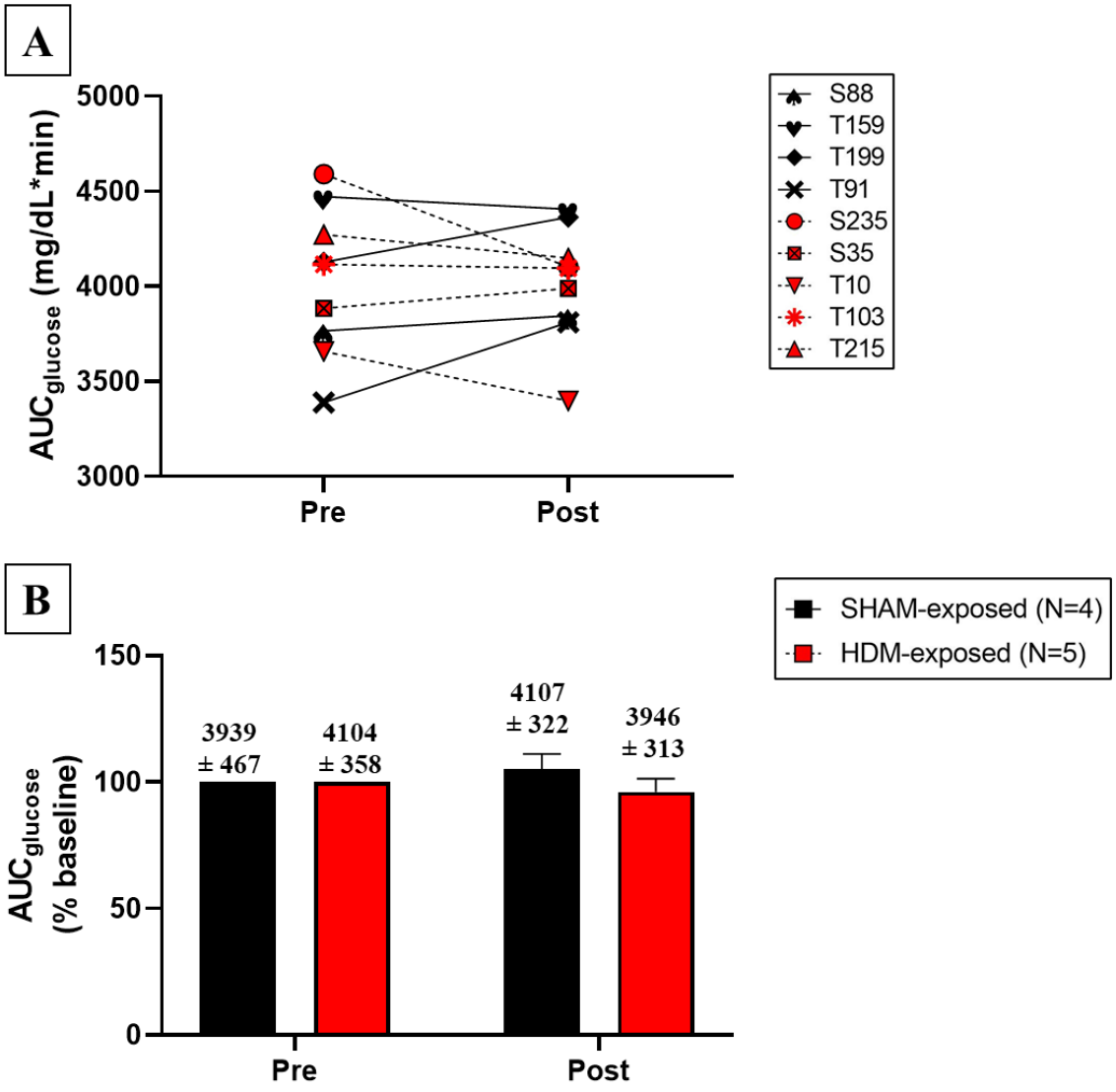

Figure 14. Raw and normalized $AUC_{Glucose}$ during IVGTT at Day -27 and Day 197

Panel (A) illustrates calculated AUC_G values for all nine study animals, pre-treatment and post-treatment. Individual animals are identified by a unique symbol: SHAM-exposed animals shown in black with a solid line; HDM-exposed animals in red with a dashed line. Panel (B) illustrates the normalized AUC_G (% relative to pre-treatment baseline), expressed as group averages (mean ± SD). SHAM-exposed animals, black bars; HDM-exposed animals, red bars. Raw group averages are shown as mean ± SD above black and red bars in Panel B. Two-factor ANOVA with repeated measures did not show statistically significant main effects for time or group and no interaction effect.

Pulmonary function and inflammation

Airway hyperresponsiveness/hyperreactivity (AHR) was assessed by measuring changes in pulmonary function and inflammation. The early asthmatic response (EAR) was assessed by measuring immediate/acute changes in pulmonary function induced by the monthly aero-HDM/SHAM exposure (specific AHR). The late asthmatic response (LAR) was assessed by measuring changes in pulmonary function induced by aero-Mch 24 hours after aero-HDM exposure (non-specific AHR); immediately following aero-Mch challenge, bronchoalveolar lavage (BAL) was performed to assess pulmonary inflammation. LAR assessments were conducted 24 hours after the first, fourth, and seventh aero-HDM/SHAM exposures.

Early asthmatic response to aero-HDM/SHAM

EAR was assessed by measuring the maximum acute pulmonary function responses to monthly airway challenges with aerosolized-HDM (HDM group) or aerosolized-saline (SHAM group). The four major PFT parameters measured included the airway challenge-induced maximum lung resistance, minimum dynamic lung compliance, maximum respiratory rate, and minimum SpO_2 (ΔR_L, ΔC_{dyn}, ΔRR and SpO_2, respectively; summary of treatment-induced changes in PFT indexes are illustrated in Figure 15).

At airway challenge/Study Day 1, compared to SHAM-treated animals, HDM induced greater increases in lung resistance and RR (Figure 15, Panels A & C respectively), greater decreases in C_{dyn} (Figure 15, Panel B), and lower minimum SpO_2 (Figure 15, Panel D): individual animal responses to HDM were highly variable but were consistent with historical responses. For SHAM animals, no overall changes in pulmonary function were observed during the study.

Therefore, assessment and discussion of changes in pulmonary function and aero-HDM-induced AHR will focus primarily on the HDM-exposed group data.

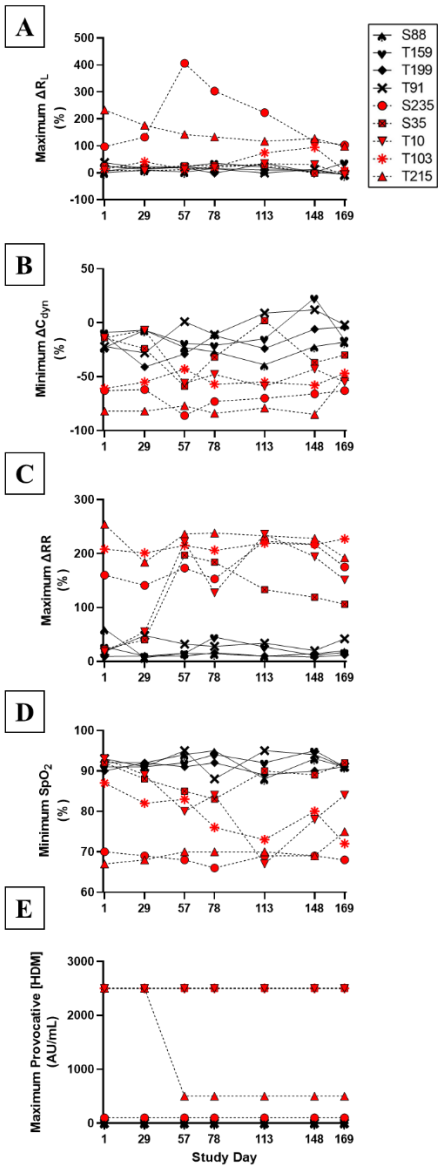

Figure 15. Maximum acute response to aero-HDM/saline- EAR PFT Summary

Illustrated are changes in lung resistance (A), dynamic compliance (B), respiratory rate (C), peripheral oxygen saturation (D), and the provocative concentration of aero-HDM (E). The raw pulmonary function measurements (normalized to daily aero-saline baseline) are shown for all nine study animals: SHAM-exposed animals are shown in black with a solid line and HDM-exposed animals in red with a dashed line. During each monthly experimental exposure, HDM-exposed animals showed greater changes in lung resistance, compliance, and respiratory rate, as well as lower minimum oxygen saturations compared to SHAM animals. Overall, a trend for increased sensitivity to aero-HDM was observed in HDM-exposed animals each month.

Maximum provocative concentration of HDM (PC_{HDM})

The maximum provocative concentration of HDM (PC_{HDM}) as previously described, is defined as the highest dose of aerosolized house dust mite antigen in antigen units/mL that induces the target changes of 100% in lung resistance, 40% decrease in lung compliance, and/or a desaturation in peripheral SpO_2 to 70% or less. Figure 16 shows the maximum provocative dose of aero-HDM for each of the HDM-exposed study animals during seven monthly aero-HDM exposures over the course of the study.

The maximum provocative dose of aero-HDM for HDM-exposed animals can be shown in Figure 13. Four of the five HDM-exposed animals received the same maximum provocative [HDM] at all study days (Figure 16). Of these four, one animal received 100 AU/mL for 4 mins and the remaining three all received the same dose of 2500 AU/mL delivered over four minutes. One animal in this group, identified as animal ID T215, received 2500 AU/mL delivered for one minute on Days 1 and 29; however, on Day 57, the aero-HDM exposure protocol was discontinued after delivery of 500 AU/mL for four minutes upon reaching a change in lung resistance greater than 100% as well as a decrease in oxygen saturation less than 70% (as required in the IACUC approved aero-HDM airway challenge protocol). Hence, on Days 57-169 the maximum provocative [HDM] for animal T215 was lower (reflecting an increased HDM sensitivity/AHR at Days 57 to 169 compared to Days 1 & 29) than for the first two aero-HDM exposures on Days 1 and 29. This decrease in PC_{HDM} at Days 57 and for the remaining monthly exposures (compared to Day 1 and 29) reflects an increased sensitivity to aero-HDM (requiring a lower dose of aero-HDM to illicit the same target changes in lung resistance and compliance), for animal T215.

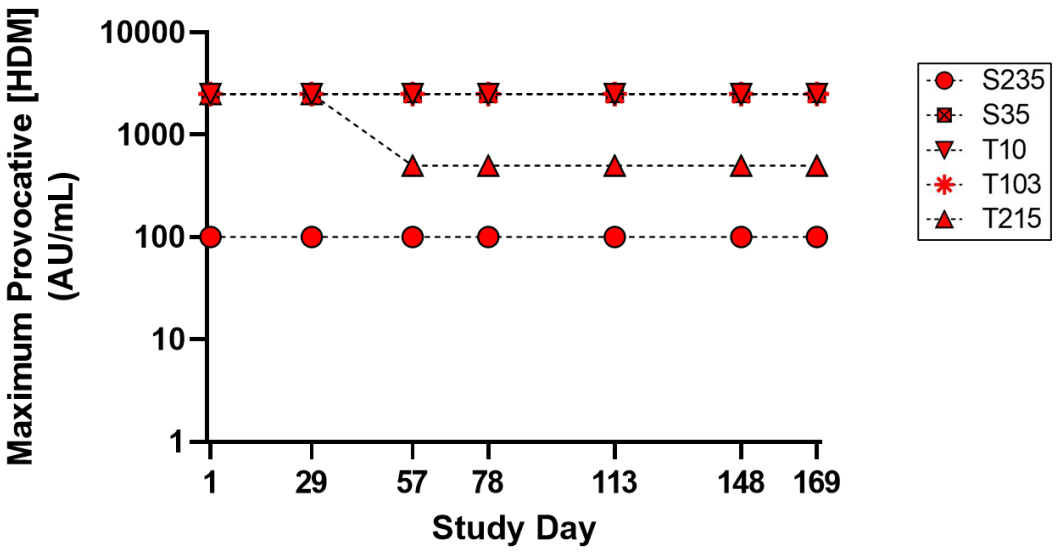

Figure 16. Maximum Provocative Concentration of aero-HDM- N=5

The maximum provocative concentration of aero-HDM for HDM-exposed animals during seven monthly aero-HDM/SHAM exposures. At each monthly exposure, four of five HDM-exposed animals received the same maximum provocative concentration of aero-HDM: Animal S235 received 100 AU/mL aero-HDM delivered for four minutes and three, historically non-sensitive/non-responders to aero-HDM, T10, T103 and S35, received the maximum concentration of aero-HDM (IACUC approved Airway Challenge to aero-HDM Protocol), 2500 AU/mL delivered over four minutes.
One HDM-exposed animal, T215, received a maximum provocative concentration of 2500 AU/mL aero-HDM delivered for one minute during the first and second monthly exposure on Days 1 and 29. However, on Day 57 the aero-HDM airway exposure protocol was discontinued after delivering 500 AU/mL for four minutes due to an >100% increase in lung resistance and oxygen desaturation less than 70%. For safety reasons, when an animal responded to an airway challenge with ≥ 100% increase in RL and/or an SpO2 ≤ 70%, we discontinued escalation of the aero-HDM dose ([aero-HDM] in AU/mL x duration of exposure in minutes) for that study day.
Note: SHAM-exposed animals (N=4) receiving consecutive aerosolized saline exposures, not exposed to aero-HDM, were not included in this figure.

Maximum change in lung resistance (R_L)

At the maximum provocative dose of aero-HDM, HDM-exposed animals had greater changes in lung resistance, lung compliance, respiratory rate, and lower oxygen saturation compared to SHAM animals receiving aero-saline (Figure 17, Panels A-D). SHAM-exposed animals did not show changes in lung resistance, or any pulmonary function parameters, over the course of the study (Figure 17, Panel C). On the other hand, a trend for increased average ΔR_L was observed in the HDM-exposed group following the first aero-HDM exposure, peaking on Day 57 after the third exposure, followed by decreasing trend at the fifth, sixth and final exposure (Figure 17, Panel C).

In HDM-exposed group, the average maximum change in lung resistance was greater than 100% at Day 57 and Day 78 (Figure 17, Panel B). Two out of five HDM-exposed animals (T215 and S235) reached a ~100% or greater increase in lung resistance at each study day (97% R_L on Day 1 for S235 and 98% R_L on Day 169 for T215; Figure 17, Panel A). For the remaining three animals, T10, T103 and S35, a trend was observed from Day 1 to Day 113 for an increase in lung resistance (Figure 17, Panel C); one of which, animal T103, reached a maximum change in lung resistance of 94% on Day 148 (Figure 17, Panel A).

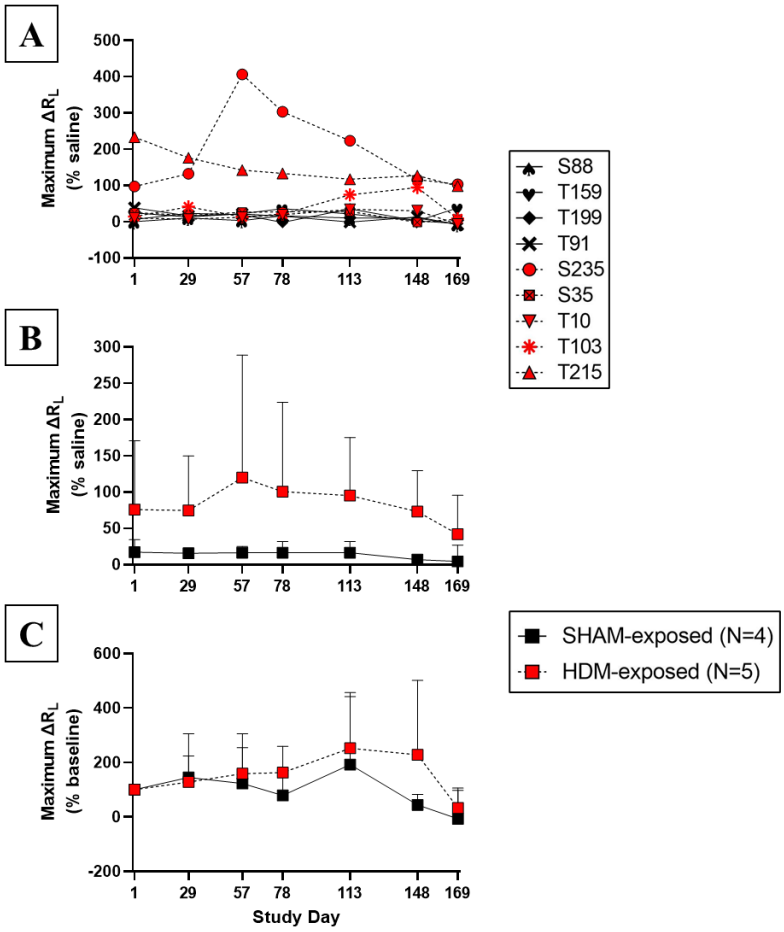

Figure 17. Maximum acute response to aero-saline or aero-HDM- ΔR_L

Maximum acute pulmonary function responses to monthly aero-HDM or aero-saline (SHAM) exposure over six months measured at Days 1, 29, 57, 78, 113, 148, & 169. Maximum △RL is expressed as a percentage of the baseline saline measurement recording prior to aero-HDM/saline delivery. The raw maximum △RL induced by delivery of the highest provocative dose of aero-HDM (or saline) at each study day for all nine study animals; SHAM-exposed animals shown in black with a solid line and HDM-exposed animals in red with a dashed line (A). The average change in lung resistance for SHAM and HDM-exposed animals are shown in Panel B; expressed as group mean ± SD. Normalized maximum △RL (to Day 1 baseline) for SHAM-exposed and HDM-exposed groups (C). Normalized data is expressed as group mean ± SD for SHAM-exposed (red square; solid line) and HDM-exposed (black square; dashed line) groups. Two-factor ANOVA with repeated measures did not show statistically significant main effects for time or group and no interaction effect.

Maximum change in lung compliance (C_{dyn})

Average change in dynamic compliance was greater in HDM-exposed animals compared to SHAM on all study days (Figure 18, Panel C), but were only statistically significant on Days 57 ($p=0.002$), Day 78 ($p=0.008$), Day 148 ($p=0.003$) and Day 169 ($p<0.001$). While SHAM-exposed animals did not show changes in C_{dyn} over the course of the study, a trend for increased ΔC_{dyn} was observed in HDM-exposed animals at each month (Figure 18, Panel C).

The average maximum decrease in dynamic lung compliance was more than 40% at every study day for HDM-exposed animals (Figure 18, Panel B). A decrease of 40% or more in dynamic lung compliance was observed for three of five animals (T103, T215 and S235) at every study day (Figure 18, Panel A). The remaining two animals (T10 and S35) showed a ≥40% decrease in lung compliance after the third and remaining aero-HDM exposures (Day 57 to Day 169), shown in Figure 18, Panels A and B.

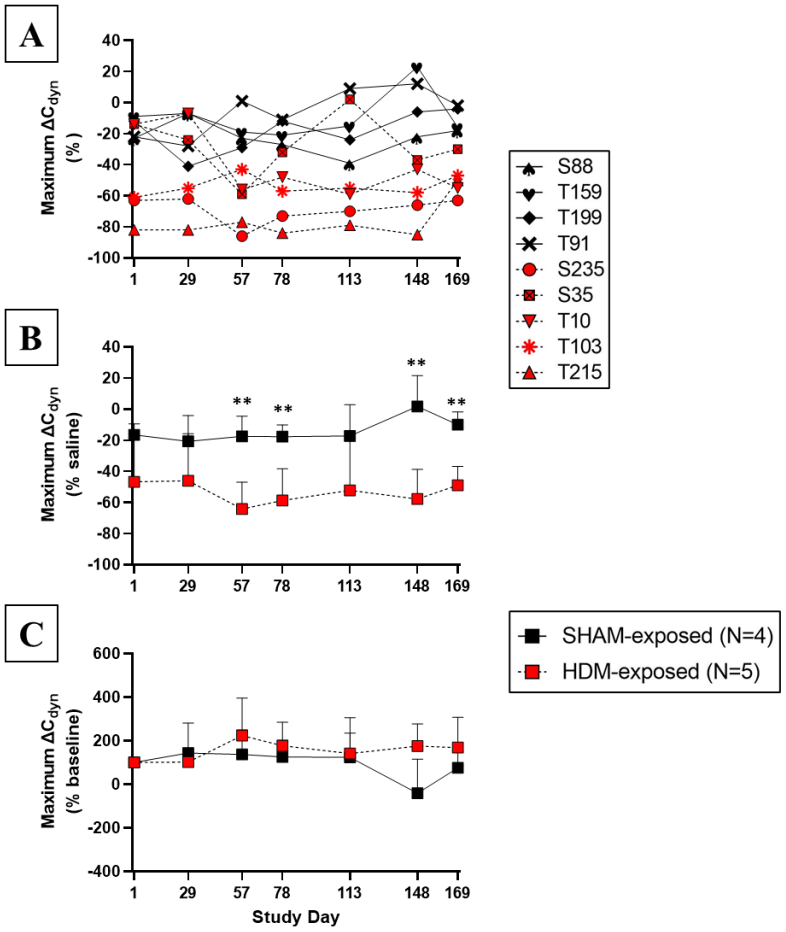

Figure 18. Maximum acute response to aero-saline or aero-HDM- ΔC_{dyn}

Maximum acute pulmonary function responses to monthly aero-HDM or aero-saline (SHAM) exposure over six months measured at Days 1, 29, 57, 78, 113, 148, & 169. Maximum ΔCdyn is expressed as a percentage of the baseline saline measurement recording prior to aero-HDM/saline delivery. The raw ΔCdyn induced by delivery of the highest provocative dose of aero-HDM (or saline) at each study day for all nine study animals; SHAM-exposed animals shown in black with a solid line and HDM-exposed animals in red with a dashed line (A). The average change in dynamic compliance for SHAM and HDM-exposed animals are shown in Panel B; expressed as group mean ± SD. Normalized maximum ΔCdyn (to Day 1 baseline) for SHAM-exposed and HDM-exposed groups (C). Normalized data is expressed as group mean ± SD for SHAM-exposed (red square; solid line) and HDM-exposed (black square; dashed line) groups. Two-factor ANOVA with repeated measures showed statistically significant main effects for treatment group ($p<0.05$), no main effects for time and no interaction effect. Two-sample t-test determined statistically significant group differences at Days 57, 78, 148, and 169 ($p<0.05$=*; $p<0.01$=**).

Maximum change in respiratory rate (RR)

On Day 1, the average change in respiratory rate was higher in HDM-exposed animals compared to SHAM. Furthermore, average ΔRR for HDM-exposed animals was significantly higher on Days 29 ($p=0.028$), 57 ($p<0.001$), 78 ($p<0.001$), 113 ($p<0.001$), 148 ($p<0.001$) and 169 ($p=0.001$), compared to SHAM controls (Figure 19, Panel B). While SHAM-exposed animals did not show changes in RR over the course of the study, a trend for increased ΔRR was observed in HDM-exposed animals at each month (Figure 19, Panel C).

The average maximum increase in respiratory rate exceeded 100% for HDM-exposed animals at every study day (Figure 19, Panel A); additionally, an average increase of 150% was observed at each study day following the 2nd monthly aero-HDM exposure (Figure 19, Panel B). Three of five animals (T103, T215, and S235) had an 150% increase or greater in respiratory rate during every monthly challenge (Figure 19, Panel A). The remaining two animals, T10 and S35, exceeded a 150% increase at Day 57 and during each subsequent exposure thereafter (Figure 19, Panel A).

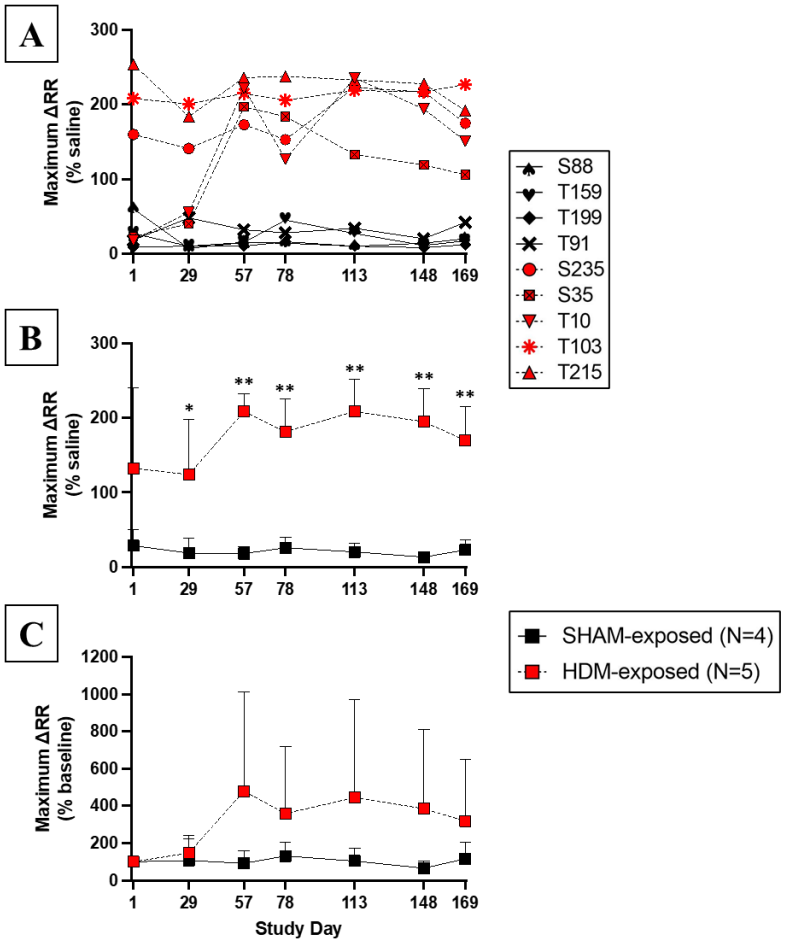

Figure 19. Maximum acute response to aero-saline or aero-HDM- ΔRR

Maximum acute pulmonary function responses to monthly aero-HDM or aero-saline (SHAM) exposure over six months measured at Days 1, 29, 57, 78, 113, 148, & 169. Maximum ΔRR is expressed as a percentage of the respiratory rate recorded during baseline saline measurement recording prior to aero-HDM/saline delivery. The raw maximum ΔRR induced by delivery of the highest provocative dose of aero-HDM (or saline) at each study day for all nine study animals; SHAM-exposed animals shown in black with a solid line and HDM-exposed animals in red with a dashed line (A). The average change in respiratory rate for SHAM and HDM-exposed animals are shown in Panel B; expressed as group mean ± SD. Normalized ΔRR (to Day 1 baseline) for SHAM-exposed and HDM-exposed groups (C). Normalized data is expressed as group mean ± SD for SHAM-exposed (red square; solid line) and HDM-exposed (black square; dashed line) groups. Two-factor ANOVA with repeated measures showed statistically significant main effects for treatment group ($p<0.05$), no main effects for time and no interaction effect. Two-sample t-test determined statistically significant group differences at Days 29, 57, 78, 113, 148, and 169 ($p<0.05$=*; $p<0.01$=**).

Minimum oxygen saturation (SpO_2)

On Day 1, the average minimum SpO_2 was lower in HDM-exposed animals compared to SHAM. Furthermore, average minimum SpO_2 for HDM-exposed animals was significantly lower on Days 29 (p=0.048), 57 (p=0.006), 78 (p=0.007), 113 (p=0.011), 148 (p=0.011) and 169 (p=0.035), compared to SHAM controls (Figure 20, Panel B). While SHAM-exposed animals did not show changes in SpO_2 over the course of the study, a trend for decreased minimum SpO_2 was observed in HDM-exposed animals at each month, although not statistically significant (Figure 20, Panel C).

An average minimum SpO_2 less than 80% was observed during the 2nd aero-HDM exposure on Day 29 as well as each monthly exposure after (Figure 20, Panel B). Two of five animals showed a decrease of 70% or less in SpO_2 during every exposure (except T215's Day 169 challenge-> minimum SpO_2 of 73%), shown in Figure 20A. At Day 113, a 70% decrease in SpO_2, requiring supplemental oxygen, was observed in three of five animals; minimum SpO_2 $\leq$74% was observed in 4/5 (Figure 20, Panel A). For the remaining animal, S35, an SpO_2 of 83, lowest of all study days, was reached at Day 78; additionally, S35 showed a trend for decreased SpO_2 from Days 1 to 78 (Figure 20, Panel A). The lowest SpO_2 observed for two of the three animals that received the maximum concentration of 2500 AU/mL aero-HDM delivery over 4 minutes (T10 and T103) occurred at Day 113 (Figure 20, Panel A).

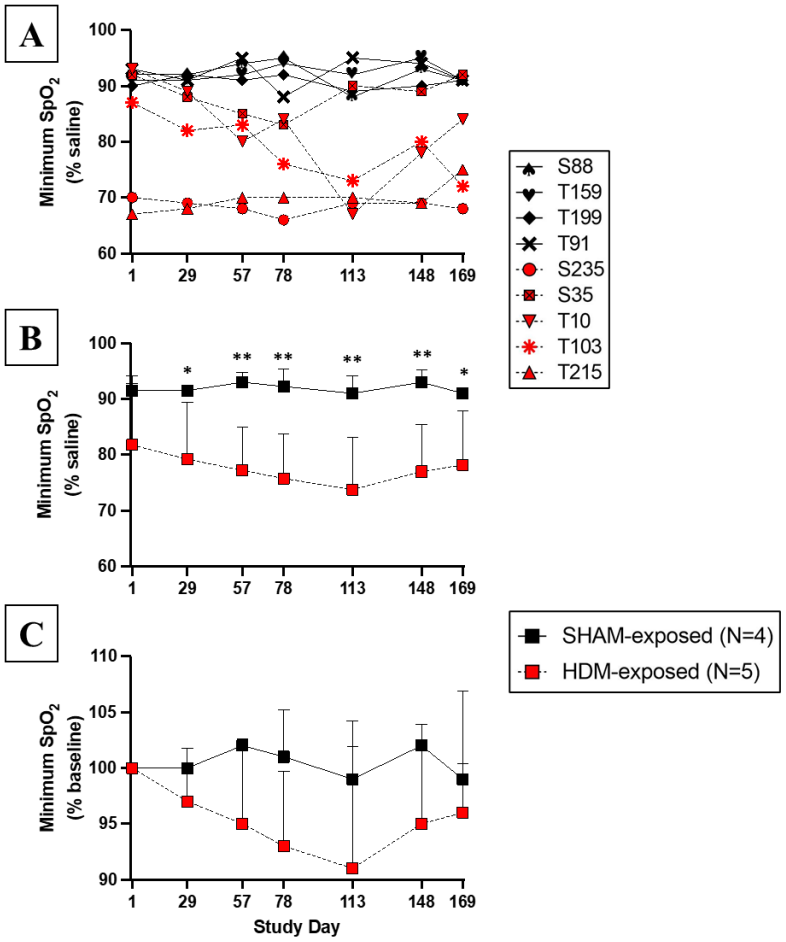

Figure 20. Maximum acute response to aero-saline or aero-HDM- Minimum SpO_2

Maximum acute pulmonary function responses to monthly aero-HDM or aero-saline (SHAM) exposure over six months measured at Days 1, 29, 57, 78, 113, 148, & 169. The raw minimum peripheral oxygen saturation (SpO2) after delivering the maximum provocative dose of aero-HDM/saline at each study day for all nine study animals; SHAM-exposed animals shown in black with a solid line and HDM-exposed animals in red with a dashed line (A). The average oxygen saturation for SHAM and HDM-exposed animals are shown in Panel B; expressed as group mean ± SD. Normalized minimum SpO2 (to Day 1 baseline) for SHAM-exposed and HDM-exposed groups (C). Normalized data is expressed as group mean ± SD for SHAM-exposed (red square; solid line) and HDM-exposed (black square; dashed line) groups. Two-factor ANOVA with repeated measures showed statistically significant main effects for treatment group ($p<0.05$), no main effects for time and no interaction effect. Two-sample t-test determined statistically significant group differences at Days 29, 57, 78, 113, 148, and 169 ($p<0.05$=*; $p<0.01$=**).

Late asthmatic response to aero-Mch- pulmonary function

LAR pulmonary function responses to aero-Mch challenge, conducted 24 hours after aero-HDM/SHAM exposures on Day 1, Day 78, and Day 169, were assessed to determine changes in non-specific AHR. Two indices used to assess non-specific AHR to aero-Mch are PC_{100} and PC_{40}. PC_{100} is defined as the highest provocative concentration of methacholine that will induce a 100% increase in lung resistance from saline and PC_{40} is defined as the provocative concentration of aero-Mch that will induce a 40% decrease in dynamic lung compliance from saline. PC_{100} and PC_{40} values at Days -41, 2, 79, and 170 are presented and described below in light of changes in non-specific AHR after the first, fourth and seventh aero-HDM/SHAM exposure.

$\underline{PC_{100}}$

The average PC_{100} for HDM-exposed animals was lower for 3 out of the 4 study days (Day -41, 79 & 170) compared to SHAM-exposed (Figure 21, Panel B). Compared to Day -41, the average PC_{100} for SHAM-exposed animals decreased by 10% on Days 2 and 79 and increased by 59% on Day 170 (Figure 21, Panel B). For HDM-exposed animals, the average PC_{100} increased by 271%, 34% and 118% on Days 2, 79, and 170, respectively, when compared to Day -41 (Figure 21, Panel C). Increases in PC_{100} compared to Day -41 were observed on Day 2 for all five HDM-exposed animals, as well as two SHAM-exposed animals (Figure 21, Panel A). On Day 79, a decrease in PC_{100} was observed for four of five HDM-exposed animals resulting in an average PC_{100} of 0.66 (although, still higher than the average PC_{100} at Day -41/Pre-HDM baseline of 0.56). Overall, no statistically significant group differences or changes over time were determined.

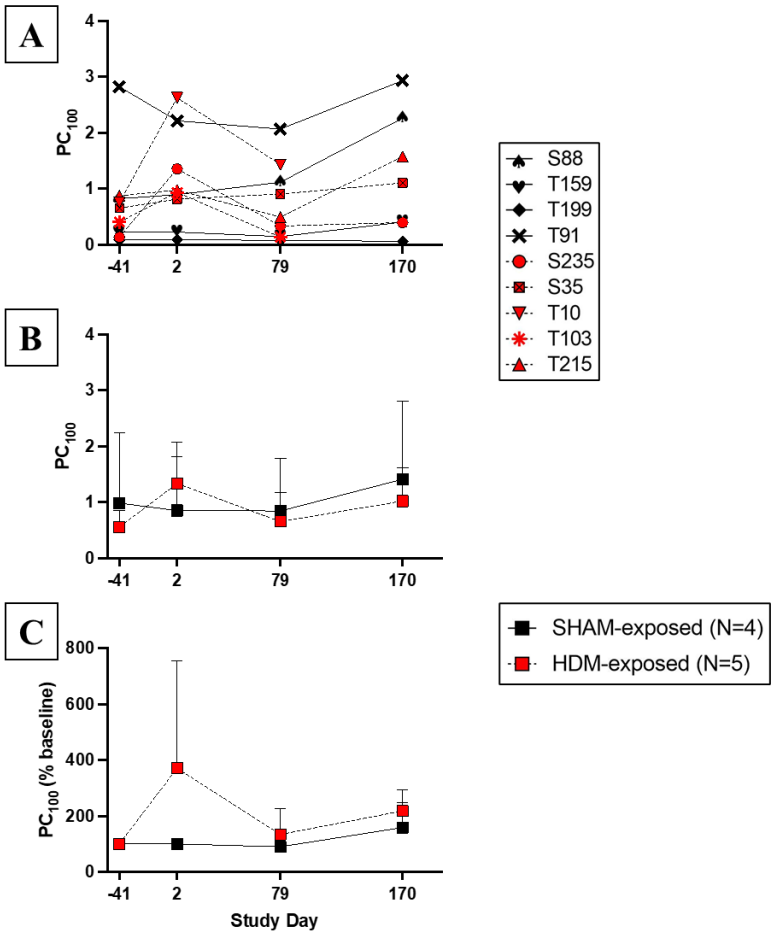

Figure 21. Raw and normalized PC_{100} at Days -41, 2, 79, and 170

The provocative concentration of aerosolized methacholine (aero-Mch) that induced a 100% increase in lung resistance (R_L) at Day -41, 2, 79 and 170. The raw PC100 values at each study day for all nine study animals; SHAM-exposed animals shown in black with a solid line and HDM-exposed animals in red with a dashed line (A). The average PC100 for SHAM and HDM-exposed animals are shown in Panel B; expressed as group mean ± SD. Normalized PC100 (to Day -41 Pre-HDM Baseline) for SHAM-exposed and HDM-exposed groups (C). Normalized data is expressed as group mean ± SD for SHAM-exposed (red square; solid line) and HDM-exposed (black square; dashed line) groups. Two-factor ANOVA with repeated measures did not show statistically significant main effects for time or group and no interaction effect.

PC_{40}

The average PC_{40} in the HDM-exposed group was lower than SHAM during each aero-Mch exposure at Days -41, 2, 79 and 170 (Figure 22, Panel B). The highest average PC_{40} for SHAM (0.41±0.49) and HDM-exposed animals (0.30±0.11) were both observed on Day -41, while the lowest average PC_{40} occurred on Day 79 for the SHAM-exposed group and Day 2 for HDM-exposed. Additionally, a relative decrease from Day -41 in average PC_{40} was observed for both groups at each of the three subsequent aero-Mch challenges on Days 2, 79 and 170 (Figure 22, Panel C).

HDM-exposed animals had a greater overall sensitivity/reactivity (based on lung compliance/PC_{40}) to aero-Mch/showed greater average non-specific AHR compared to SHAM (Figure 22, Panels A &B). Also, both groups showed relative increases in non-specific AHR to aero-Mch (observed as decreases in PC_{40}) after the first, fourth and seventh exposure when compared to Day -41/Pre-HDM baseline, although not statistically significant (Figure 22, Panel C).

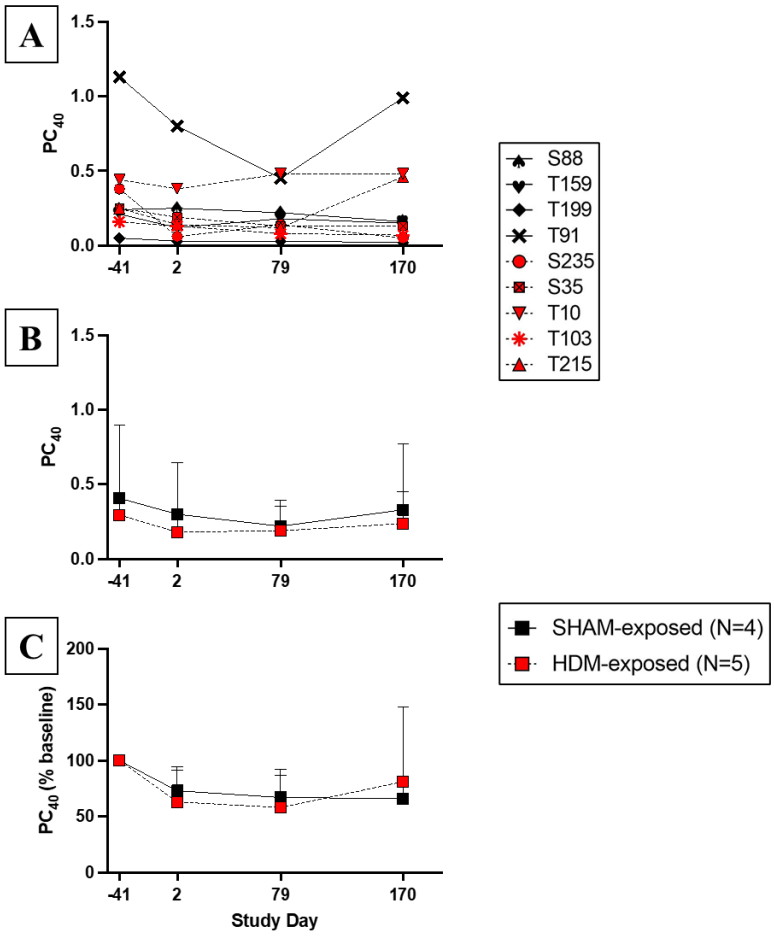

Figure 22. Raw and normalized PC_{40} at Days -41, 2, 79, and 170

The provocative concentration of aerosolized methacholine (aero-Mch) that induced a 40% decrease in dynamic lung compliance (Cdyn) at Day -41, 2, 79 and 170. The raw PC40 values at each study day for all nine study animals; SHAM-exposed animals shown in black with a solid line and HDM-exposed animals in red with a dashed line (A). The average PC40 for SHAM and HDM-exposed animals are shown in Panel B; expressed as group mean ± SD. Normalized PC40 (to Day -41 Pre-HDM Baseline) for SHAM-exposed and HDM-exposed groups (C). Normalized data is expressed as group mean ± SD for SHAM-exposed (red square; solid line) and HDM-exposed (black square; dashed line) groups. Two-factor ANOVA with repeated measures did not show statistically significant main effects for time or group and no interaction effect.

Late asthmatic response- pulmonary inflammation

Pulmonary inflammation responses to monthly aero-HDM or aero-saline (SHAM) exposure were assessed by bronchoalveolar lavage (BAL) 24 hours after the first, fourth and seventh exposures. Total WBC counts and BAL cellularity for lymphocytes, eosinophils and neutrophils will be presented and described below, in order to assess changes in pulmonary inflammation over the course of the six-month study.

Total WBC

At all four study days, the average Total WBC for HDM-exposed animals was greater compared to SHAM, largely due to high Total WBC counts for animal T10 (Figure 23, Panels A & B). Compared to Day -41, average total WBC increased after the first, fourth and seventh aero-HDM/SHAM challenge for both groups (Figure 23, Panel C). Additionally, both exposure groups showed similar trends for increases in average total WBC at Day 2 and Day 79, followed by a decrease from Day 79 to Day 170 (Figure 23, Panel B). Overall, relative group differences and changes in Total WBC counts over time were not statistically significant.

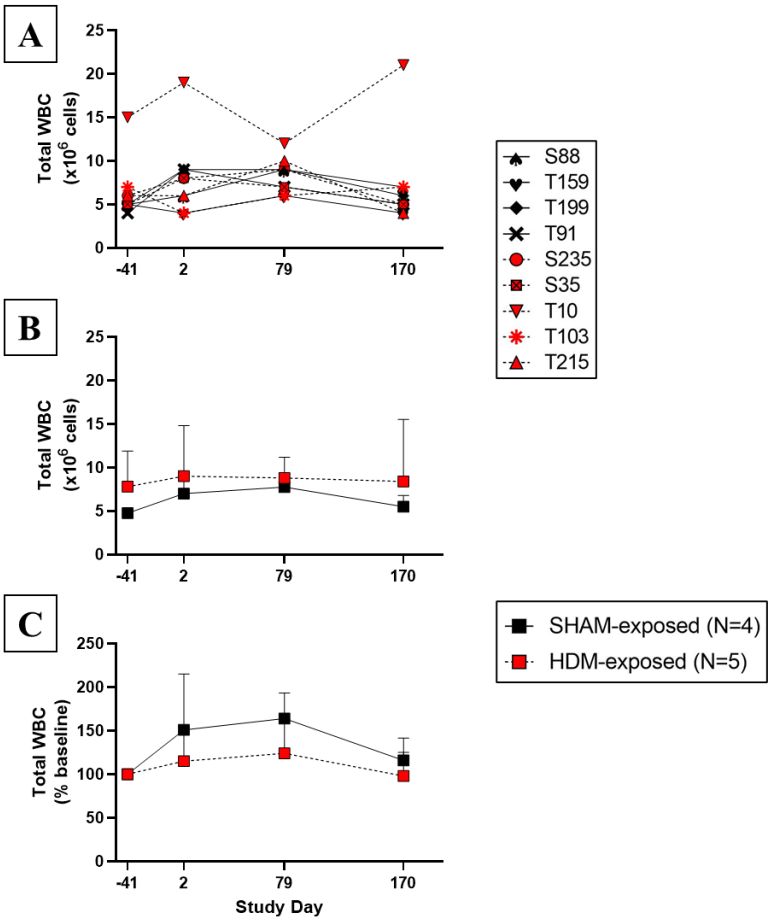

Figure 23. Raw and normalized total WBC at Days -41, 2, 79, and 170

Total WBC cell counts, assessed by bronchoalveolar lavage (BAL) 24 hours after the first (Day 2), fourth (Day 79) and seventh (Day 170) aero-HDM/saline exposures. The raw total WBC values at each study day for all nine study animals; SHAM-exposed animals shown in black with a solid line and HDM-exposed animals in red with a dashed line (A). The average total WBC for SHAM and HDM-exposed animals are shown in Panel B; expressed as group mean ± SD. Normalized total WBC (to Day -41 Pre-HDM Baseline) for SHAM-exposed and HDM-exposed groups (C). Normalized data is expressed as group mean ± SD for SHAM-exposed (red square; solid line) and HDM-exposed (black square; dashed line) groups. Two-factor ANOVA with repeated measures did not show statistically significant main effects for time or group and no interaction effect.

Lymphocytes

Except for Day 2, in which both exposure groups average % lymphocytes was 18%, a greater average % lymphocytes was observed on Days -41, 79, and 170 in SHAM-exposed animals compared to HDM-exposed (Figure 24, Panel B). No change in average % lymphocytes was observed in SHAM animals; an average ~18% lymphocytes was observed at all 4 time points (Figure 24, Panel B). However, in the HDM-exposed group, an average 23% increase was observed on Day 2 (relative to Day -41) followed by a 35% and 20% decrease in % lymphocytes after the fourth and seventh exposure on Days 79 and 170, respectively (Figure 24, Panel C). Overall, relative group differences and changes in % lymphocytes over time were not statistically significant.

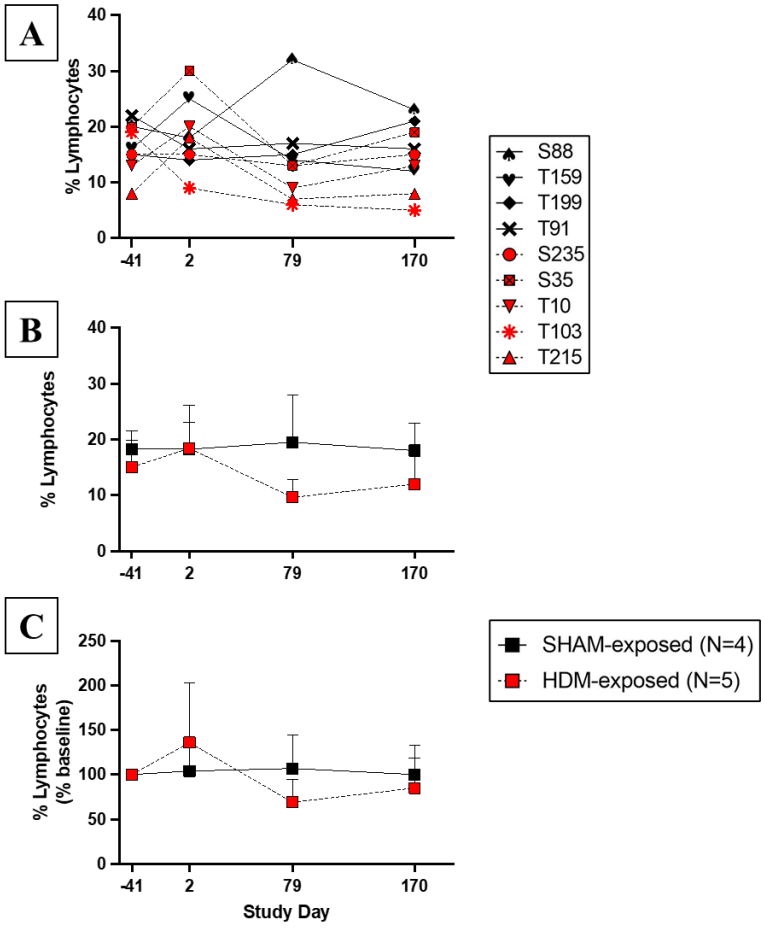

Figure 24. Raw and normalized % lymphocytes at Days -41, 2, 79, and 170

Pulmonary inflammation, assessed by bronchoalveolar lavage (BAL) 24 hours after the first (Day 2), fourth (Day 79) and seventh (Day 170) aero-HDM/saline exposures. The raw % lymphocytes at each study day for all nine study animals; SHAM-exposed animals shown in black with a solid line and HDM-exposed animals in red with a dashed line (A). The average % lymphocytes for SHAM and HDM-exposed animals are shown in Panel B; expressed as group mean ± SD. Normalized % lymphocytes (to Day -41 Pre-HDM Baseline) for SHAM-exposed and HDM-exposed groups (C). Normalized data is expressed as group mean ± SD for SHAM-exposed (red square; solid line) and HDM-exposed (black square; dashed line) groups. Two-factor ANOVA with repeated measures did not show statistically significant main effects for time or group and no interaction effect.

Eosinophils

On Days -41, 2, 79 and 170, the average % eosinophils were greater in the HDM-exposed group compared to SHAM (Figure 25, Panel B). On Days 2, 79 and 179 (relative to Day -41), an average increase in % eosinophils were observed in both exposure groups. Additionally, both exposure groups showed similar trends for increases in average % eosinophils at Day 2 and Day 79, followed by a relative decrease from Day 79 to Day 170 (Figure 25, Panel B).

Compared to Day -41, average % eosinophils in SHAM-exposed animals increased by 806%, 1613%, and 1063% on Days 2, 79, and 170, respectively (Figure 25, Panel C). Similarly, the average % eosinophils in HDM-exposed animals, relative to Day -41, increased significantly by 415% on Day 2 ($p=0.0024$), 753% on Day 79 ($p=0.035$) and 486% on 170 ($p=0.014$), shown in Figure 25, Panel C). Average peak % eosinophils of 17% for SHAM and 24% for HDM-exposed group was observed on Day 79, after the fourth experimental exposure (Figure 25, Panel B). On Day 79, 42% and 19% eosinophils were observed for two SHAM-exposed animals T199 and S88, respectively (Figure 25, Panel A).

Interestingly, the maximum pulmonary inflammation responses for HDM-exposed animals occurred at different study days/after different number of monthly aero-HDM exposures. More specifically, animal T10's peak % eosinophils occurred on Day 2, 24-hours after the first aero-HDM exposure; 2 animals, T215 and S35, peak occurred on Day 79, after 4th exposure; and the remaining 2 animals, T103 and S235, peak responses occurred on Day 170, after the seventh exposure (Figure 25, Panel A).

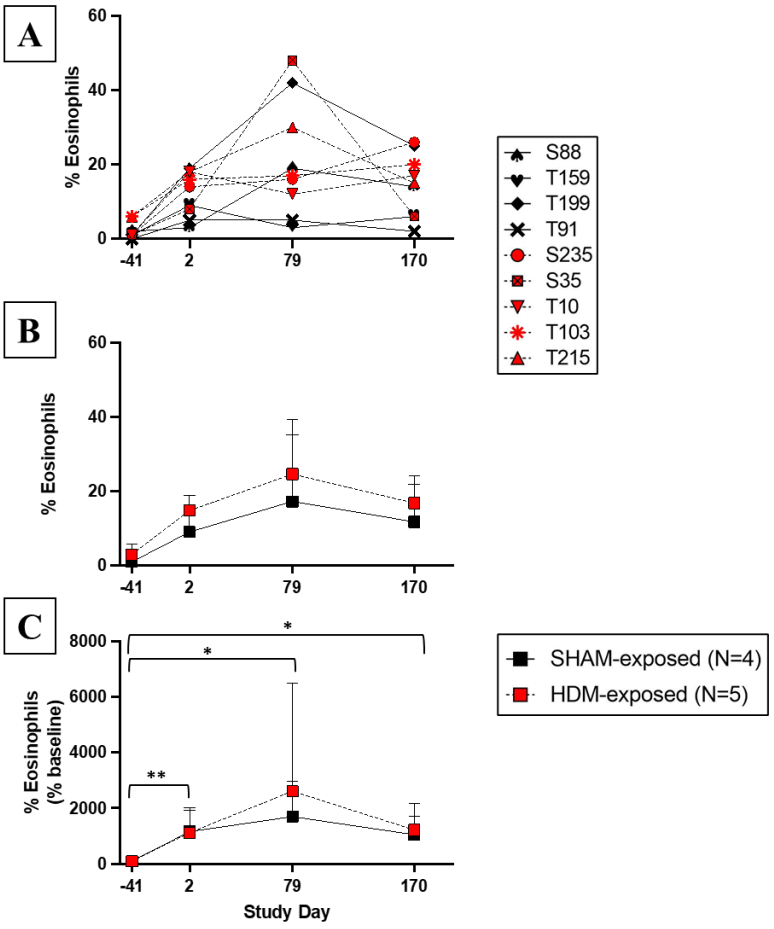

Figure 25. Raw and normalized % eosinophils at Days -41, 2, 79, and 170

Pulmonary inflammation, assessed by bronchoalveolar lavage (BAL) 24 hours after the first (Day 2), fourth (Day 79) and seventh (Day 170) aero-HDM/saline exposures. The raw % eosinophils at each study day for all nine study animals; SHAM-exposed animals shown in black with a solid line and HDM-exposed animals in red with a dashed line (A). The average % eosinophils for SHAM and HDM-exposed animals are shown in Panel B; expressed as group mean ± SD. Normalized % eosinophils (to Day -41 Pre-HDM Baseline) for SHAM-exposed and HDM-exposed groups (C). Normalized data is expressed as group mean ± SD for SHAM-exposed (red square; solid line) and HDM-exposed (black square; dashed line) groups. Two-factor ANOVA with repeated measures showed statistically significant main effects for time ($p<0.05$), no main effects for treatment and no interaction effect. One-way ANOVA showed statistically significant difference in % eosinophils over time in HDM-exposed animals. Paired t-test to evaluate pairs of study days showed a statistically significant difference in % eosinophils in HDM-exposed group between Day -41 and 2 ($p=0.0024$), Day -41 and 79 ($p=0.035$), and Day -41 and 170 ($p=0.014$); $p<0.05$=*, $p<0.01$=**

Neutrophils

On Day -41/Pre-HDM baseline, average % neutrophils were similar in SHAM-exposed (0.6±0.2%) and HDM-exposed (0.4±0.3%) animals (Figure 26, Panel B). However, average % neutrophils for the HDM-exposed group was higher compared to SHAM after the first, fourth and seventh exposure (Figure 26, Panel B).

Compared to Day -41, average % neutrophils for SHAM-exposed animals increased by 111% on Day 2, 478% on Day 79, and 67% on Day 170, although not statistically significant (Figure 26, Panel C). This trend for increased % neutrophils, particularly on Day 79, for the SHAM-exposed groups was largely due to animal T91. On Day 79, SHAM-exposed animal T91 manifested an increase in neutrophils in the BAL fluid to 11% (Figure 26, Panel A), reflected as an increase in SHAM-exposed group average for % neutrophils (Figure 26, Panels B & C).

After the first aero-HDM exposure, conducted 24 hours before BAL, the average percentage of neutrophils in the BAL fluid for the HDM-exposed groups increased from 0.4% to ~3% of the total cells recovered (Figure 26, Panel B). Furthermore, average % neutrophils, compared to Day -41, increased significantly by 1129% on Day 79 ($p=0.0011$) and 971% on Day 170 ($p=0.0024$), in the HDM-exposed group (Figure 26, Panel C).

Interestingly, the maximum pulmonary inflammation responses for HDM-exposed animals occurred at different study days/after different number of monthly aero-HDM exposures. More specifically, animal T10's peak % neutrophils occurred on Day 2, 24-hours after the first aero-HDM exposure; 2 animals, T215 and S35, peak occurred on Day 79, after 4th exposure; and the remaining 2 animals, T103 and S235, peak responses occurred on Day 170, after the seventh exposure (Figure 26, Panel A).

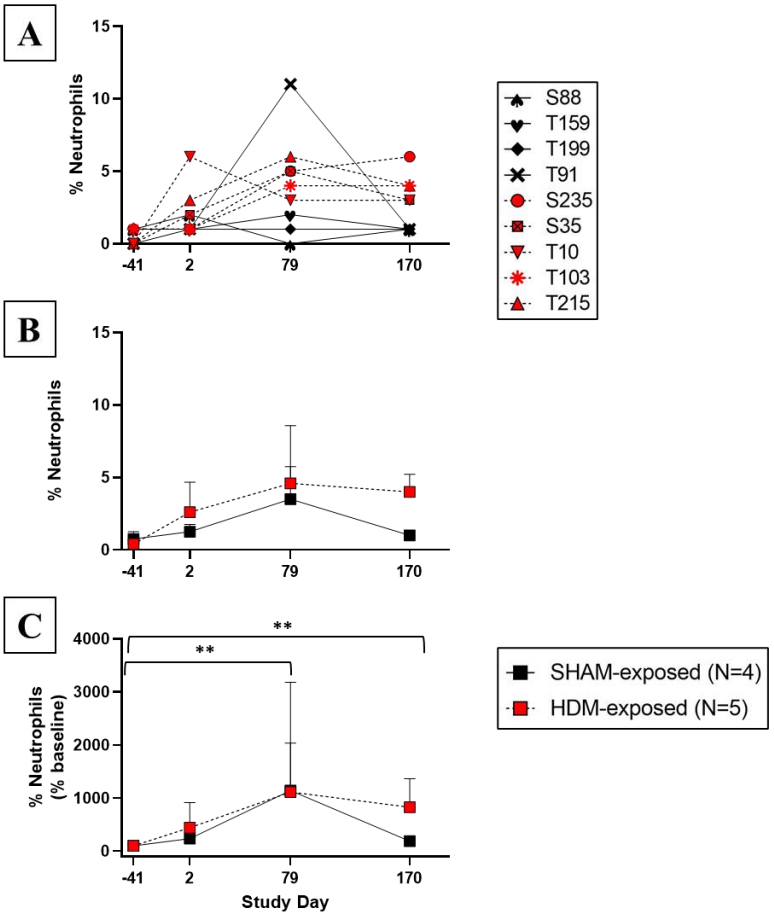

Figure 26. Raw and normalized % neutrophils at Days -41, 2, 79, and 170

Pulmonary inflammation, assessed by bronchoalveolar lavage (BAL) 24 hours after the first (Day 2), fourth (Day 79) and seventh (Day 170) aero-HDM/saline exposures. The raw % neutrophils at each study day for all nine study animals; SHAM-exposed animals shown in black with a solid line and HDM-exposed animals in red with a dashed line (A). The average % neutrophils for SHAM and HDM-exposed animals are shown in Panel B; expressed as group mean ± SD. Normalized % neutrophils (to Day -41 Pre-HDM Baseline) for SHAM-exposed and HDM-exposed groups (C). Normalized data is expressed as group mean ± SD for SHAM-exposed (red square; solid line) and HDM-exposed (black square; dashed line) groups. Two-factor ANOVA with repeated measures showed statistically significant main effects for time ($p<0.05$), no main effects for treatment and no interaction effect. One-way ANOVA showed statistically significant difference in % neutrophils over time in HDM-exposed animals. Paired t-test to evaluate pairs of study days showed a statistically significant difference in % neutrophils for the HDM-exposed group between Day -41 and 79 ($p=0.0011$) and Day -41 and 170 ($p=0.0024$); $p<0.05$=*, $p<0.01$=**

DISCUSSION AND CONCLUSIONS

Introduction

In the study conducted, we hypothesized chronic exposure to aero-HDM will induce chronic pulmonary inflammation that will synergize with obesity related inflammation to exacerbate the development of obesity-related insulin resistance – with the severity of IR correlated to the degree of aero-HDM sensitivity. To test this hypothesis, we exposed one cohort of macaques (N = 5) monthly to aero-HDM, and a second cohort (N = 4) monthly to aerosolized saline/sham only, for six months.

Major findings

Body composition

Decades of longitudinal research and surveying thousands of animals provided a general time of the development of obesity in NHP the eventual development of overt T2DM (Abee et al., 2012; Hansen, 2014; Hansen, 2012). Multiple similar hallmark characteristics of spontaneously induced obesity are observed in both nonhuman primates and humans(Abee et al., 2012; Barbara C. Hansen & Xenia T. Tigno, 2007; Wagner et al., 2001). Obesity has only been observed in sexually mature, post-pubescent NHPs; this occurs over the age of eight for rhesus macaques(Abee et al., 2012; Hansen, 2014; Hansen, Barbara C., Newcomb, Chen, & Linden, 2013). In addition, rhesus macaques reach peak body weight at age 15. (Hansen, 2014)

Based on the three criteria used to define obesity in nonhuman primates described in the methods and supported in the literature, all nine study animals were obese and remained obese for the entirety of the six-month study. A greater degree/greater severity (‘more obese’) of obesity was observed in HDM-exposed animals, compared to SHAM. Lastly, two HDM-exposed animals,

S35 and S235, showed a 7% and 5% decrease, respectively, in body weight at Day 169 relative to Day -41.

Insulin resistance

Insulin resistance is first evident by the hypersecretion of insulin resulting in elevated insulin levels despite no changes or improvements in glucose clearance (Abee et al., 2012). This is characterized by fasting hyperinsulinemia and increased insulin secretion during both phases as assessed by IVGTT (Bremer et al., 2011; Havel et al., 2017). Elevated FPI and dramatic increases in $AUC_{Insulin}$ are typical in animals developing insulin insensitivity/insulin resistance as it reflects a state of compensation for the decline in glucose uptake by the progressing insulin resistance tissues (Abee et al., 2012; Hansen, Barbara C., 2017).

Overtime, compensation in the form of insulin hypersecretion can no longer be sustained and can no longer compensate to maintain glucose balance due to insulin resistant peripheral tissues (Wang, Xiaoli et al., 2013). At this point, insulin levels decline evident by a decrease in $AUC_{Insulin}$ and impaired glucose tolerance occurs (Staup, Aoyagi, Bayless, Wang, & Chng, 2016b). As beta cell function decline and the pancreatic exhaustion occurs, increased insulin levels can no longer effectively respond to increased glucose levels induced by IVGTT or postprandial (Abee et al., 2012; Defronzo, 2009). This severe state of insulin resistance and impaired glucose tolerance in which $AUC_{Insulin}$ dramatically declines coincident with significantly higher $AUC_{Glucose}$ and dramatic decline in glucose disappearance rate (K_G) characterizes the progression to an overt T2DM disease state (Hansen, B. C. & Bodkin, 1986). Hallmark characteristics suggesting development/progression of insulin resistance include significantly higher insulin levels but comparable glucose values as well as increases in HOMA-IR and $AUC_{Insulin}$. On Day 197, FPI for both SHAM and HDM-exposed animals decreased by

32% and 23%, respectively (**Figure 8**, Panel B), and HOMA-IR decreased by 32% and 29%, respectively (**Figure 9**, Panel B), although not statistically significant. Additionally, while not statistically significant, a 3% and 5% decrease in $AUC_{Insulin}$ for SHAM and HDM-exposed groups, respectively, was observed on Day 197 compared to Day -27. The relative changes in IR parameters observed in both exposure groups does not show evidence of insulin resistance, quite the contrary.

Overall, the IVGTT measurements did not provide meaningful data to indicate the presence of IR in the 9 study animals nor changes in IR as a result of monthly aero-HDM exposures. However, based on the literature, this finding is not surprising. The literature reports peak body weight for rhesus macaques (on average reached at 15 years of age) is reached ~1-3 years prior to the first signs of T2DM manifestation (Abee et al., 2012; Hansen, 2014). This has been supported since by Hansen and others reporting the average age of diabetes onset in the male rhesus monkey is ~18 years (Abee et al., 2012; Hansen, 2014; Hansen & Bodkin, 1986).

Pulmonary function and inflammation

Human asthma is highly complex. Most classified as a pulmonary obstructive disease(West, 1979), the National Heart, Lung, and Blood Institute also defines asthma as a "chronic inflammatory disorder" (Chabra & Gupta, 2021). Hallmark characteristics include increased AHR, airway edema, hypersecretion of mucus, and inflammatory cell infiltration (West, 1998). Allergic asthma manifests as a biphasic response involving an early and late phase (Dorsch, 1990; Kavuru, 2006). The early asthmatic response (EAR) occurs within minutes to two hours after airway provocation and is characterized by elevated serum IgE and acute bronchoconstriction reflected as an increase in lung resistance and a decrease in lung compliance

(Dorsch, 1990; Plopper & Hyde, 2008; Van Scott et al., 2004). The late asthmatic response (LAR) occurs within 6-8 hours following provocation but can last up to 24 hours (Dorsch, 1990; Kavuru, 2006). The LAR manifests as non-specific bronchoconstriction (AHR to a non-specific stimulus such as methacholine) as well as pulmonary inflammation observed in the bronchoalveolar lavage fluid (BALF) (Miller et al., 2017; Slonim & Hamilton, 1976).

EAR and LAR- Pulmonary function

During each monthly experimental exposure, HDM-exposed animals showed greater changes in lung resistance, compliance, and respiratory rate, as well as lower minimum oxygen saturations compared to SHAM animals. Overall, a trend for increased sensitivity to aero-HDM was observed in HDM-exposed animals each month.

Both exposure groups showed relative increases in average PC_{100} at Day 170 compared to Day -41, Pre-HDM baseline. A decrease in PC_{40} induced by aero-Mch was observed 24 hours after the 1st, 4th and last aero-HDM/SHAM challenge for both exposure groups. This reflects a relative increase in non-specific AHR to aero-Mch in terms of lung compliance for both exposure groups (relative to Day -41/Pre-HDM baseline), although not statistically significant.

The five HDM-exposed animals manifested increasing AHR to aero-HDM after the seven total exposures (Figure 27), although as a group they showed highly variable and changes in the seven IR indices pre- and post-treatment were not statistically significant. While changes in IR were not statistically significant, noteworthy/interesting trends/associations were observed in the HDM-exposed animals when HOMA-IR and AHR rank were analyzed before and after the six-month study. Figure 27 illustrates the association between HOMA-IR and AHR rank before and after the study for the HDM-exposed animals. Animals S235 and T215, two historically HDM-

sensitive animals, showed essentially no change in AHR rank associated with ~23% and 13% increase in HOMA-IR after the exposure protocol, respectively.

Conversely, the remaining three HDM-exposed animals with less historical aero-HDM responsivity, T103, T10, and S35, manifested the opposite trend/association between AHR rank and HOMA-IR observed for S235 and T215 (Figure 27). All 3 animals manifested increased AHR reflected as a decrease in AHR rank from Day 1 to Day 169; a 15% decrease in AHR rank was observed for T103 and S35 with an even greater decrease of ~30% was observed for animal T10. The decrease in AHR rank/increased HDM-sensitivity/AHR to aero-HDM were associate with a 7% decrease in HOMA-IR for both T10 and T103 and a 72% decrease for S35, suggesting increased AHR was associated with an improvement in IR (reflected as a decrease in HOMA-IR after 6-month exposure protocol). Regarding aim 1, these findings do not support our hypothesis that increased AHR via monthly exposures would be associated with worsening IR.

One animal in HDM-exposed group should be mentioned- Animal S35 was the least HDM-sensitive of the five HDM-exposed animals, however, three important observations on S35's changes in IR, AHR, and body composition. From Day 1 to Day 169, S35 lost ~5% of his body weight and also manifested increased AHR to aero-HDM as reflected in his changes in AHR rank (Figure 27). These observations were associated with a ~70% decrease in HOMA-IR suggesting an improvement in IR. One possible explanation for improved IR is the coincident weight loss. A 5-7% decrease in BW has been associated with improvements in obesity related sequalae, including insulin resistance/sensitivity, according to the literature (Hansen, Barbara & Bray, 2008; Pite et al., 2020).

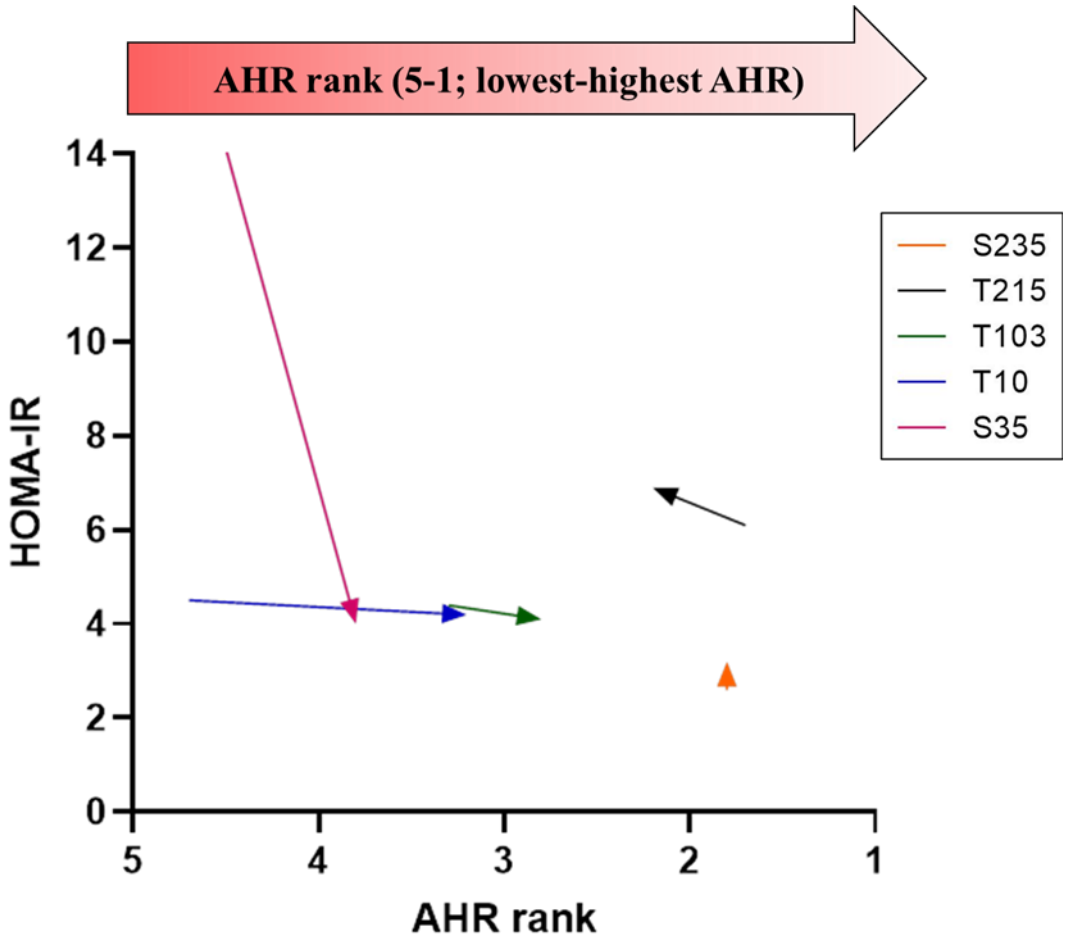

Figure 27. Changes in AHR rank vs. HOMA-IR- HDM-exposed group (N=5)

Illustrated is the association between HOMA-IR and AHR rank before and after the study for the HDM-exposed animals (N=5). The origin of each arrow represents the AHR rank and HOMA-IR on Days 1 and -27, respectively, and the arrowhead represents the AHR rank and HOMA-IR on Days 169 and 197, respectively (after monthly aero-HDM/SHAM exposures for six months). The two historically aero-HDM sensitivity animals, S235, showed no change in AHR associated with a 23% increase in HOMA-IR pre vs. post treatment, while T215 showed an increase in AHR rank associated with a 13% increase in HOMA-IR. The three historically less aero-HDM sensitive/responsive animals, T103, T10, and S35 showed the opposite trend/association between AHR rank and HOMA-IR pre and post treatment. All three animals showed a decrease in AHR rank (aka increased sensitivity to aero-HDM after the six-monthly exposures/increase in AHR) associated with a decrease in HOMA-IR- suggesting increased AHR to aero-HDM was associated with an improvement in IR (reflected as a decrease in HOMA-IR). This does not support our hypothesis that increased AHR via monthly aero-HDM exposures would be associated with worsening IR.

LAR- Pulmonary inflammation

The second feature of allergic asthma is increased inflammation of the airways. Multiple inflammatory cells including macrophages, mast cells, eosinophils, neutrophils, epithelial cells, T-lymphocytes and basophils contribute to the pulmonary inflammation observed after airway provocation (Dorsch, 1990; Kavuru, 2006; West, 1998). Two major asthma phenotypes of airway inflammation have been identified and used for diagnoses and treatment of asthma patients: Th2-high (eosinophilic) and Th2-low (non-eosinophils; neutrophilic) (Jennifer Louten et al., 2012; Kuruvilla, Lee, & Lee, 2019). These endotypes are characterized by different clinical manifestations such as time of onset and responsiveness to steroid treatment, as well as the specific molecular mechanisms and biomarkers such as major inflammatory mediators and cytokines production observed (Akar-Ghibril, Casale, Custovic, & Phipatanakul, 2020; Jennifer Louten et al., 2012; Kavuru, 2006; Kuruvilla et al., 2019; Sinyor & Concepcion Perez, 2021). LAR pulmonary inflammation increased significantly in % eosinophils and % neutrophils in the HDM-exposed animals after the 1st, 4th and last aero-HDM exposure. Interestingly, inflammation also increased in the SHAM-exposed animals reflected as an increase in % eosinophils (for two animals) and % neutrophils (for one animal). Increases in lung inflammation in % eosinophils and neutrophils observed in the HDM-exposed animals supports the major two asthma phenotypes, eosinophilic and neutrophil, identified in the literature (Akar-Ghibril et al., 2020; Dixon & Poynter, 2016; Tashiro & Shore, 2019). Overall, regarding aim 2, the findings illustrated in Figure 28 do not support our hypothesis that increased non-specific AHR to methacholine or increased pulmonary inflammation would be associated with worsening IR. HDM-exposed animals manifested increased aero-HDM sensitivity/AHR with coincident increased pulmonary inflammation after the monthly aero-HDM exposures. Significant increases

% eosinophils and % neutrophils were observed for all five animals 24 hours after the first, fourth, and seventh exposure (Figure 28). The HDM-exposed animals exhibited mixed, eosinophil-dominate pulmonary inflammation consistent with the features of one of the obese asthma endotypes reported in the literature, characterized as early-onset, atopic asthma with eosinophilic inflammatory profile (Carr & Kraft, 2018; Tashiro & Shore, 2019).

Furthermore, increased pulmonary inflammation was also observed in the SHAM-exposed group (Figure 28). Increased % eosinophil inflammation was manifested by two SHAM-exposed animals, S88 and T199. We did not expect to observe this degree of pulmonary inflammation in the SHAM animals, paralleling the expected lung inflammation induced by aero-HDM in the HDM-exposed group.

These two animals, S88 and T199, were historically highly HDM-sensitive: one animal, T199, being the most HDM-sensitive/responsive of the entire colony with a PC_{HDM} of 100 AU/mL. Are we observing an intermediate inflammatory endotype of the early-onset, atopic, eosinophilic obese asthma phenotype in which eosinophilic pulmonary inflammation first induced by asthma (aero-HDM sensitization and periodic maintenance airway challenges) is now driven by obesity when not challenged to aero-HDM?

Very interestingly, one SHAM-exposed animal, T91, with historically poor responsivity/sensitivity to aero-HDM, manifested increased neutrophilic inflammation similar to the second major obese asthma endotype seen in late-onset obese asthmatics with non-eosinophil/neutrophil-dominate lung inflammation (Dixon & Poynter, 2016; Kuruvilla et al., 2019; Peters et al., 2018). The late-onset, non-atopic, neutrophil-dominant endotype is described in the literature as asthma due to/resulting from obesity (non-asthmatic individual develops usually age-related obesity and related sequalae leading to late-onset asthma) (Israel & Reddel,

2017; Tashiro & Shore, 2019). These unique inflammatory profiles resemble the clinical and inflammatory phenotypes/endotypes manifested in obesity associated human asthma warranting further investigation. In addition, this data corroborates/supports the superiority/usefulness of the nonhuman primate (specifically macaques) animal model in the study of obesity, allergic asthma and associated co-morbidities (Abee et al., 2012; Barbara C. Hansen & Xenia T. Tigno, 2007; Havel et al., 2017).

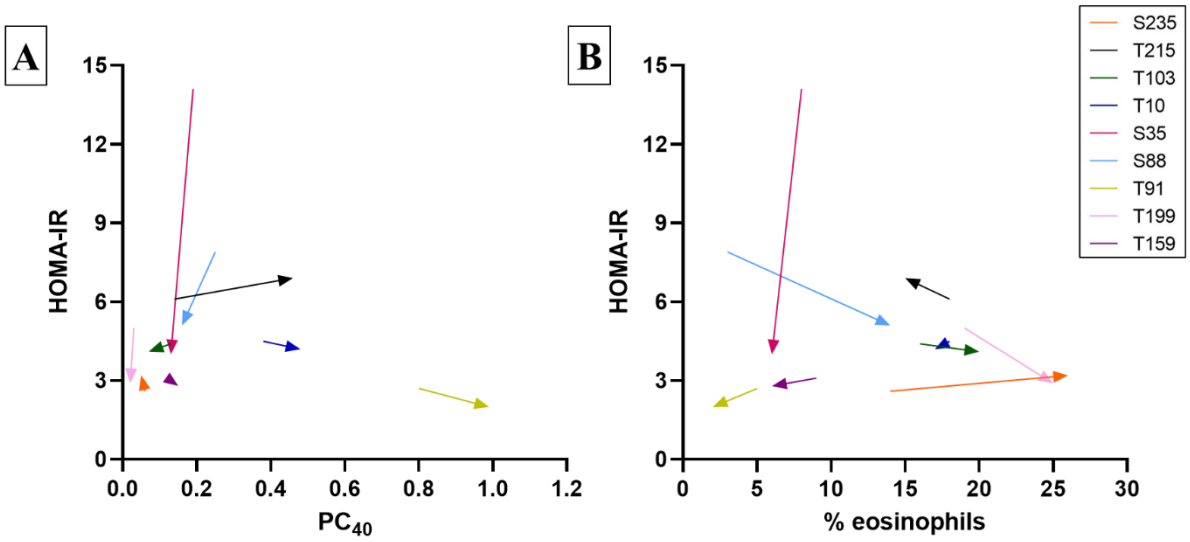

Figure 28. Changes in PC_{40} and % eosinophils vs. HOMA-IR- N=9

Illustrated is the association between HOMA-IR and PC_{40} (A) and % eosinophils (B) before and after the study for all nine study animals (N=9). The origin of each arrow represents the PC_{40}, % eosinophils and HOMA-IR on Days 2 and -27, respectively, and the arrowhead represents the PC_{40}, % eosinophils and HOMA-IR on Days 170 and 197, respectively (after monthly aero-HDM/SHAM exposures for six months).

Limitations

The study was limited primarily by the IVGTT assessments. Insulin resistance assessment via IVGTT was measured twice during the study (without any historical reference values for proper comparison) and the two IVGTT were conducted only six months apart. Only drastically significant changes in IR/IGT would be observed after only six months. We were limited by only two IVGTT measurements and that those measurements were done at ~10-11 years of age, after the development of spontaneous obesity and presumably in the process of IR development, making it very difficult to determine the stage of individual animals IR/T2DM disease progression (Abee et al., 2012; Barbara C. Hansen & Xenia T. Tigno, 2007; Hansen, 2017). Although the literature describes a highly reproducible and supportive timeline of disease progression, NHP like humans have unique insulin responses and age of onset which is why IR via IVGTT should be measured consecutively beginning when spontaneous obesity is first detected to properly measure disease progress, diagnosis, and treatment inventions (Hansen & Bodkin, 1986; Staup et al., 2016). Each animal is its own best control and unfortunately, we were limited by the two assessments (Staup et al., 2016). An alternative approach includes direct measurement of insulin sensitivity via the hyperinsulinemia/euglycemic clamp (*Laboratory animal medicine* 2015; Abee et al., 2012; Staup et al., 2016).

Future studies

The inflammatory mechanisms linking obesity, IR, and allergic asthma are still not clear and will likely become more complicated by multiple disease co-morbidities including cardiovascular disease, cancer, etc. Clearly the next step is to identify common biomarkers of the mixed disease states particularly studies investigating inflammatory cytokines (focus on IL-6, TNF-α, leptin,

adiponectin) produced systemically and tissue specific. Further investigation measuring coincident inflammatory cytokines and metabolites associated with IR and AHR inflammation, with specific focus on cytokines TNF-α and IL-6 and adipokines, adiponectin and leptin are necessary in identifying the inflammatory mediators linking obesity, metabolic dysfunction, asthma and the further related mechanisms and pathways underlying these chronic inflammation disease states.

Future studies evaluating the interacting effect(s) of multiple modifying factors of metabolic dysfunction (adiposity and insulin resistance) as well as genetic and environmental aspects must be conducted using a more multidisciplinary approach in order to fully understand the link between obesity and severe asthma development and provide the urgent need for therapeutics uniquely designed for the treatment and possible prevention of obese asthmatics (Bantulà et al., 2021; Miethe et al., 2020; Peters et al., 2018).

Overall conclusions

No significant changes in body composition were observed in either exposure group; all study animals were obese during the entirety of the study; however, HDM-exposed animals were larger/more obese compared to the small, obese SHAM-exposed animals. IVGTT data including the seven indices of insulin resistance were highly variable within exposure groups and no statistically significant changes in any of the IR outcome measures were observed within exposure groups, between groups nor over time. Monthly aero-HDM exposures for six months induced increased AHR and significant pulmonary inflammation (eosinophilic and neutrophilic) in the five HDM-exposed animals, although AHR to aero-HDM was not statistically significant and highly variable within individual animals.

Associations between AHR and HOMA-IR at the beginning and end of the six-month exposure protocol was assessed from HDM-exposed animals. Three of the five animals showed a negative association between changes in AHR and HOMA-IR (IR index used) suggesting increased AHR was associated with a decrease in HOMA-IR. In other words, contrary to our hypothesis, increased AHR/increase sensitivity to aero-HDM was associated with improved insulin resistance, not worsened.

Interestingly, animals in both the aero-HDM and aero-saline exposed groups manifested increased pulmonary inflammation. All five HDM-exposed animals and two SHAM-exposed animals exhibited predominately eosinophilic pulmonary inflammation and one SHAM-exposed animal manifested increased neutrophilia very similar to the early-onset, atopic, eosinophil-dominate obese asthma phenotype and the late-onset, non-atopic, neutrophil-dominate endotype reported in the literature (Dixon & Poynter, 2016; Tashiro & Shore, 2019). Overall, these finding warrant further investigation of the role of insulin resistance in the obese asthma phenotypes/endotypes using a larger cohort of animals and more IVGTT measurements to determine stage of insulin resistance progression.

REFERENCES

Abate, K. H., Abebe, Z., Abil, O. Z., Afshin, A., Ahmed, M. B., Alahdab, F., . . . Zucker, I. (2018). Global, regional, and national incidence, prevalence, and years lived with disability for 354 diseases and injuries for 195 countries and territories, 1990–2017: A systematic analysis for the global burden of disease study 2017. *The Lancet (British Edition), 392*(10159), 1789-1858. doi:10.1016/S0140-6736(18)32279-7

Abee, C. R., Mansfield, K., Tardif, S. D., & Morris, T. (2012). *Nonhuman primates in biomedical research: Diseases* (2nd ed.). Saint Louis, UNITED STATES: Elsevier Science & Technology. Retrieved from http://ebookcentral.proquest.com/lib/eastcarolina/detail.action?docID=902781

Akar-Ghibril, N., Casale, T., Custovic, A., & Phipatanakul, W. (2020). Allergic endotypes and phenotypes of asthma. *The Journal of Allergy and Clinical Immunology in Practice (Cambridge, MA), 8*(2), 429-440. doi:10.1016/j.jaip.2019.11.008

AYANOGLU, G., DESAI, B., WARDLE, R. L., FICK, R. B., GREIN, J., DE WAAL MALEFYT, R., . . . VAN SCOTT, M. R. (2011). Modelling asthma in macaques: Longitudinal changes in cellular and molecular markers. *The European Respiratory Journal, 37*(3), 541-552. doi:10.1183/09031936.00047410

Bantulà, M., Roca-Ferrer, J., Arismendi, E., & Picado, C. (2021). Asthma and obesity: Two diseases on the rise and bridged by inflammation. *Journal of Clinical Medicine, 10*(2) doi:10.3390/jcm10020169

Barbara C. Hansen, & Xenia T. Tigno. (2007). The rhesus monkey (macaca mulatta) manifests all features of human type 2 diabetes. In E. Shafrir (Ed.), *Animal models of diabetes: Frontiers in research* (1st ed., pp. 249-268). Boca Raton, FL: CRC Press.

Bremer, A. A., Stanhope, K. L., Graham, J. L., Cummings, B. P., Wang, W., Saville, B. R., & Havel, P. J. (2011). Fructose-Fed rhesus monkeys: A nonhuman primate model of insulin resistance, metabolic syndrome, and type 2 diabetes. *Clinical and Translational Science, 4*(4), 243-252. doi:10.1111/j.1752-8062.2011.00298.x

Camargo, C. A., Weiss, S. T., Zhang, S., Willett, W. C., & Speizer, F. E. (1999). Prospective study of body mass index, weight change, and risk of adult-onset asthma in women. *Archives of Internal Medicine, 159*(21), 2582-2588. doi:10.1001/archinte.159.21.2582

Cardet, J. C., Ash, S., Kusa, T., Camargo, J., Carlos A, & Israel, E. (2016). Insulin resistance modifies the association between obesity and current asthma in adults. *The European Respiratory Journal, 48*(2), 403-410. doi:10.1183/13993003.00246-2016

Carr, T. F., & Kraft, M. (2018). Use of biomarkers to identify phenotypes and endotypes of severe asthma. *Annals of Allergy, Asthma, & Immunology, 121*(4), 414-420. doi:10.1016/j.anai.2018.07.029

Centers for disease control and prevention.national center for chronic disease prevention and health promotion,
division of nutrition, physical activity, and obesity.data, trend and maps.

Chabra, R., & Gupta, M. (2021). *Allergic and environmental induced asthma*. Treasure Island, FL: StatPearls Publishing. Retrieved from https://www.ncbi.nlm.nih.gov/books/NBK526018/

Coffman, R. L., & Hessel, E. M. (2005). Nonhuman primate models of asthma. *The Journal of Experimental Medicine, 201*(12), 1875-1879. doi:10.1084/jem.20050901

Das, U. N. (2001). Is obesity an inflammatory condition? *Nutrition, 17*(11), 953-966. doi:https://doi.org/10.1016/S0899-9007(01)00672-4

Defronzo, R. A. (2009). Banting lecture. from the triumvirate to the ominous octet: A new paradigm for the treatment of type 2 diabetes mellitus. *Diabetes (New York, N.Y.), 58*(4), 773. Retrieved from https://www.ncbi.nlm.nih.gov/pubmed/19336687

Dixon, A. E., & Poynter, M. E. (2016). Mechanisms of asthma in obesity. pleiotropic aspects of obesity produce distinct asthma phenotypes. *American Journal of Respiratory Cell and Molecular Biology, 54*(5), 601-608. doi:10.1165/rcmb.2016-0017PS

Dixon, A. E., & Rincón, M. (2016). Metabolic dysfunction: Mediator of the link between obesity and asthma? *The Lancet. Respiratory Medicine, 4*(7), 533-534. doi:10.1016/S2213-2600(16)30104-7

Dixon, A. E., & Holguin, F. (2019). Diet and metabolism in the evolution of asthma and obesity. *Clinics in Chest Medicine, 40*(1), 97-106. doi:10.1016/j.ccm.2018.10.007

Dorsch, W. (1990). *Late phase allergic reactions*. Boca Raton, FL: CRC Press.

Ellulu, M. S., Patimah, I., Khaza'ai, H., Rahmat, A., & Abed, Y. (2017). Obesity and inflammation: The linking mechanism and the complications. *Archives of Medical Science : AMS, 13*(4), 851-863. doi:10.5114/aoms.2016.58928

Fantuzzi, G. (2005). Adipose tissue, adipokines, and inflammation. *Journal of Allergy and Clinical Immunology, 115*(5), 911-919. doi:10.1016/j.jaci.2005.02.023

Forno, Erick, MD, MPH, Han, Y., PhD, Muzumdar, R. H., MD, & Celedón, Juan C., MD, DrPH. (2015). Insulin resistance, metabolic syndrome, and lung function in US adolescents with and without asthma. *Journal of Allergy and Clinical Immunology, 136*(2), 304-311.e8. doi:10.1016/j.jaci.2015.01.010

Freeman, A. M., & Pennings, N. (2021). Insulin resistance. *StatPearls* (). Treasure Island, FL: StatPearls Publishing. Retrieved from http://www.ncbi.nlm.nih.gov/books/NBK507839/

Gomez-Llorente, M., Romero, R., Chueca, N., Martinez-Cañavate, A., & Gomez-Llorente, C. (2017). *Obesity and asthma: A missing link* MDPI AG. doi:10.3390/ijms18071490

Haldar, P., Pavord, I. D., Shaw, D. E., Berry, M. A., Thomas, M., Brightling, C. E., . . . Green, R. H. (2008). Cluster analysis and clinical asthma phenotypes. *American Journal of Respiratory and Critical Care Medicine, 178*(3), 218-224. doi:10.1164/rccm.200711-1754OC

Hales, C. M., Carroll, M. D., Fryar, C. D., & Ogden, C. L.*Prevalence of obesity and severe obesity among adults: United states, 2017-2018 key findings data from the national health and nutrition examination survey*

Hansen, B. C. (2014). In Bray B. (Ed.), *Handbook of obesity: Epidemiology, etiology, and pathophysiology. 3rd ed.* (3rd ed.). New York: Marcel Dekker.

Hansen, B. C., & Bodkin, N. L. (1986). Heterogeneity of insulin responses: Phases leading to type 2 (non-insulin-dependent) diabetes mellitus in the rhesus monkey. *Diabetologia, 29*(10), 713-719. doi:10.1007/BF00870281

Hansen, B. C. (2004). Primates in the study of aging-associated obesity. In George A. Bray, & Claude Bouchard (Eds.), *Handbook of obesity* (2nd ed., pp. 238-299). New York: Mercel Dekker, Inc. doi:10.3109/9780203913376-13

Hansen, B. C. (2012). Investigation and treatment of type 2 diabetes in nonhuman primates. *Methods in Molecular Biology (Clifton, N.J.), 933*, 177-185. doi:10.1007/978-1-62703-068-7_11

Hansen, B. C. (2017). Progressive nature of obesity and diabetes in nonhuman primates. *Obesity, 25*(4), 663-664. doi:https://doi.org/10.1002/oby.21818

Hansen, B. C., Newcomb, J. D., Chen, R., & Linden, E. H. (2013). Longitudinal dynamics of body weight change in the development of type 2 diabetes. *Obesity (Silver Spring, Md.), 21*(8), 1643-1649. doi:10.1002/oby.20292

Hansen, B., & Bray, G. (2008). In Hansen B. C., Bray G. A. (Eds.), *The metabolic syndrome:: Epidemiology, clinical treatment, and underlying mechanisms* (1st ed.). Totowa, NJ: Humana Press. Retrieved from https://www.springer.com/gp/book/9781588297389

Havel, P. J., Kievit, P., Comuzzie, A. G., & Bremer, A. A. (2017). Use and importance of nonhuman primates in metabolic disease research: Current state of the field. *ILAR Journal, 58*(2), 251-268. doi:10.1093/ilar/ilx031

Hotamisligil, G. S. (2017). Foundations of immunometabolism and implications for metabolic health and disease. *Immunity (Cambridge, Mass.), 47*(3), 406-420. doi:10.1016/j.immuni.2017.08.009

Husemoen, L. L. N., Glümer, C., Lau, C., Pisinger, C., Mørch, L. S., & Linneberg, A. (2008). Association of obesity and insulin resistance with asthma and aeroallergen sensitization. *Allergy*, *63*(5), 575-582. doi:10.1111/j.1398-9995.2007.01613.x

Ioannou, G. N., Bryson, C. L., & Boyko, E. J. (2007). Prevalence and trends of insulin resistance, impaired fasting glucose, and diabetes. *Journal of Diabetes and its Complications*, *21*(6), 363-370. doi:10.1016/j.jdiacomp.2006.07.005

Israel, E., & Reddel, H. K. (2017). Severe and difficult-to-treat asthma in adults. *The New England Journal of Medicine*, *377*(10), 965-976. doi:10.1056/NEJMra1608969

Jen, K. C., & Hansen, B. C. (1988). Glucose disappearance rate in rhesus monkeys: Some technical considerations. *American Journal of Primatology*, *14*(2), 153-166. doi:10.1002/ajp.1350140206

Jennifer Louten, Jeanine D. Mattson, Maria-Christina Malinao, Ying Li, Claire Emson, Felix Vega, . . . Maribel Beaumont. (2012). Biomarkers of disease and treatment in murine and cynomolgus models of chronic asthma. *Biomarker Insights*, *2012*(7), 87-104. doi:10.4137/BMI.S9776

Kavuru, M. S. (2006). *Diagnosis and management of asthma* (3rd ed.). Caddo, OK: Professional Communications, Inc.

Kemnitz, J. W., & Francken, G. A. (1986). Characteristics of spontaneous obesity in male rhesus monkeys. *Physiology & Behavior*, *38*(4), 477-483. doi:10.1016/0031-9384(86)90414-2

Kim, K., Kim, S., Lee, S., Song, W., Chang, Y., Min, K., & Cho, S. (2014). Association of insulin resistance with bronchial hyperreactivity. *Asia Pacific Allergy*, *4*(2), 99-105. doi:10.5415/apallergy.2014.4.2.99

Kumar, S., & O'Rahilly, S. (2005). *Insulin resistance* (1. Aufl. ed.). Hoboken, NJ: Wiley. Retrieved from http://ebooks.ciando.com/book/index.cfm/bok_id/493680

Kuruvilla, M. E., Lee, F. E., & Lee, G. B. (2019). Understanding asthma phenotypes, endotypes, and mechanisms of disease. *Clinical Reviews in Allergy & Immunology*, *56*(2), 219-233. doi:10.1007/s12016-018-8712-1

Laboratory animal medicine (2015). In Anderson L. C., Otto G., Pritchett-Corning K. R. and Whary M. T. (Eds.), . San Diego: Elsevier Science & Technology. Retrieved from http://ebookcentral.proquest.com/lib/eastcarolina/detail.action?docID=2084974

Lee, H., Muniyappa, R., Yan, X., Yue, L. Q., Linden, E. H., Chen, H., . . . Quon, M. J. (2011). Comparison between surrogate indexes of insulin sensitivity/resistance and hyperinsulinemic euglycemic glucose clamps in rhesus monkeys. *Endocrinology*, *152*(2), 414-423. doi:10.1210/en.2010-1164

Liddie, S., Okamoto, H., Gromada, J., & Lawrence, M. (2019). Characterization of glucose-stimulated insulin release protocols in african green monkeys (chlorocebus aethiops). *Journal of Medical Primatology, 48*(1), 10-21. doi:10.1111/jmp.12374

Loeb, W. F., & Quimby, F. W. (1989). *The clinical chemistry of laboratory animals* (1st ed.). Elmsford, NY: Pergamon Press.

Lundbaek, K. (1962). Intravenous glucose tolerance as a tool in definition and diagnosis of diabetes mellitus. *British Medical Journal, 1*(5291), 1507-1513. doi:10.1136/bmj.1.5291.1507

Mattiuzzi, C., & Lippi, G. (2020). Worldwide asthma epidemiology: Insights from the global health data exchange database. *International Forum of Allergy & Rhinology, 10*(1), 75-80. doi:10.1002/alr.22464

Miethe, S., Karsonova, A., Karaulov, A., & Renz, H. (2020). Obesity and asthma. *The Journal of Allergy and Clinical Immunology, 146*(4), 685-693. doi:10.1016/j.jaci.2020.08.011

Miller, L. A., Royer, C. M., Pinkerton, K. E., & Schelegle, E. S. (2017). Nonhuman primate models of respiratory disease: Past, present, and future. *ILAR Journal, 58*(2), 269-280. doi:10.1093/ilar/ilx030

National diabetes statistics report, 2020 | CDC. (2020). Retrieved from https://www.cdc.gov/diabetes/data/statistics-report/index.html

Periyalil, H. A., Gibson, P. G., & Wood, L. G. (2013a). Immunometabolism in obese asthmatics: Are we there yet? *Nutrients, 5*(9), 3506-3530. doi:10.3390/nu5093506

Periyalil, H. A., Gibson, P. G., & Wood, L. G. (2013b). Immunometabolism in obese asthmatics: Are we there yet? *Nutrients, 5*(9), 3506-3530. doi:10.3390/nu5093506

Peters, U., Dixon, A. E., & Forno, E. (2018). Obesity and asthma. *Journal of Allergy and Clinical Immunology, 141*(4), 1169-1179. doi:10.1016/j.jaci.2018.02.004

Peters, U., Suratt, B. T., Bates, J. H. T., & Dixon, A. E. (2018). Beyond BMI: Obesity and lung disease. *Chest, 153*(3), 702-709. doi:10.1016/j.chest.2017.07.010

Peterson, J. D., Nehrlich, S., Oyer, P. E., & Steiner, D. F.Determination of the amino acid sequence of the monkey, sheep, and dog proinsulin C-peptides by a semi-micro edman degradation procedure. *The Journal of Biological Chemistry, 247*(15), 4866-4871. Retrieved from https://agris.fao.org/agris-search/search.do?recordID=US201302316576

Pite, H., Aguiar, L., Morello, J., Monteiro, E. C., Alves, A. C., Bourbon, M., & Morais-Almeida, M. (2020). Metabolic dysfunction and asthma: Current perspectives. *Journal of Asthma and Allergy, 13*, 237-247. doi:10.2147/JAA.S208823

Plopper, C. G., & Hyde, D. M. (2008). The non-human primate as a model for studying COPD and asthma. *Pulmonary Pharmacology & Therapeutics, 21*(5), 755-766. doi:10.1016/j.pupt.2008.01.008

Pound, L. D., Kievit, P., & Grove, K. L. (2014). The nonhuman primate as a model for type 2 diabetes. *Current Opinion in Endocrinology, Diabetes, and Obesity, 21*(2), 89-94. doi:10.1097/MED.0000000000000043

Raman, A., Colman, R. J., Cheng, Y., Kemnitz, J. W., Baum, S. T., Weindruch, R., & Schoeller, D. A. (2005). Reference body composition in adult rhesus monkeys: Glucoregulatory and anthropometric indices. *The Journals of Gerontology. Series A, Biological Sciences and Medical Sciences, 60*(12), 1518-1524. doi:10.1093/gerona/60.12.1518

Sadeghimakki, R., & McCarthy, H. D. (2019). Interactive effects of adiposity and insulin resistance on the impaired lung function in asthmatic adults: Cross-sectional analysis of NHANES data. *Annals of Human Biology, 46*(1), 56-62. doi:10.1080/03014460.2019.1572223

Schelegle, E. S., Gershwin, L. J., Miller, L. A., Fanucchi, M. V., Van Winkle, L. S., Gerriets, J. P., . . . Plopper, C. G. (2001a). Allergic asthma induced in rhesus monkeys by house dust mite (dermatophagoides farinae). *The American Journal of Pathology, 158*(1), 333-341. doi:10.1016/S0002-9440(10)63973-9

Schelegle, E. S., Gershwin, L. J., Miller, L. A., Fanucchi, M. V., Van Winkle, L. S., Gerriets, J. P., . . . Plopper, C. G. (2001b). Allergic asthma induced in rhesus monkeys by house dust mite (dermatophagoides farinae). *The American Journal of Pathology, 158*(1), 333-341. doi:10.1016/S0002-9440(10)63973-9

Serafino-Agrusa, L., Spatafora, M., & Scichilone, N. (2015). Asthma and metabolic syndrome: Current knowledge and future perspectives. *World Journal of Clinical Cases, 3*(3), 285-292. doi:10.12998/wjcc.v3.i3.285

Shore, S. A. (2008). Obesity and asthma: Possible mechanisms. *The Journal of Allergy and Clinical Immunology, 121*(5), 1087-1095. doi:10.1016/j.jaci.2008.03.004

Singh, S., Prakash, Y. S., Linneberg, A., & Agrawal, A. (2013). Insulin and the lung: Connecting asthma and metabolic syndrome. *Journal of Allergy, 2013* doi:10.1155/2013/627384

Sinyor, B., & Concepcion Perez, L. (2021). Pathophysiology of asthma. *StatPearls* (). Treasure Island (FL): StatPearls Publishing. Retrieved from http://www.ncbi.nlm.nih.gov/books/NBK551579/

Slonim, N. B., & Hamilton, L. H. (1976). *Respiratory physiology* (3rd ed.). Saint Louis, MI: The C. V. Mosby Company.

Staup, M., Aoyagi, G., Bayless, T., Wang, Y., & Chng, K. (2016a). Characterization of metabolic status in nonhuman primates with the intravenous glucose tolerance test. *Journal of Visualized Experiments*, (117) doi:10.3791/52895

Staup, M., Aoyagi, G., Bayless, T., Wang, Y., & Chng, K. (2016b). Characterization of metabolic status in nonhuman primates with the intravenous glucose tolerance test. *Journal of Visualized Experiments*, (117) doi:10.3791/52895

Tashiro, H., & Shore, S. A. (2019). Obesity and severe asthma. *Allergology International, 68*(2), 135-142. doi:10.1016/j.alit.2018.10.004

Thuesen, B. H., Husemoen, L. L. N., Hersoug, L. -., Pisinger, C., & Linneberg, A. (2009). Insulin resistance as a predictor of incident asthma-like symptoms in adults. *Clinical and Experimental Allergy, 39*(5), 700-707. doi:10.1111/j.1365-2222.2008.03197.x

Van Scott, M. R., Aycock, D., Cozzi, E., Salleng, K., & Stallings, H. W. (2005). Separation of bronchoconstriction from increased ventilatory drive in a nonhuman primate model of chronic allergic asthma. *Journal of Applied Physiology (Bethesda, Md.: 1985), 99*(6), 2080-2086. doi:10.1152/japplphysiol.00537.2005

Van Scott, M. R., Hooker, J. L., Ehrmann, D., Shibata, Y., Kukoly, C., Salleng, K., . . . Nyce, J. (2004). Dust mite-induced asthma in cynomolgus monkeys. *Journal of Applied Physiology (Bethesda, Md.: 1985), 96*(4), 1433-1444. doi:10.1152/japplphysiol.01128.2003

Van Scott, M. R., Reece, S. P., Olmstead, S., Wardle, R., & Rosenbaum, M. D. (2013). Effects of acute psychosocial stress in a nonhuman primate model of allergic asthma. *Journal of the American Association for Laboratory Animal Science, 52*(2), 157-164.

Wagner, J. D., Cline, J. M., Shadoan, M. K., Bullock, B. C., Rankin, S. E., & Cefalu, W. T. (2001). Naturally occurring and experimental diabetes in cynomolgus monkeys: A comparison of carbohydrate and lipid metabolism and islet pathology. *Toxicologic Pathology, 29*(1), 142-148. doi:10.1080/019262301301418955

Wang, X., Reece, S., Olmstead, S., Wardle, R. L., & Van Scott, M. R. (2010). Nocturnal thoracoabdominal asynchrony in house dust mite-sensitive nonhuman primates. *Journal of Asthma and Allergy, 3*, 75-86. doi:10.2147/JAA.S11781

Wang, X., Hansen, B. C., Shi, D., Fang, Y., Du, F., Wang, B., . . . Wang, Y. J. (2013). Quantification of β-cell insulin secretory function using a graded glucose infusion with C-peptide deconvolution in dysmetabolic, and diabetic cynomolgus monkeys. *Diabetology & Metabolic Syndrome, 5*(1), 40. doi:10.1186/1758-5996-5-40

Wang, X., Wang, B., Sun, G., Wu, J., Liu, Y., Wang, Y., & Xiao, Y. (2015). Dysglycemia and dyslipidemia models in nonhuman primates: Part I. model of naturally occurring diabetes. doi:10.4172/2155-6156.S13-010

West, J. B. (1979). *Respiratory physiology* (2. ed. ed.). Oxford u.a: Blackwell.

West, J. B. (1998). In Paul J. Kelly (Ed.), *Pulmonary pathophysiology* (5th ed.). Philadelphia, PA: Lippincott Williams & Wilkins. Retrieved from http://scans.hebis.de/HEBCGI/show.pl?27904063_aub.html

Woolard, H. G., Fisher-Wellman, K. H., Gowdy, K. M., Reece, S., Collier, D. N., & Wardle, R. L. (2020). Early metabolic syndrome (MetS) in chronic rhesus macaque model of human allergic asthma. *The FASEB Journal, 34*(S1), 1. doi:10.1096/fasebj.2020.34.s1.04162

Wu, H., & Ballantyne, C. (2020). Metabolic inflammation and insulin resistance in obesity. *Circulation Research, 126*(11), 1549-1564. doi:10.1161/CIRCRESAHA.119.315896

Wu, T. D. (2021). Diabetes, insulin resistance, and asthma: A review of potential links. *Current Opinion in Pulmonary Medicine, 27*(1), 29-36. doi:10.1097/MCP.0000000000000738

XIUQIN ZHANG, RONGLI ZHANG, KAITAO LI, HUILIANG ZHANG, YAN ZHANG, CHAO HAN, . . . JIAMING MAO. (2011). Rhesus macaques develop metabolic syndrome with reversible vascular dysfunction responsive to pioglitazone. *Circulation (New York, N.Y.), 124*(1), 77-86. doi:10.1161/CIRCULATIONAHA.110.990333

Younas, H., Vieira, M., Gu, C., Lee, R., Shin, M., Berger, S., . . . Polotsky, V. Y. (2019). Caloric restriction prevents the development of airway hyperresponsiveness in mice on a high fat diet. *Scientific Reports, 9*(1), 279. doi:10.1038/s41598-018-36651-2

Young, S. S., Skeans, S. M., Austin, T., & Chapman, R. W. (2003). The effects of body fat on pulmonary function and gas exchange in cynomolgus monkeys. *Pulmonary Pharmacology & Therapeutics, 16*(5), 313-319. doi:10.1016/S1094-5539(03)00073-7

APPENDIX A: IACUC APPROVAL LETTER

Animal Care and Use Committee
003 Ed Warren Life Sciences Building | East Carolina University | Greenville NC 27834 - 4354
252-744-2436 office | 252-744-2355 fax

March 5, 2021

Robert Wardle, Ph.D.
Department of Physiology, ECU

Subject: Protocol Q218e, original approval date 06/10/2019

Dear Dr. Wardle:

The amendment#8 to your Animal Use Protocol entitled, "Nonhuman Primate Chronic Asthma Shared Resource Program" (AUP#Q218e) was reviewed by this institution's Animal Care and Use Committee on 03/4/2021. The following action was taken by the Committee:

"Approved as submitted"

Please contact Aaron Hinkle prior to any hazard use

A copy of the protocols is enclosed for your laboratory files. Please be reminded that all animal procedures must be conducted as described in the approved Animal Use Protocol. Modifications of these procedures cannot be performed without prior approval of the ACUC. The Animal Welfare Act and Public Health Service Guidelines require the ACUC to suspend activities not in accordance with approved procedures and report such activities to the responsible University Official (Vice Chancellor for Health Sciences or Vice Chancellor for Academic Affairs) and appropriate federal Agencies. Please ensure that all personnel associated with this protocol have access to this approved copy of the AUP/Amendment and are familiar with its contents.

Sincerely yours,

Sue McRae, Ph.D. Chair, Animal Care and Use Committee

SM/GD

enclosure